

## ABSTRACT

Title of dissertation:                   TOOL DEVELOPMENT TO  
  CONSTRAIN AND OPTIMIZE  
  SHELLFISH AQUACULTURE GEAR  
  PERFORMANCE

Brendan Philip Campbell, Doctor of  
Philosophy, 2022

Dissertation directed by:            Professor Matthew W. Gray  
  Department of Marine Estuarine  
  Environmental Science

To produce virginica cultured Crassostrea more efficiently, current grow out techniques require better understanding to allow for more consistent growth and quality. While the basic physical conditions that influence shellfish growth have been well researched, there are limited studies that consider how physical conditions (i.e. water flow and wave motion) influence shellfish growth within the context of an off-bottom aquaculture farm. Since oysters are suspension feeders, they require food to be delivered to their siphons through ambient processes. Changes in water flow can influence the overall survival, growth rate, and quality of oysters. Additionally, the motion, or jostling, of cages are thought to cause chipping on the outer portion of oyster shells, influencing the overall shape and growth of oysters. There are many techniques and equipment that have the potential to influence the water delivery and movement of oysters in

containerized culture; however, little research has addressed how culture practices influence physical forcing surrounding cultured oysters and what impact those changes have on oyster performance. The biophysical relationship occurring in shellfish aquaculture is not being properly characterized partially due to a lack of affordable tools capable of monitoring physical forces in constrained spaces.

This dissertation summarizes the current understanding of how culture practices influence oyster aquaculture production and demonstrates the novel use of affordable and commonly available tools that can be utilized in shellfish aquaculture research across multiple operational scales. The development of a novel clod card method and predictive model was attempted for use in characterizing mass transfer rate of water. The clod card, along with accelerometer loggers were utilized to understand the effects of physical forcing on the production of off-bottom cultured oysters when exposed to a range of biofouling mitigation treatments, grown using different culture methods, and spatially across an active shellfish aquaculture lease. These experiments validated the value in characterizing physical forcing in shellfish aquaculture and identified trade-offs between oyster shell growth and market quality that are linked to changes in the physical environment, which were produced by changing culture practices. Additionally, these validation experiments determined that variability in oyster growth and performance can change over small spatial scales, smaller than the typical grow-out shellfish aquaculture lease, which can influence water movement inside cages, water quality, and the efficiency of a commercial shellfish operation. By considering the local physical environment, growers can strategically employ culture practices that optimize the water flow through and movement of oysters to enhance farm profitability.

TOOL DEVELOPMENT TO CONSTRAIN AND OPTIMIZE SHELLFISH  
AQUACULTURE GEAR PERFORMANCE

by

Brendan Philip Campbell

Dissertation submitted to the Faculty of the Graduate School of the  
University of Maryland, College Park in partial fulfillment  
of the requirements for the degree of  
Doctor of Philosophy  
2022

Advisory Committee:

Professor Matthew W. Gray, Chair  
Professor Jeffrey Cornwell  
Professor Louis Plough  
Professor Larry Sanford  
Professor William Walton

# Table of Contents

Table of Contents .....	ii
List of Tables .....	v
List of Figures .....	vi
List of Abbreviations .....	viii
Chapter 1: Working towards optimized commercial oyster aquaculture: A review on the effects of commercial practices on the production of oysters during the grow-out phase .....	1
Abstract .....	1
Introduction .....	1
Stocking density .....	4
Biofouling control .....	7
Cultivation method and gear .....	8
Farm layout and site selection .....	10
Future considerations .....	14
Discussion .....	16
Chapter 2: Modifications of plaster clod cards to monitor mass transfer rate for shellfish aquaculture systems in low-energy environments .....	20
Abstract .....	20
Introduction .....	21
Methods .....	25
Construction and sampling procedure .....	26
Laboratory experiments .....	28
Experimental flow field .....	28
Trend of plaster dissolution over time .....	30
Effect of temperature and salinity on plaster dissolution rate .....	30
Predictive model to convert plaster dissolution to water motion .....	31
Field experiments .....	33
Comparing predicted clod card measurements to an ADCP .....	33
Influence of tidal cycle on clod card accuracy .....	33
Influence of protective cage surrounding clod cards .....	33
Results .....	34
Trend of plaster dissolution over time .....	34
Effects of water flow, temperature, and salinity on plaster dissolution rate .....	35
Predictive model to convert plaster dissolution to water motion .....	35
Comparing predicted clod card measurements to an ADCP .....	36

Influence of tidal cycle on clod card accuracy .....	37
Influence of protective cage surrounding deployed clod cards .....	38
Discussion .....	38
Chapter 3: Biofouling treatment on long-line cages alters the growth strategies of cultured eastern oysters by affecting cage motion .....	45
Abstract .....	45
Introduction .....	46
Methods .....	48
Study area .....	49
Sample design .....	50
Biofouling coverage .....	51
Physical forcing .....	52
Environmental monitoring .....	52
Oyster performance .....	53
Statistical analysis .....	53
Results .....	54
Environmental monitoring .....	54
Biofouling coverage during field experiments .....	55
Physical forcing .....	57
Oyster performance .....	57
Discussion .....	60
Chapter 4: Effect of off-bottom oyster grow-out method on physical forces and oyster production .....	64
Abstract .....	64
Introduction .....	65
Methods .....	67
Study area .....	67
Experimental design .....	68
Oyster growth and performance .....	69
Physical forcing .....	70
Environmental monitoring .....	70
Statistical analysis .....	71
Results .....	73
Environmental monitoring .....	73
Physical forcing .....	74
Oyster performance .....	75
Discussion .....	79
Chapter 5: Assessing the variability of the physical environment surrounding an off-bottom oyster lease and its influence on eastern oyster growth performance .....	83

Abstract .....	83
Introduction .....	84
Methods .....	86
Study area .....	87
Experimental design .....	87
Oyster growth and performance .....	90
Physical forcing .....	90
Environmental monitoring .....	91
Results .....	92
Environmental monitoring .....	92
Physical forcing .....	94
Oyster performance .....	97
Discussion .....	102
Bibliography .....	107

## List of Tables

Table 1: Symbols used in equations during chapter 1 .....	30
Table 2: Summary of clod card predictive models .....	37
Table 3: Mean response and confidence interval of all monitored parameters .....	57
Table 4: Results from Dunn tests .....	59
Table 5: Average and confidence interval of measured chapter 4 parameters .....	75
Table 6: Average and confidence interval of all water quality and physical parameters .....	98
Table 7: Average and confidence interval of oyster performance parameters with statistical comparisons .....	101

## List of Figures

Figure 1: Diagram of clod card design .....	27
Figure 2: Diagram of recirculating flow field .....	31
Figure 3: Clod card dissolution over time .....	35
Figure 4: Clod card dissolution compared to water flow, temperature, and salinity with linear trendlines .....	36
Figure 5: Comparison between clod card predictive models using the air-dried technique .....	40
Figure 6: Comparison between clod card predictive models using the oven-dried technique ....	41
Figure 7: Comparison between predicted clod card measurements and ADCP measurements ..	41
Figure 8: Tidal effect on clod card dissolution .....	42
Figure 9: Comparison between protected and unprotected clod cards .....	42
Figure 10: Map of experimental design for chapter 3 .....	49
Figure 11: Pictures taken of biofouling accumulation on cages over time .....	52
Figure 12: Binary time series describing when cages were desiccated .....	55
Figure 13: Boxplot of final accumulated biofouling .....	56
Figure 14: Biofouling accumulation over time per cage type .....	56
Figure 15: Time series of jostling per biofouling treatment method .....	58
Figure 16: Boxplots of shell length and condition index of cages treated for biofouling .....	59
Figure 17: Comparison between time-to-market and relative quality of oysters .....	62
Figure 18: Diagram of cage placement used for chapter 4 .....	68
Figure 19: Diagram of accelerometer placement in bags .....	71
Figure 20: Average and variance of cage movement per culture method .....	75
Figure 21: Time series of cage jostling per cage type .....	76
Figure 22: Trend of shell length growth per cage type .....	77
Figure 23: Violin plots of all growth parameters per cage type .....	78
Figure 24: Principal component analysis comparing the spread between cage types .....	78

Figure 25: Theoretical chart depicting environments created by different cage types .....	82
Figure 26: Map of the field site including physical characteristics .....	88
Figure 27: Map of experimental design for chapter 5 .....	89
Figure 28: Diagram of how test bags were placed on bottom cages .....	89
Figure 29: Maps of water quality parameters along the oyster farm .....	93
Figure 30: Histogram of ADCP water velocity measurements around the study site .....	95
Figure 31: Time series of tidal height during the ADCP deployment .....	96
Figure 32: Maps of physical parameters monitored along the oyster farm .....	96
Figure 33: Spatial correlation of clod card dissolution along the field site .....	96
Figure 34: Identification of notable regions on farm based on physical properties .....	99
Figure 35: Maps of final oyster performance parameters monitored along the farm .....	100
Figure 36: Hypothetical growth strategies and oyster performance outcomes .....	105

## List of Abbreviations

Abbreviation	Meaning	Page
ADCP	Acoustic Doppler Current Profiler	20
GIS	Geographic Information Systems	24
CFD	Computational Fluid Dynamics	24
MLEM	Mixed Linear Effect Model	31
Log-GLM	Logarithmic-Transformed Generalized Linear Model	31
STIC	Stream, Temperature, Intermittency, and Conductivity Logger	63
ODO	Optical Dissolved Oxygen	73
HPLDF	Horn Point Laboratory Demonstration Farm	77
ARIMA	Autoregressive Integrated Moving Average	82
PCA	Principal Component Analysis	82

# Chapter 1: Working towards optimized commercial oyster aquaculture: A review on the effects of commercial practices on the production of oysters during the grow-out phase

## **Abstract**

As the need for sustainable protein sources mounts, the oyster aquaculture industry is drawing increasingly more attention as one of the most sustainable sources of animal-based protein. While innovations have provided an influx of new off-bottom cultivation methods that span the water column and creative farm management techniques offered to growers, there are significant gaps in research limiting the optimization of these new innovative techniques. For example, oysters have responded differently to culture practices in varying environments and species; however, much of the current understanding of aquaculture production research makes a ‘one-size-fits-all’ assumption. This review summarized the current knowledge of the grow-out phase of containerized oyster aquaculture while highlighting important research gaps that, when filled, will provide guidance to growers to further improve the production of cultured oysters using. We also focused this review to highlight current disagreements within results among published oyster aquaculture production research and identified potential reasons for their disagreement. Specifically, this review discussed comparisons among off-bottom oyster cultivation methods, farm site selection, layout, standard husbandry practices, and suggestions for gaps in current oyster aquaculture production research.

## **Introduction**

Global oyster production has increased tremendously over the past century. Within this industrious growth, oyster cultivation has dominated global production (Botta et al. 2020). Oysters are among the top ten cultured aquatic animals and the top three in North America (FAO 2020). The culture of oysters and other mollusks will likely contribute to the overall global expansion of aquaculture production, termed the ‘blue revolution’ (Garlock et al. 2019). The high nutritional value of oysters compared to other land and sea-based protein sources (Dong 2009, Willer et al. 2021) combined with the array of ecosystem services provided by cultivating oysters (Coen et al. 2011, Shumway et al. 2003, Ray et al. 2019) deems oyster aquaculture as an ideal candidate for fulfilling the projected needs for water-based protein (Kobayashi et al. 2015).

However, the future growth of oyster aquaculture is limited by production inefficiencies that will deter growth until improvements and innovations are made to increase production efficiency (Willer et al. 2021). Perhaps the most considerable challenge to optimization occurs in the grow-out phase of production. Containerized aquaculture was first proposed in the 1930s (Needler 1935) and began to gain popularity in the 1950s (Shaw 1969). Since the popularization of off-bottom oyster aquaculture, an influx of different commercial cultivation methods and gear flourished, giving growers a large selection of equipment and techniques to choose from. Each method used to grow oysters varies greatly in terms of the effort, risk, and costs associated with maintaining the farming operation (Rauch et al. 1975, Bihan et al. 2013, Martinell et al. 2019). The annual operations cost also varies significantly with the operational scale (Ho et al. 2016). For example, biofouling accumulation on cages is a considerable labor expense to effectively

mitigate and varies greatly across cultivation methods (Adams et al. 2011) and likely location. Suggested stocking density also varies widely among the cages and cultivation methods now available to growers. When scaled, suboptimal stocking caused reductions in growth, survival, and farm profits (Filgueira et al. 2013). The cumulation of husbandry practices and gear costs created an extensive range of expenses for the grower and could affect farm profitability (Huang & Lee 2013, Hood et al. 2020, Engle et al. 2021).

Aside from gear operation and maintenance, tailoring cultivation methods to the prevailing environmental conditions on the farm represents a new avenue for optimization. Each method occupies different vertical positions in the water column, and each gear type has a unique shape and surface area; the combination of these factors and their interactions with a suite of biophysical influences likely creates unique growth experiences for crops during grow-out. For example, oysters grown at the water's surface in bobbing cages exposed to wave action and relatively high current velocity is stressful during development due to excess jostling and feeding inhibition, respectively (Mallet et al. 2009). Alternatively, oysters grown near the bottom in a low-energy environment may not receive enough agitation, creating thinner, lower-quality oysters. There is currently a dearth of knowledge surrounding how specific gear, and the crops within them, respond to prevailing biophysical characteristics. However, much of the recent studies addressing this topic do not fully agree with each other, likely due to changes in responses across oyster species, husbandry practices performed, and experimental settings.

This review will summarize and discuss the current research on the grow-out phase of containerized oyster aquaculture. Cultivation method, husbandry practices, and site location and

productivity models will be discussed concerning their impact on shellfish production across varying environmental conditions and species. We will emphasize research areas where the results of recent studies disagree and identify the conditions that likely explain the disagreement. This analysis highlights optimal conditions for growing oysters in different environments and gaps in oyster aquaculture research and technology within this maturing industry.

### **Stocking density**

The stocking density within one bag, across a farm space, and throughout a waterbody is indicative of overall shellfish quality (Filgueira et al. 2013). While oysters of lower stocking densities tend to have better shell quality, the scale of a shellfish aquaculture operation positively correlates with farm profitability (Ho et al. 2016). The scale at which oysters are grown must remain balanced to allow the grower to maximize profitability while not reducing crop quality or degrading the environment.

There is a general understanding that stocking density correlates negatively with growth, quality, and survival. Honkoop & Bayne (2002) determined that throughout the first year of growth for Pacific oysters (*C. gigas*), increasing stocking density in trays resulted in a small yet significant change in somatic tissue growth, possibly due to food depletion. A similar study observing the effect of stocking density on early *C. virginica* and *C. ariakensis* spat grown in upwelling systems were not significantly affected by stocking density (Bishop & Hooper 2005). A different study focusing on adult oysters observed larger, significant changes in shell growth and final weight in oysters grown for one season using rack-and-bag culture grown at varying densities (Grizzle et al. 2020). This effect was also observed in stocking density studies

conducted in suspended cultures (Marshall & Dunham 2013). Comparing the effects of stocking density and ploidy showed that diploid and triploid oyster growth was equally and negatively affected by increases in stocking density (Tan et al. 2021). This relationship also holds in a hatchery setting where oyster larvae stocked at a high density are subject to slower growth rates and higher mortality (Wang et al. 2018). The studies mentioned above indicate that the definition of density varies across studies and that density effects on crop growth depend on culture methods, culture conditions, and location. Additionally, disagreement between stocking density research appears to be attributed by a combination of location, size class, oyster species, and culture method (both in the nursery and grow-out phase). Ploidy did not appear to influence the effect of stocking density on oyster performance. Longitudinal studies or repeating similar studies in other locations under very different conditions would test how well-preserved density effects are. For example, density effects may be present in sensitive low-seston environments (e.g. Maine), while in eutrophic estuaries, such as the Chesapeake Bay, acceptable density levels with gear may be substantially greater.

After animal density within gear is optimized for the local environment, how individual pieces of gear are positioned relative to others and oriented within the farm warrants scrutiny. Theoretically, a series of bags full of oysters well separated from each other should be equally productive as a series of half-filled bags placed close to each. No stocking density experiment has analyzed the potential influence of water flow among densely packed cages or how food depletion may arise if water/food moves lamina rly from upstream cages to those located downstream.

Stocking density may influence the culture conditions by influencing gear movement. Few studies have evaluated gear movement with wave activity nor modeled its effects (But see Wang et al. 2014). The added weight of a more densely stocked bag would also provide more resistance to motion against the force of water movement, which may result in changes in shell and meat quality, which is highly correlative to value in the half-shell market (Brake et al. 2003). A similar relationship was observed in fish pens, where weights were added to the bottom of the nets to resist motion due to hydrodynamic forces (Klebert et al. 2013). More research is needed to better validate the results of stocking density studies such as these and to provide more applicable data for growers on how to best stock farms.

While stocking density has, at the least, minimal influence on the growth and quality of oysters, most studies only demonstrate these effects on the order of a single bag or cage. Different cultivation methods naturally lend themselves to varying ranges of stocking density. Floating cages have comparably lower stocking densities than off-bottom rack culture, much less than the more natural, on-bottom culture (Comeau et al. 2013). This suggests that, with current technology, the stocking density of a farming operation of caged oysters is not likely to reach a point of overcapacity. One exception could be in areas with low flushing rates, which are less capable of supporting large populations of suspension-feeding organisms (Cranford 2019). Currently, models are being developed to quantify the farm-scale stocking densities required to exceed local ecological and economic carrying capacity (Byron et al. 2015, Filgueira et al. 2014). However, with the continued expansion of shellfish aquaculture, it is vital to consider the carrying capacity as technology advances. Some blue mussel operations have observed examples

of shellfish culture exceeding the natural carrying capacity (Cranford et al. 2008). Continued work in monitoring and standardizing a procedure for assessing oyster carrying capacity will allow for a maximization of production per area that can prevent production penalties and adverse environmental effects associated with large-scale operations.

### **Biofouling control**

Biofouling is an unavoidable presence in shellfish aquaculture, especially in eutrophic estuaries. It requires extensive time and effort to effectively manage the fouling on the animals, cages, and other pieces of submerged equipment (Adams et al. 2011). Improper management of biofouling on these surfaces can be considered a detriment to many growers as the fouling degrades shell quality and increases post-harvest costs (Handley & Bergquist 1997, Adams et al. 2011). However, growth and survival trends of cultured oysters exposed to varied rates of biofouling accumulation lack consistency. One study on the pearl oyster, *Pinctada imbricata*, grown in trays with and without biofouling treatment, resulted in a significant decrease in shell growth of oysters not treated for fouling after 16 weeks compared to trays cleaned every 4-8 weeks (Pit & Southgate 2003). A similar study using the same oyster species grown on ropes did not see any significant differences in growth nor survival after one year; however, they did observe a high settlement of fouling within the first three months of deployment, which then slowed down for the remainder of their experiment (Lacoste et al. 2014). Generally, biofouling accumulation has a neutral effect on the growth and survival of oysters (Mallet et al. 2009, Sala & Lucchetti 2008, Lodeiros et al. 2007). It is also important to note that the excessive treatment

of biofouling on oysters is considered a detriment to the growth and survival of *C. virginica* and *P. margaritifera* (Mallet et al. 2009, Pit & Southgate 2003, respectively).

The process of biofouling management has been said to be complex and vary greatly in effect across species and cultivation method employed (Lacoste & Gaertner-Mazouni 2015) and requires great consideration to manage the costs associated with the practice and the final output that is received. Disagreement in research regarding the effects of biofouling are driven by multiple factors such as: the intensity of fouling treatment, oyster species, biofouling species present, culture method used, and biofouling communities present at the time of experimentation. A seemingly unexplored aspect of biofouling-shellfish aquaculture research is to analyze the effects of epibiont assemblages on the structures associated with aquaculture and determine to what extent biofouling reduces the durability and lifespan of shellfish aquaculture cages and gear. Further work in this area will likely lead to important findings that will better inform the true value of biofouling mitigation and the costs associated with neglecting this procedure. Such work may help to better inform models to predict the optimal cost per unit effort of biofouling management against production.

### **Cultivation method and gear**

Many research efforts have helped to understand the effect of different cultivation methods on the growth and quality of oysters. In previous sections, we determined that different culture methods have varying influence on the effects of biofouling and stocking density on oysters. This is likely due to these cage methods providing different localized environments that ultimately affects the growth of the oysters inside. A comparison of *C. virginica* oysters grown in

off-bottom, suspended, and floating cages in Sandy Bay, AL, showed significant changes in oyster survival, shell growth, and tissue weight across different culture methods. The use of bottom cages resulted in slower growth and decreased survival compared to suspended and floating cages (Walton et al. 2013b). To leverage the capabilities of floating culture to improve shell shape, which draws a premium on the half-shell market, another study conducted in Chesapeake Bay, MD, assessed the benefits of using floating culture as a finishing step in the grow-out process, which yielded significantly increased tissue weights and higher quality shells according to a 3:2:1 shell ratio (Thomas 2016). This result, however, is not species-specific. A study on the performance of *C. ariakensis* cultured using different methods suggests that these thinner-shelled species of oyster exhibit faster shell growth in fixed, off-bottom cages than in floating and suspended systems (Bishop & Petersen 2005).

The growth of oysters could also be affected by the type of gear used within respective cultivation methods. The cultivation of oysters through off-bottom culture methods typically involves using two gear types that influence the density of the contained oysters. Rack-and-bag systems hold bags of oysters along a 1xn formation. Bottom cages hold bags of oysters in a 2x2, 2x3, or 3x2 configuration stacking rows of bags on top of one another. Grizzle et al. (2020) demonstrated that oyster growth (*C. virginica*) is likely faster when using bottom cages compared to rack-and-bag systems. The use of box-shaped bags for both methods also resulted in better growth compared to envelope-style bags. Additionally, while the data was not statistically significant, this work suggests that there may be differences in growth between the bags placed in each section of the bottom cage configuration. Similar work assessed the differences between

different floating cage designs. When comparing the use of singular floating bags and a floating rope-rack, using a rope-rack style cage was more effective in quickly growing oysters (Mallet et al. 2013). Another study comparing the performance of singular floating bags and a Taylor float determined that floating bags resulted in faster shell growth with similar survival (Hamilton et al. 2004). The orientation of long-line cages has also been shown to influence oyster shell growth significantly and is a significant factor influencing production (Davis 2013). These studies indicate how crop quality and production vary among gear types, typically among two gear types. However, in these studies, there is little effort to explain why production or shell quality varies among gear types. Additionally, how bag or system orientation relative to the dominant flow direction, for example, affects the crop within the system (e.g. neighbor effects) or total farm production is unclear. Mechanistic production experiments that explain differences among gear types are currently lacking.

Given the variety of cultivation methods used for oyster aquaculture, it is important to adopt a farm method most complementary to the local environment. Since cultured oysters can become stressed in areas with high turbulence (Mallet et al. 2009), a cage system that produces high-quality oysters in low-energy environments may be less effective in higher-energy environments. A direct comparison between oysters grown using varied cultivation methods in areas of high and low water flow and turbulence would be a valuable study for the expansion of the industry as it would be another environmental layer growers could use when identifying suitable substrates. Such a comparison would be beneficial to better understanding the physical environment's role in the production and begin to generate quantitative ranges of water flow and

turbulence that result in optimal use of the varying culture methods. Some practices might be more ecologically sustainable when considering gear and culture effects on the local landscape. While there has been some debate over the potential impacts of oyster aquaculture practices (Munroe et al. 2020, Dumbauld & McCoy 2015, Naylor et al. 2001), recent studies suggest that the impacts of culture on local fauna such as seagrasses would be much less affected by floating bag culture since they block less light compared to long-line and tray systems (Ferretto et al. 2022).

### **Farm layout and site selection**

To optimize the long-term production of oysters, it is essential to consider the interactions between animal physiology, culture conditions, and farm-scale biophysical features of the farming site. Many studies researching oyster production fail to describe the overall layout of a farm site and the physical characteristics of that experimental site. The primary physiological functions pertaining to oyster growth (i.e. filtration, clearance rate, respiration) are directly affected by fluctuations in environmental conditions, such as temperature and salinity (Guzmán-Agüero et al. 2012). While oysters as a species live can inhabit a fairly large range of saline conditions (i.e. 5-30), the realized range at which a group of oysters can optimally perform is governed by their adaptation to their local environment (Proestou et al. 2016); hence, the relationship between growth and local environmental conditions is stronger when formed at the population level rather than the species level. Additionally, origin and temperature drive the gamete production in broodstock conditioning. Warmer conditioning waters significantly increase the proportion of mature gametes among adults (Chávez-Villalba et al. 2002). Similar

findings show that adult oysters are susceptible to high mortality events during heatwaves where temperatures exceed 30 degrees Celsius (Scanes et al. 2020). While salinity is a large indicator of oyster success, the ability of an oyster to perform in varying salinities is largely dependent on family history and origin, as their ability to tolerate changes in salinity is moderate to highly heritable (McCarty et al. 2020) and therefore will have varied affects from one genetic family to the next. The ranges of optimal salinity for oysters of various species and origins have been well researched (Bi et al. 2021, Wang et al. 2018); however, more work is needed to better understand optimal salinity ranges for oysters that live in both high and low salinity as well as those that live in areas with a dynamic range of salinity.

As suspension feeders, oysters rely heavily on the ambient physical environment for food delivery. Variation in water flow and direction forces oysters to adapt their feeding strategies and can influence filtration rates (Lenihan et al. 1995, Wilson-Ormond et al. 1997, Whalen & Stachowicz 2017) and, ultimately, productivity (Lee et al. 2017). Additionally the filtration and assimilation rate of food is also strictly correlated with the ambient environment and fluctuates in periods of physiological stress. While some studies on the relationship between oyster feeding activity and water movement, they lack consistency and are predominantly laboratory-based experiments (Campbell & Hall 2018); therefore, these studies often lack the dynamic range of environmental conditions found commonly in estuaries and, as a result, have limited ecological applicability. Of the field/model experiments conducted on wild reefs, oysters can alter the local movement of water significantly enough to influence carrying capacity (Liu & Huguenard 2020). This relationship likely applies to oyster aquaculture settings, especially with the presence of

cages that interfere with water motion and create alterations in the environment that would scale with farm size. Model studies of aquaculture gear demonstrated that oyster aquaculture gear alters water movement downstream by creating drag forces and attenuating water motion (Delaux et al. 2011, Gaurier et al. 2011). More field research is needed to understand how oyster aquaculture influences local hydrodynamics. Additionally, research to connect shellfish aquaculture production with these altered physical environments is crucial for future technology in this industry.

A major impediment to gear optimization research is the lack of tools capable of sampling physical conditions within the limited confines of aquaculture gear that is both affordable and rigid enough to be safely deployed for an extended timeframe. Interestingly, some techniques and tools used for marine research may apply to aquaculture studies. Clod cards may provide cost-effective estimates of relative mass transfer rate to characterize water movement (Muus 1968, Jokiel & Morrissey 1993, Thomas & Glenn 1994, Porter et al. 2000). Using clod cards, experiments could then be developed to understand how to optimally deploy cages to promote water flow, food delivery to suspension-feeding animals, and animal growth. Additionally, the movement of oysters and cages in the water has been rarely observed, especially in field applications. A small accelerometer such as the HOBO Pendant® G logger from Onset can observe the movement of oysters and cages over a continuous timeframe which may provide crucial data for optimizing gear use in new environments.

Numerous studies model environmental conditions using various approaches to enhance site selection for shellfish leases (Ross et al. 2013, Newell et al. 2013, Jiang et al. 2022). These

range in scale from within gear-level (i.e. Buitrago et al. 2005) to whole coastlines (Snyder et al. 2017, Newell et al. 2021). Several generalized models exist that allow for an input of environmental conditions to predict the production capabilities of a site (Silva et al. 2011, Hawkins et al. 2013). A standard method of site selection modeling uses Geographic Information System (GIS) to map specific geographic locations and use measured environmental and hydrodynamic data to determine site carrying capacity and production capability (Jiang et al. 2022, Newell et al. 2013, Buitrago et al. 2005). Others have applied a series of physical and biogeochemical models to predict aquaculture productivity along a more conceptual space (Ferreira et al. 2007). A model developed by Bricker et al. (2016) successfully utilizes a combination of these approaches to predict the potential production of several waterbodies within Long Island Sound, Connecticut.

Combining field and modeling techniques have been demonstrated when assessing the effects of water flow, food availability, and other factors on culture conditions within aquaculture structures, such as mussel long-lines (Stevens & Petersen 2011). Understanding the culture or environmental impacts of culture gear improves decision-making during farm design (Newell et al. 2014). While computational fluid dynamics (CFD) models described the water movement through rack-and-bag style cages (Delaux et al. 2011), more research combining field and modeling techniques is needed. A combined field and modeling study would be especially useful for understanding the orientation of oyster aquaculture structures and the physical changes that occur across a farmscape to enhance production further.

### **Future considerations**

As with most environmental entities, climate change trends are likely to influence the future of the oyster aquaculture industry. While the oyster has been argued to have enough plasticity to adapt to the predicted increases in temperature (Li et al. 2017), the exacerbation of hypoxia, added prevalence of disease, and increased intensity of storm activity, among other factors, will complicate the successful cultivation of shellfish. Perhaps the most vulnerable life stage to these effects is larvae. The production of oyster larvae is impacted slightly by water pH (Thiyagarajan & Ko 2012, Barton et al. 2014), although this is not a factor in some areas and likely varies by species (Gray et al. 2022). Hypoxic conditions negatively impact the development of post-settled oyster larvae, likely by reducing feeding rates; however, this is of less concern to adult oysters (Baker & Mann 1994), and research has suggested that adult oysters could mitigate local hypoxic and eutrophic waters (Yu & Gan 2021). Adult oysters are more robust to changes in pH and dissolved oxygen but are more vulnerable to interannual fluctuations of temperature and salinity, which cause physiological stress in the animals and can significantly influence production (Mizuta et al. 2012). To better understand the implications of climate change on oyster aquaculture, a model was constructed in Thau Lagoon, France, which predicted that harvests are sensitive to climate change effects and will result in growth losses and summer mortality events (Gangnery et al. 2004). These models help to provide adaptive strategies as environmental conditions change. Palmer et al (2021) speculated on the potential for growing oysters offshore in an offshore environment, there is more environmental stability; however, more research is needed to provide lease areas and understand the capabilities of this cultivation strategy.

The internal cage conditions inside oyster aquaculture gear deployed in the field are poorly understood. The lack of understanding within these systems could lead to false assumptions about the behaviors and possible stress of cultured animals, which may lead to inappropriate use of husbandry practices and reduce production efficiency. The limited understanding of internal cage conditions is likely due to a lack of identified, reasonably attainable tools designed to monitor the physical conditions inside these small areas that are also rigid enough to sustain long-term deployments in highly active environments. The conditions of finfish aquaculture nets have been studied extensively (Klebert et al. 2013, Chen & Christensen 2017, BI et al. 2018, Dong et al. 2020, Tsarau et al. 2021) and have demonstrated how changes in flow regimes within these structures have led to changes in animal behavior and production (Madin et al. 2010). It is reasonable to assume that there is an unquantified influence that physical forcing, such as water flow and turbulence, have on containerized oyster production. Further research is needed to understand how physical forces change within oyster aquaculture gear and what effect those forces have on oyster growth, quality, and aquaculture production.

To ensure that husbandry practices on oyster farms are economically practical, developing a bioeconomic model to optimize the labor and resources required to perform farm tasks given a range of environmental conditions could be a valuable tool for growers looking to optimize their grow-out operations (But see Hood et al. 2020, Hensey 2020, Parker et al. 2020). Such a model could help growers to optimize resource efficiency and make better management decisions about what husbandry practices they should employ. Several economic models have been developed for aquaculture (Martinell et al. 2019, Llorente & Luna 2016). Models have also

been developed to understand the effects of mortality (Girard & Perez Agundez 2014), scale (Ho et al. 2016), and use of on-bottom and off-bottom aquaculture (Engle et al. 2021). However, a model incorporating specific husbandry practices tailored to prevailing environmental conditions is unavailable.

## **Discussion**

The growing oyster aquaculture industry will be valuable in fulfilling the need for sustainable protein sources globally. A better understanding of the grow-out process will be a necessary step to ensuring a continued increase in production in a sustainable manner. Since the industry relies on ambient conditions, it is essential to focus future research efforts focus on understanding how the effects of husbandry practices on oyster production change in various biological and physical conditions. It is also important to consider how different oyster species and size classes respond to the environment while in culture.

Since changes in culture gear have varied influence on the effects of different husbandry practices and overall shell quality, understanding how culture cages and bags interact across varying environmental conditions and commercial uses will greatly improve shellfish quality and production by informing growers on the optimal uses, benefits, and limitations of each method. Additionally, culture equipment must be adapted to consider the region and specific oyster species. Growers commonly will rotate crops between a series of culture methods throughout the grow-out stage appears to help improve oysters' production however, there is little quantitative evidence to suggest how effective this procedure is on improving the growth and quality of oysters. Early-phase grow-out can focus on developing long and thicker shells (typically using

bottom cages) to reduce farm mortality, while the late phase can focus on growing meat (typically long-line or floating cages) to improve yield. However, more research is needed to better understand how this transition changes amongst different ambient environments and at different stocking densities and farm scales.

Current models for determining site selection and estimating productivity will continue to be necessary for optimizing the shellfish aquaculture industry; however, more research on validating these models, especially in areas with low salinity and/or high temperature, would be helpful to determine the potential areas for expansion. Low salinity and high-temperature regions may be more likely due to climate change effects, and the future expansion of oyster aquaculture will likely need to grow into these less optimal areas. Additionally, offshore shellfish aquaculture would allow for massive potential growth as leasing and zoning will be less conflicted with other stakeholders and are more likely to combat the effects of climate change. The only caveat potentially is food limitation, which requires even further consideration.

Research regarding the stocking density of oysters in current literature needs to provide a stronger consideration of carrying capacity, gear stocking density, and farm density. Research suggests that stocking density has either a negative or null effect on shellfish growth and survival. Additionally, since increased stocking density enhances overall farm profitability, it is crucial to understand the potential effects of stocking density when considering these factors. Similarly, the effects of biofouling on cultured oysters have also been well studied. However, there are contrasting results on the effect of biofouling organisms on culture equipment and oysters. Future studies should more strongly quantify fouling communities' species diversity and

richness and relate those metrics to a potential influence on oyster production. Additionally, an economic cost-benefit analysis of biofouling mitigation intensity versus overall production would be an invaluable tool for growers, as biofouling mitigation is labor intensive and is a high day-to-day cost for growers.

## Chapter 2: Modifications of plaster clod cards to monitor mass transfer rate for shellfish aquaculture systems in low-energy environments

### **Abstract**

The biophysical conditions within shellfish cages have not been characterized well partially due to a lack of technology. A novel clod card design was developed and tested for its use in measuring water flow through oyster cages for 4–12-hour deployments. Clod cards are made by mixing plaster of Paris and deionized water into 2.5 cm diameter spherical molds with an aluminum tether placed through the center. When formed, the cards were fit inside an aluminum bait cage used for protection. We tested the dissolution rate of plaster of Paris across a range of temperature (15 – 30 °C) and salinity (0 – 30 ppt) in a steady flow field to develop a predictive model used to convert units of dissolution rate (% mass lost/ hr) into units of velocity (m/s). The model predictions of clod cards deployed in the field were then compared to measurements of a nearby acoustic doppler current profiler (ADCP) to determine the accuracy of the predictive model. We also tested the clod cards in a series of small laboratory and field trials to understand the environmental limits of this clod card design. We determined that this clod card design was not effective in monitoring relative water flow among oyster aquaculture gear in low-flow environments because of the high range of error that occurs when using this sampling method. Additionally, producing a model to translate clod card dissolution rate to standard units

of velocity given known environmental parameters was not successful in field deployments. The poor predictability of the model in the field suggests that clod card measurements respond to the collective mass transfer through a system instead of strictly water velocity. As a result, noise in clod card dissolution is higher than the responding velocity in less energetic environments. While clod cards have been shown to be useful tools for measuring relative mass transfer in the past, further research is necessary to improve upon this design for use in oyster aquaculture systems and in low-flow environments.

## **Introduction**

Due to the expansion of shellfish aquaculture in recent years, the use of containerized gear to hold animals off the bottom of the water has become more common. The presence of nets, cages, floats, and other structural materials associated with aquaculture practices alter the ambient fluid dynamics by interacting with flow fields, resulting in reduced water velocity, and increased turbulent, drag, and shear forces (Liu & Huguenard 2020, Klebert et al. 2012, Grant & Bacher 2001, Folkard & Gascoigne 2009, Lin et al. 2016, Newell & Richardson 2014, Delaux et al. 2011). Biological influences, such as biofouling on cage structures, exacerbate the effects on the local flow regime (Bi et al. 2018, Claereboudt et al. 1994). It is possible to manage these biological factors by changing the orientation, scale, or dimensions of deployed equipment so that the effects of gear on the local flow regime are minimized (Gaurier et al. 2011, Richardson & Newell 2008). Such alterations have led to conclusions suggesting that specific gear deployments can improve feeding behavior in cultured animals (Duarte et al. 2014).

Understanding biophysical interactions associated with the culture of bivalves is essential since bivalves rely on ambient water flow to deliver food from the water column. Filter feeding bivalves require a specific range of water flow and turbulence to produce a feeding current that can successfully capture food particles. However, the range of optimal flow levels for feeding and growth for shellfish are inconsistent and not generally agreed upon (Campbell & Hall 2018). Additionally, while aquaculture structures influence local hydrodynamics (Stevens & Petersen 2011, Pilditch et al. 2001), it is uncertain how commercial production is affected by these changes.

Model and laboratory techniques are typically conducted to determine the effect of physical influences on the annual harvestable biomass of shellfish. Farm-scale production models, such as the FARM and AquaShell<sup>TM</sup> models (Ferreira et al. 2007, Silva et al. 2011) or the ShellGIS and ShellSIM models (Newell et al. 2013, Hawkins et al. 2013), generate an estimate of harvestable biomass by accounting for environmental parameters of a given farm then coupling these characteristics with biological growth models. While these models answer questions regarding production, site selection, and ecosystem service provision, they require extensive data to make accurate assessments that may not be available for a specific region. Additionally, they rarely consider the influence of gear types on the ambient environment or crop accessibility to the overlying water. The use of flume-based models (Gaurier et al. 2011, Folkhard & Gascoigne 2009, Grizzle et al. 1992) and computational fluid dynamic models (CFD) (Vo et al. 2018, Richardson & Newell 2008, Delaux et al. 2011) have also been widely used to describe changes in suspension feeding in response to a water flow gradient and changes

in hydrodynamic forces across culture gear. While these studies can draw basic conclusions on the effects between the equipment and the physical environment, they do not consider the fluctuations in flow and turbulence that characterize natural environments. Of the research conducted in situ that describes the influence of a bivalve farm on local conditions, acoustic doppler current profilers (ADCP) are typically used to characterize the physical environment upstream and downstream of a given farm (Turner et al. 2019, Xu et al. 2019, Liu and Huguenard 2018, Poizot et al. 2016, Stevens and Petersen 2011). These studies successfully monitor environmental conditions surrounding a farm space and adjacent areas but typically cannot monitor flow fields inside farms, only along the perimeter, as obstructions interfere with ADCP readings. This information helps to optimize farm orientation on a large scale but cannot address potential production changes within a farm.

While all the studies mentioned above help characterize the overlying eco-physical system of shellfish farms and the environment, an applied, in situ method of describing shellfish behavior inside culture gear is required. Internal condition of cages could vary substantially between farms due to irregularities in how cages may be stocked with crops or how densely packed cages may be positioned by growers. Additionally, optimizing growth conditions within cages is likely highly dependent on local environmental factors (e.g. food abundance & flow regime). Furthermore, previous research methods cannot fully capture flow dynamics due to fluctuations in cage conditions such as biofouling accumulation and changes in primary productivity across a growing season. The capability to cost-effectively measure small-scale physical interactions related to shellfish production will provide invaluable insight to shellfish

culturists looking to optimize production by informing management decisions specific to a grower's operation. To appropriately model small-scale physical processes in aquaculture, new and affordable tools are needed to monitor water flow inside cages to improve culture conditions and shellfish production.

Clod cards are a potential candidate for monitoring forces acting upon shellfish cages. Clod cards are easily adaptable apparatuses made from plaster or gypsum material that measure the mass transfer of material in a localized area. Early examples of clod card designs came from Muus (1968) and Doty (1971), using plaster of Paris in small molds (~30g) to monitor water exposure and motion through localized environments. In an attempt to increase the deployment time of cards, Kawai et al. (1982) attempted to increase the size of the cards. Adding new materials to clod cards, such as resin glue (Grovhoug 1978) or latex (Gerard & Mann 1979), extends deployment time by reducing the dissolution rate. Alternative materials to plaster can also effectively monitor mass transfer (Bartol et al. 1999). To improve the functionality and accuracy of clod cards, Jokiel and Morrissey (1993) advised that the dissolution of cards should not exceed 30% of the original mass, and environmental parameters will influence the dissolution rate. Thompson and Glenn (1994) further refined calibration standards for plaster dissolution and noted that still-water calibrations are ineffective for proper calibration. Lastly, Porter et al. (2000) highlighted that the energy level of the ambient environment could alter clod card dissolution rate, so calibrations need to consider the intensity of the sampling environment.

While past aquaculture research has utilized clod cards (Yokoyama et al. 2004, Wildish and Kristmanson 1997), modifications are needed to monitor water motion inside shellfish

culture cages over shorter deployments to properly monitor the water motion directly experienced by cultured shellfish without damaging the clod cards. In this study, we will discuss the development of a clod card specifically designed for use inside off-bottom shellfish aquaculture cages. Our design includes a 2.5 cm diameter spherical plaster card with a wire tether protruding through the center. The card is placed inside a protective cage to prevent chipping damage while deployed inside cages. Additionally, with parallel monitoring of ambient temperature and salinity, a calibration model will be constructed to convert the relative measurement of clod card dissolution (percent mass lost / hour) into a more widely applicable water flow measurement (m/s). We repeated this model using two methods to dry the cards after deployment, an air-dried technique, and an oven-dried technique. Through a combination of laboratory and field tests, we tested the characteristics of clod card dissolution concerning deployment time, ambient temperature, ambient salinity, and desiccation events. We will then produce a calibration model to convert relative dissolution rate to velocity and compare the accuracy of this clod card technique by comparing its ability to measure water flow to an Acoustic Doppler Current Profiler (ADCP).

## **Methods**

We will describe a procedure for constructing 2.5 cm diameter spherical clod cards inside shellfish aquaculture cages. A protective cage will surround the clod cards to prevent contact with shellfish inside the cages. We created a recirculating, linear flow tank in the laboratory that evenly moves water past cards at known velocities. In this recirculating system, we changed the temperature and salinity across a range of ambient conditions to better understand how

environmental conditions affect the dissolution rate of plaster of Paris in our clod cards. Using the known water velocity, temperature, and salinity, we also generated a series of predictive models to convert clod card dissolution rate into units of meters per second. Using the predictive model and laboratory studies, we then compared a commonly used ADCP and the clod cards to assess the accuracy of these tools in measuring water velocity. Since clod cards dissolve proportionally to turbulence as well, we conducted this comparison during times with low and high wave action to dissociate any effects of turbulent wave action on the dissolution rate of our cards. Lastly, we conducted a series of small experiments to test the capability of clod cards to respond to potential environmental changes such as tidal period, desiccation events, and the presence or absence of the protective cage. The cumulation of these tests will improve the interpretation of field measurements using these tools and highlight sampling periods or occasions where clod card deployments should not be performed.

#### *Construction and sampling procedure*

Use a 2.5 cm spherical ice tray with holes drilled into the center of each mold that can fit a twenty-gauge wire when forming the plaster spheres. The twenty-gauge fencing wire cut into 1.5 g sections was used to tether the clod cards to structures and secure them to its protective cage, which was placed inside each mold before filling. A 2:1 volume deionized water to plaster of Paris dry mix was used based on specifications from the “F-Type” design by Jokiel and Morrissey (1993). Quickly stir the mixture until homogenous and carefully fill each mold using a 50 mL syringe to prevent bubbles from forming inside the cards. After filling the molds, weight

was added to the top of the mold to ensure a consistent shape and left to rest at room temperature for 24 hours.

After setting the molds, cards can be removed and cleaned of any surface impurities to create a spherical shape. Any cards with surface defects, such as holes or cards that did not attach to the tether, should be discarded. The cleaned cards will rest for 24 hours before being weighed and ready to assemble and deploy. Place the cards inside a wire bait cage (45 mm diameter x 55 mm tapered height) to protect the clod cards from physical disturbances and secure them by attaching fishing weights to the tethers extending past the cage (Figure 1).



Figure 1: Our clod card design featuring a 2.5 cm diameter plaster of Paris sphere, the surrounding bait cage, twenty-gauge tether running through the center of the card, and fishing weights to secure the card in the center of the cage.

The range of linear dissolution occurs between roughly four to twelve hours for a clod card of this size, depending on the intensity of flow conditions. Deployed cards should not lose more than thirty percent of their original mass; otherwise, the dissolution will no longer be linear with time. During deployment, monitor the length of deployment, water temperature, and salinity. When completing a deployment, it is vital to remove all cards from the water within a

similar time (< 30 minutes) so that each card has the same amount of time to dry out before being weighed. After deployment, cards will be air-dried for 24 hours or placed in a drying oven at 60 °C for 24 hours. The drying will remove excess water from the card and likely negate the effects of ambient humidity on the water content inside the cards. Once the cards have rested, they can be removed from the wire bait cage and weighed again for final measurement.

Some initial computations were required to obtain final readings of the rate of dissolution. The initial and final mass of the clod card needs to be subtracted by 1.5 g to account for the weight of the wire tether (Eqn. 1). Given the corrected initial and final dry mass of the cards, total percent mass loss can be calculated (Eqn. 2), then divided by the time of deployment (Eqn. 3) to solve for the rate of clod card dissolution. This value represents the mass transfer rate of water through the surrounding environment relative to deployments associated with equal ambient temperature and salinity. To convert this reading to a universal metric of velocity (m/s), the dissolution values must be input along with ambient salinity and temperature to a predictive, multilinear model (Table 1).

$$\text{Eqn. 1: } m_{i,f} = m_{ia,fa} - 1.5g$$

$$\text{Eqn. 2: } d = \frac{m_i - m_f}{m_i}$$

$$\text{Eqn. 3: } dt = \frac{d}{t}$$

### Laboratory experiments

#### *Experimental flow field*

A laboratory linear flow field was constructed using a 200L head tank with either a chiller or heater to maintain the desired temperature (Figure 2). Water pumped from this tank into a 20L intermediate tank placed above a 100L raceway will flow through three holes in the intermediate tank into the upstream section of the raceway. The water then flows downstream through a set of straws, streamlining the flow in the experimental area of the raceway. The water then returns to the head tank, completing the circuit. One to four aquaria (21.5 x 40.5 cm) were added to the raceway to decrease the cross-sectional area by 21.5 cm per aquaria added and increase the velocity of water moving past the cards. These aquaria sat flush between the straws and the end of the raceway to minimize alterations in flow caused by the water bending around these structures. Clod cards were not deployed along the boundaries of the raceway walls to ensure that the velocity of water moving past each card was equal. Additionally, dye tests were performed in the raceway to ensure the water was properly streamlined before experimentation.

#### *Trend of plaster dissolution over time*

Clod cards are designed to dissolve linearly with water flow. The relationship of dissolution may change based on the characteristics of the card. This assessment looks to describe the rate by which this clod card design dissolves in flowing water. In our experimental tank, we deployed three clod cards every two hours to create exposure treatments at 0, 2, 4, 6, 8, 10, and 12 hours. Card deployment was staggered so that they could all be removed at the same time and have equal drying time under similar atmospheric conditions before being weighed. The change in plaster dissolution over each exposure time to characterize the rate at which these plaster cards dissolve in identical conditions.

Table 1: A list of symbols used in each equation, including a description of the symbol and respective units.

Symbol	Description	Units
$m_{ia}$	Initial mass of clod card with tether	g
$m_{fa}$	Final mass of clod card with tether	g
$m_i$	Initial mass of clod card not including tether	g
$m_f$	Final mass of clod card not including tether	g
$d$	Clod card dissolution	-
$t$	Deployment time	hr
$dt$	Clod card dissolution rate	hr <sup>-1</sup>
$A$	Cross sectional area of clod card	cm <sup>2</sup>
$\Delta C$	Concentration difference between the dissolved solid from the card to the ambient water	g/L
$k$	Mass transfer coefficient	L/cm <sup>2</sup>
$d_A$	Clod Card dissolution considering the change of shape throughout deployment	hr <sup>3</sup>
$T$	Water temperature	°C
$T_{ref}$	Reference water temperature	°C
$\mu$	Dynamic viscosity of water	Pa*s
$\mu_{ref}$	Reference viscosity of water	Pa*s
$d_T$	Clod Card dissolution considering the change of shape throughout deployment and standardizing temperature	hr <sup>3</sup>

*Effect of temperature and salinity on plaster dissolution rate*

Temperature and salinity have previously been found to significantly influence the dissolution rate of other clod card designs (Jokiel & Morrissey 1993, Thompson & Glenn 1994). We deployed clod cards at known flow rates (0.6 – 4.2 cm/s) in varying ranges of temperature (15, 20, 25, 30 °C) and salinity (0, 10, 20, 30 ppt) in an experimental flow field under controlled laboratory conditions. After monitoring the average dissolution per flow rate, temperature, and salinity, we produced a linear regression to understand the effect that flow, temperature, and

salinity have on the dissolution rate of this clod card design. We repeated this experiment for both the air-dried and oven-dried techniques.

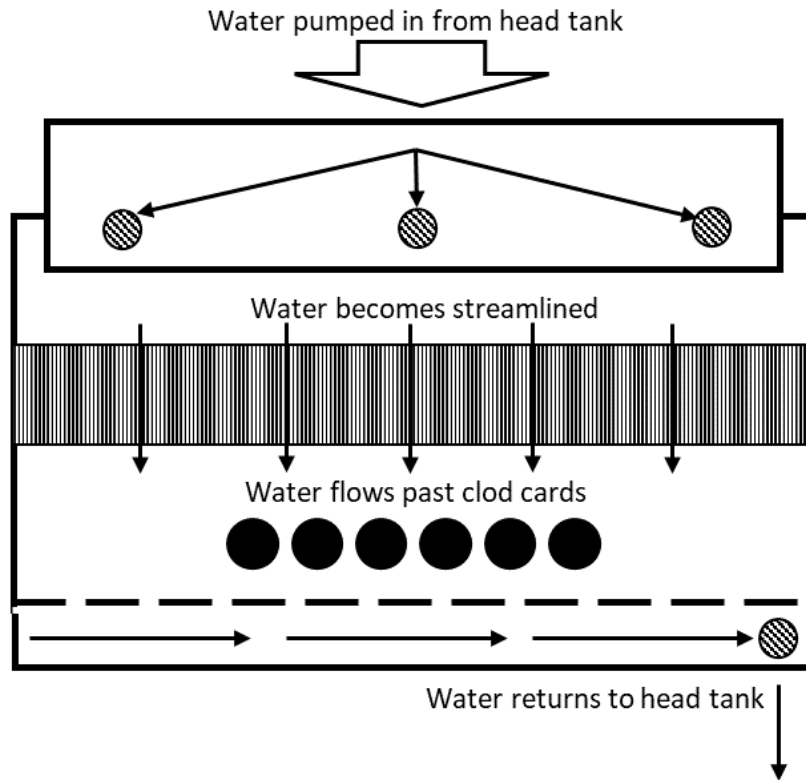


Figure 2: Diagram of the laboratory flow field used in the conversion model. Heated or chilled water from a head tank is pumped into a holding container above the raceway. This water pours into the raceway and runs through a closely packed bundle of straws (i.e. honeycomb) to diffuse turbulence and streamline water flow. Water then passes by the cards, drains, and is recirculated back into the head tank.

*Predictive model to convert plaster dissolution to water motion*

We conducted a calibration study to inform a model capable of predicting ambient flow conditions based on ambient conditions and the rate of plaster dissolution. Triplicate

deployments of clod cards (n = 58) were conducted in our experimental flow field across a range of known temperatures, salinities, and flow velocity using a gravity-fed, laminar flow field for six hours. We replicated the experiment for both the air-dried and oven-dried techniques. We then took the average response in plaster dissolution from the triplicate deployment as a function of temperature and salinity to produce a mixed linear effect model (MLEM) and a log-transformed, generalized linear model (log-GLM). Additionally, we compared the raw dissolution and environmental data to a series of modifications by Thompson and Glenn (1994). For both transformations, the mass transfer coefficient of the plaster sphere,  $k$  (Eqn. 4), needed to be calculated. The first modification considers the reduction in the surface area of the plaster sphere (Eqn. 5). Equation 5 describes the modified dissolution rate  $d_A$ , where  $\Delta C$  is the concentration difference between the dissolved solid immediately surrounding the surface area and the ambient water, taken from figure 5 from Thompson and Glenn (1994). The second dissolution rate adjustment,  $d_T$ , considers the standardization to a reference temperature using ambient temperature,  $T$ , and the dynamic viscosity of saltwater,  $\mu$  (Eqn. 6). To provide validity, all model variants were tested and compared for their ability to predict flow velocity given known plaster dissolution rates, temperatures, and salinities. The best performing models were then compared to the experimental data to determine overall model fitness.

$$\text{Eqn. 4: } k = \frac{1 - \left(\frac{m_f}{m_i}\right)^{-3}}{2 * \left(\frac{A}{m_i}\right) * \Delta C}$$

$$\text{Eqn. 5: } d_A = 1 - \left[1 - \left(\frac{1}{3} k * \frac{A}{m_i} * \Delta C t\right)\right]^3$$

$$\text{Eqn. 6: } d_T = d_A * \left(\frac{T}{T_{ref}} * \frac{\mu_{ref}}{\mu}\right)^{-1}$$

## Field experiments

### *Comparing predicted clod card measurements to an ADCP*

A side-by-side comparison was conducted to compare the clod card's ability to estimate velocity with other currently established methods. We deployed a 2 Mhz Nortek™ Aquadopp Acoustic Doppler Current Profiler next to a vertical profile of clod cards using the air-dry method to compare the similarity in measurements between sampling methods. We deployed both devices for eight hours, and the average flow velocity at 30, 50, 70, and 90 cm depth bins were recorded and compared (n = 28). Similar readings from the clod cards and the ADCP would provide evidence that this clod card design is an accurate method of measuring velocity in the field.

### *Influence of tidal cycle on clod card accuracy*

Since tidal fluctuations alter local water movement on a time scale similar to the clod card deployment time, we conducted a trial to determine how the tidal cycle influences the accuracy of clod card measurements. We also aimed to find a range of deployment lengths that would be robust against changes in tide over the sampling period. Triplicate cards were deployed at time zero at high tide for six hours. Every following hour, we deployed another replicate of cards for six deployments to model the tidal cycle fully. This experiment utilized the air-drying technique for desiccating cards to be weighed.

### *Influence of protective cage surrounding clod cards*

It was uncertain whether the presence of the cages surrounding the clod cards influences the dissolution rate of clod cards. Clod cards were deployed with and without cages (n=21) over a range of flow rates to determine any significant changes in plaster dissolution in various flow conditions. This experiment utilized the air-dry technique for desiccating cards to be weighed.

## **Results**

This research intended to better understand the characteristics of a novel clod design and determine its capability for use in aquaculture research. Through a series of small-scale studies, we addressed the dissolution rate of clod cards over time, the influence of temperature and salinity, and the effects of desiccation events to describe behaviors of clod card dissolution during changing environmental controls. We developed a mixed linear model to predict ambient water motion based on ambient salinity and clod card dissolution rate. We then tested the model's ability to predict water flow. We compared the model with readings from an established water flow monitoring tool to determine whether clod cards are practical tools for monitoring water velocity in shellfish aquaculture.

### *Trend of plaster dissolution over time*

There was a significant linear relationship between the dissolution of clod cards across the entire time series ( $r^2 = 0.9177$ ,  $p < 0.001$ ). The rate at which these cards dissolve may begin to lose linearity after losing roughly 25 percent of their mass. The linear relationship of clod card dissolution, excluding the cards that exceeded 25 percent dissolution, strengthens the linear correlation ( $r^2 = 0.9690$ ,  $p < 0.001$ ) (Figure 3).

Effects of water flow, temperature, and salinity on plaster dissolution rate

For the air-dried technique, there was a significant linear relationship between water flow and salinity ( $p = 0.004$ ,  $p = 0.032$ , respectively). Under the range tested in our experiments, the temperature did not significantly influence the dissolution rate of the air-dried cards ( $p = 0.130$ ). The dissolution rate of the oven-dried cards was significantly influenced by water flow, salinity, and temperature ( $p = 0.002$ ,  $p = 0.001$ ,  $p = 0.019$ , respectively). The dissolution rate had a positive linear relationship with water flow and a slightly negative linear relationship with salinity for both clod card techniques. The effect of temperature appeared to change depending on the technique used. The oven-dried clod cards appeared to be less influenced by temperature. In contrast, the dissolution rate of air-dried cards appeared to be heavily positively correlated with temperature, although this relationship is not statistically significant (Figure 4).

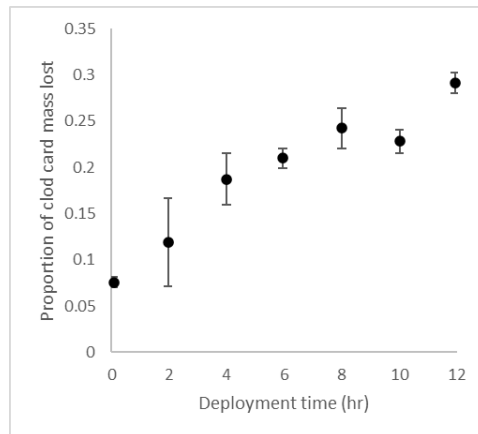


Figure 3: Strong linear correlation exists between the dissolution of clod cards and the length of the deployment time until roughly 25 percent total dissolution.

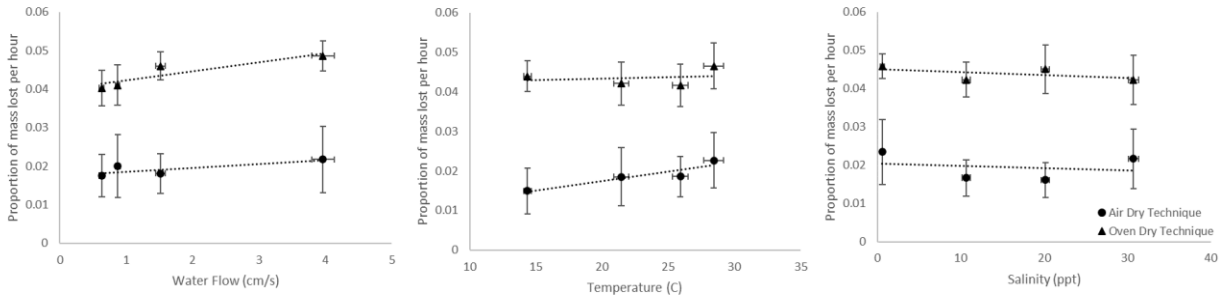


Figure 4: Linear relationships between clod card dissolution and water flow (left), temperature (center), and salinity (right) for both the air-dried (circle) and the oven-dried (triangle) desiccation techniques.

### Predictive model to convert plaster dissolution to water motion

The oven-dried clod card technique offered higher overall predictability than the air-dried method when comparing the coefficient of determination and the model AIC values (Table 2).

The shape and temperature adjustments improved the  $R^2$  of the model fit for the air-dried technique and had similar predictability during the oven-dried technique. The applied log-GLM appeared to be more effective in predicting water flow than the MLEM. When comparing each of the six model runs for the air-dried technique, the log-GLM model considering both the rate of change of the surface of the card and the standardization for the temperature to 20 °C, had the most optimal predictive power (AIC = 100.02,  $R^2 = 0.79$ ) (Figure 5). For the oven-dried technique, the log-GLM model, only considering the rate of change of the card's surface, had the highest predictive power (AIC = 90.69,  $R^2 = 0.83$ ). In both models, there is a slight overprediction at higher velocities and underprediction at intermediate and low velocities that could be stressed when applied to a broader range of flow velocities (Figure 6). While all model

runs have reasonable predictability based on statistical evidence, the range in modeled measures of water velocity spans nearly 50% of the range of water velocities analyzed during this experiment, indicating a large range of error across the predictive model at these water velocities.

Comparing predicted clod card measurements to an ADCP

Clod cards deployed in tandem with an ADCP across several vertical profiles in the Choptank River showed little to no overlap in the measurements taken (n = 28). Considering all the model runs trialed, the clod card measurements were not statistically similar to the ADCP measurements (Students T-Test, p < 0.001). The clod card data overestimated the environmental measurements and showed little change in velocity predictions across the known range from the ADCP measurements. Figure 7 highlights four of the six model runs. These model runs had the most comparable results compared to the ADCP data.

Table 2: Summary of all predictive models ran using the calibration data collected in a controlled laboratory setting for both the air-dried and the oven-dried desiccation technique.

Technique	Model	Adjustments	AIC	R <sup>2</sup>
Air-Dried	MLEM	Raw	127.74	0.57
Air-Dried	MLEM	Shape	127.74	0.57
Air-Dried	MLEM	Temperature + Shape	121.24	0.64
Air-Dried	Log-GLM	Raw	154.59	0.55
Air-Dried	Log-GLM	Shape	106.27	0.76
Air-Dried	Log-GLM	Temperature + Shape	100.02	0.79
Oven-Dried	MLEM	Raw	106.96	0.74
Oven-Dried	MLEM	Shape	110.83	0.72
Oven-Dried	MLEM	Temperature + Shape	122.25	0.61
Oven-Dried	Log-GLM	Raw	129.08	0.74
Oven-Dried	Log-GLM	Shape	90.69	0.83
Oven-Dried	Log-GLM	Temperature + Shape	107.94	0.75

### *Influence of tidal cycle on clod card accuracy*

The dissolution of plaster deployed for six hours throughout a semi-diurnal tidal cycle was robust against the tide period. The trend of plaster dissolution over time remained constant when averaged over the six-hour period and did not reflect the low-frequency waves associated with the tidal pattern (Figure 8).

### *Influence of protective cage surrounding deployed clod cards*

Using a bait cage to protect clod cards was not found to significantly alter the dissolution rate of plaster media ( $P = 0.711$ ). Across a range of dissolution proportions, there was a strong linear correlation, near 1:1, between cages deployed with and without cages (Figure 9). Given this result, it is possible to deploy this type of clod card with or without a protective case depending on the application while still retaining comparable measures of clod card dissolution.

## **Discussion**

The modified clod card design is not a practical tool for monitoring water movement inside aquaculture gear. This clod card design has a close linear dissolution rate with time until more than thirty percent of the mass has been lost, as suggested by Jokiel and Morrissey (1993). The dissolution rate was also not affected by the presence or absence of a protective cage, which allows for additional customization in future applications. The dissolution rate of clod cards appeared to range greatly within experimental treatments conducted in low flow environments (0 – 4 cm/s) despite evidence which suggests much higher predictability at higher flow velocities (5 – 100 cm/s, Jokiel & Morrissey 1993, Thompson & Glenn 1994) hence, we conclude that this

design, in its current state, was unsuccessful in measuring water motion in low flow environments. It is likely that the noise that exists within clod card measurements at low flow velocities is too high compared to the measured flow velocity and therefore cannot sample accurately. Additionally, developing a model to convert clod card measurements to more widely applicable units was only moderately successful in laboratory applications. More development on the use of this technique is required to be capable of accurately measuring relative mass transfer rate. If performed correctly, clod cards can be utilized as a highly cost-effective tool for commercial shellfisheries who wish to gain initial insight into the relative mass transfer of material through their cages. Mass transfer rate refers to the relative exposure of material being removed from an area.

Since monitoring the turbulence of a local watershed requires specialized training and is costly, it was likely not a procedure that would be available to aquaculturists, who are the target audience of this study. The dissolution models and laboratory tests assume that turbulent forces are constant with water flow. This assumption is likely the reason for the poor agreement between the clod card and ADCP measurements. The dissolution rate of this card is subject to change with turbulent conditions, such as wave action. This assumption violates the suggestions made by Porter et al. (2000) that cards need to be calibrated in a similar environment as the test site. In our attempt to convert clod card dissolution to water flow, we used a streamlined flow across a range of temperature and salinity. The generated model results will overestimate the water flow in more turbulent conditions and likely worsen with faster flow speeds. The comparison between the sampling methods would likely agree better in a controlled laboratory

setting. Additionally, since we conducted laboratory experiments in a device that produced a linear current, laboratory studies were not accounting for the potential for water to flow in all directions, as would be more characteristic of the field testing, resulting in another potential source of error that influenced the lack of predictability in our calibration model when compared to established tools.

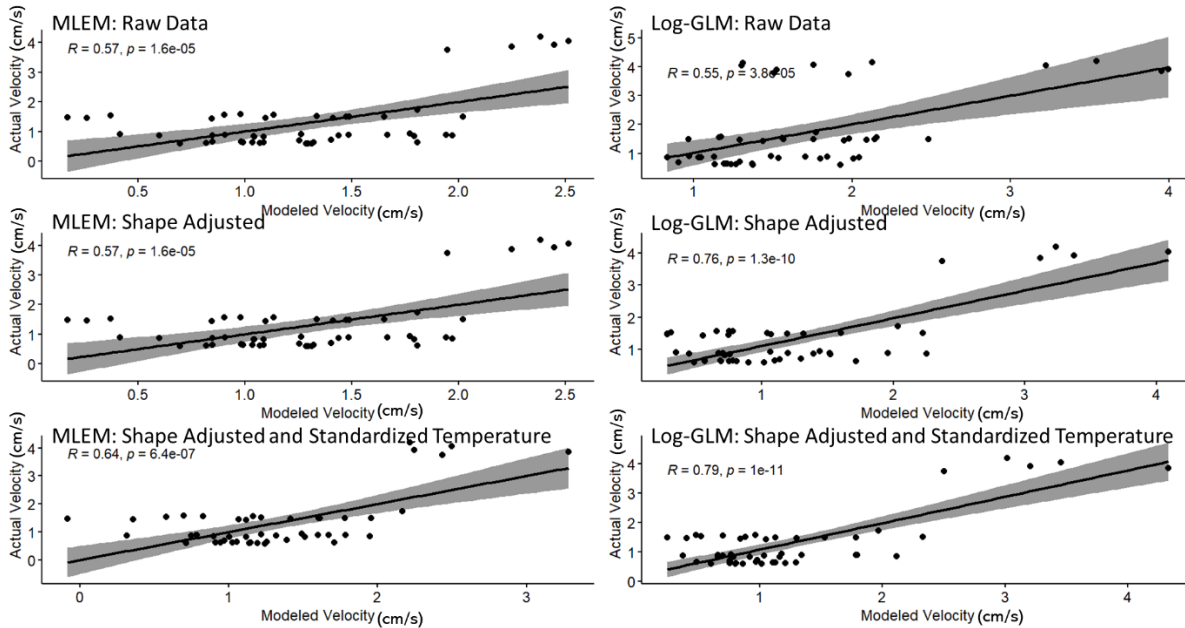


Figure 5: Comparison between the known and predicted water velocity using the predictive clod card model on the air-dried technique. Both MLEM (left) and Log-GLM (right) models were applied to the raw data (top), transformed data considering the rate of change of the clod cards' shape over time (center), and a combination of the shape transformation and standardization of temperature to 20 °C (bottom). Each figure shows a coefficient of determination, p-value, and a 95 percent confidence interval.

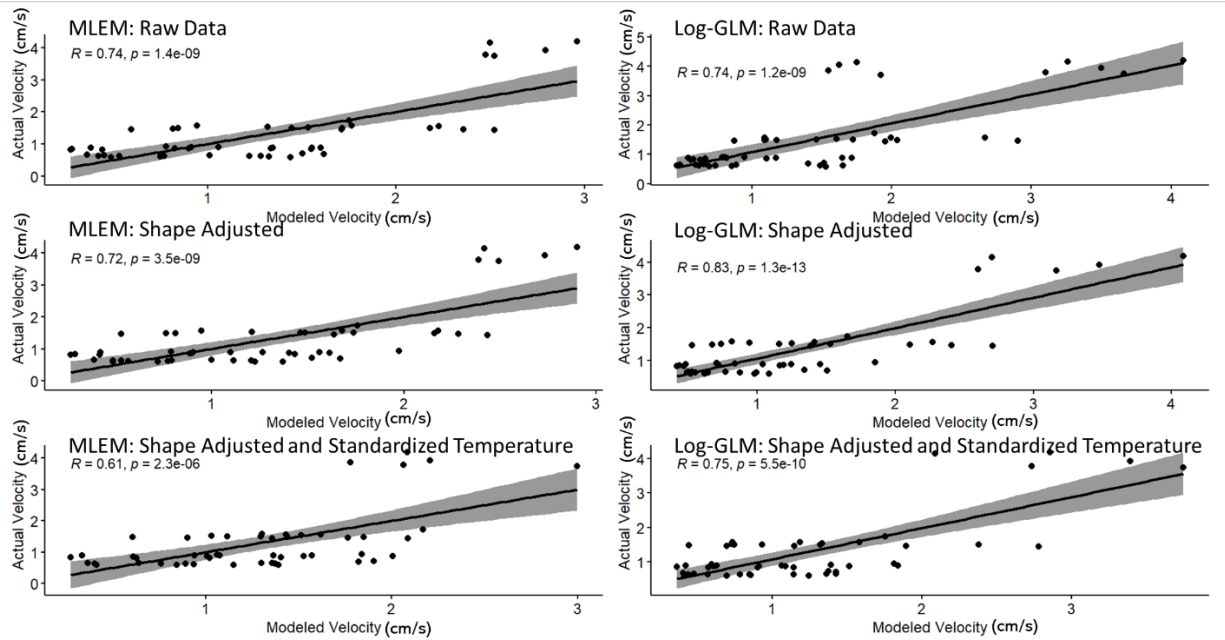


Figure 6: Comparison between the known and predicted water velocity using the predictive clod card model on the oven-dried technique. Both MLEM (left) and Log-GLM (right) models were applied on the raw data (top), transformed data to consider the rate of change of the clod cards' shape over time (center), and a combination of the shape transformation and standardization of temperature to 20 °C (bottom). Each figure shows a coefficient of determination, p-value, and a 95 percent confidence interval.

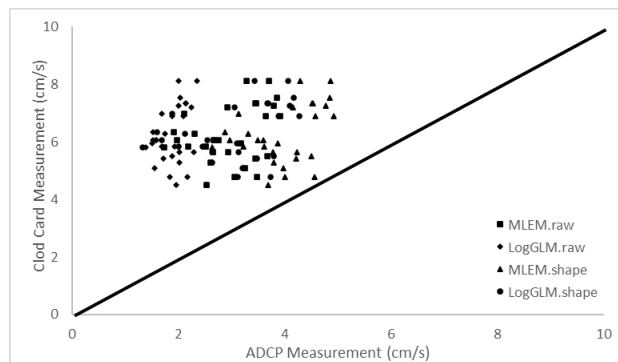


Figure 7: Model predictions of clod card velocity measurements using the air-dried method compared to measurements taken by a 1 MHz Nortek Aquadopp Profiler (ADCP). We included the four most accurate model predictions in this figure. We did not include the other two models due to considerable disagreement from the ADCP measurements.

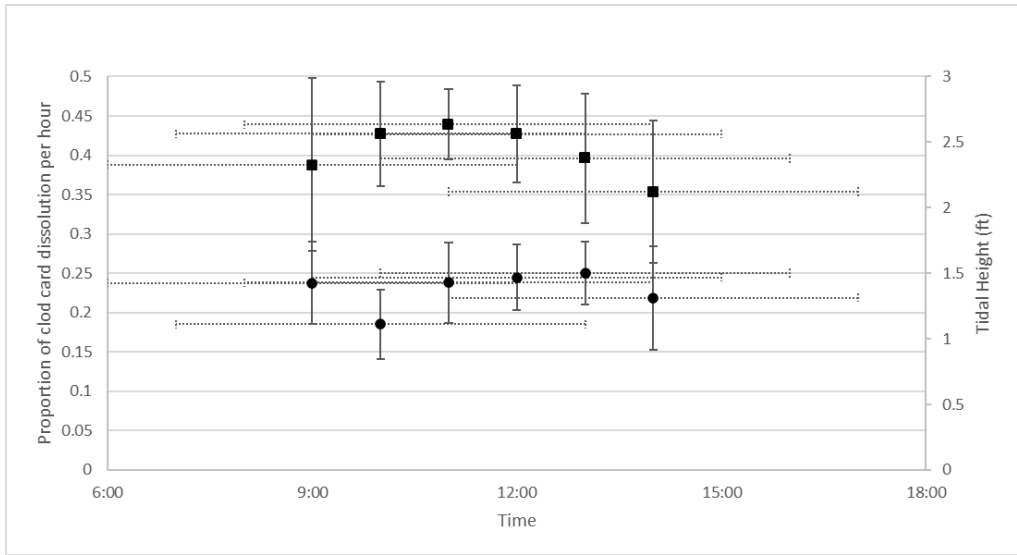


Figure 8: Dissolution of clod cards (circle) deployed in six-hour lengths across half a tidal cycle. Tidal height was monitored hourly and averaged every six hours to match the time the cards were deployed (square).

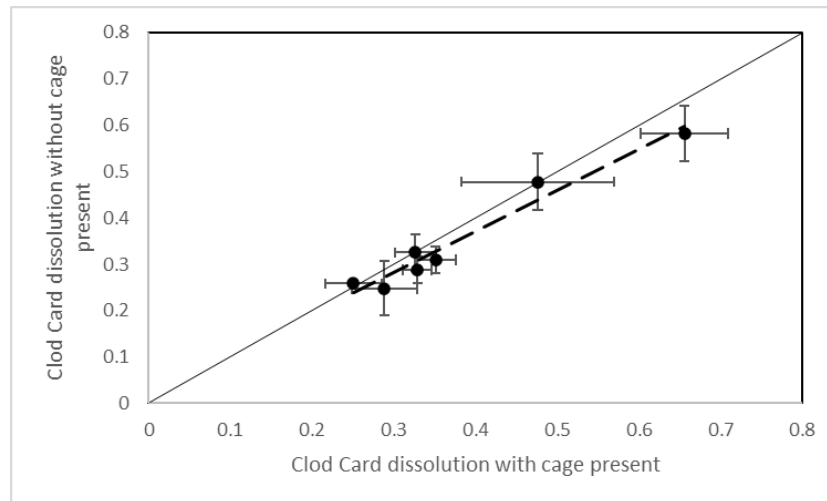


Figure 9: Strong linear correlation between protected and unprotected clod cards.

The oven-dried technique showed to have more accurate predictions of the laboratory treatments than the air-dried technique. While the oven-dried technique is more precise, the air-

dried technique requires less equipment and might be more applicable for commercial operations. Considering the change in surface area and standardizing temperature when producing the predictive model based on Thompson and Glenn (1994) improved the overall predictability of the model with the laboratory data for both card drying techniques. However, when applying the models to field data, the model runs, considering both the shape adjustments and temperature standardization, produced unreasonable velocity predictions. This study did not fully consider the potential effects that ambient humidity might have on the initial and final weight of not oven-dried cards. While we did not consider this during experimentation, ambient humidity might have influenced the initial weight of the cards for both methods. Future versions of this method should attempt to use an oven drying technique before the weighing and deployment of cards and after deployments so that the initial weight of the card is not affected by the humidity where the cards are stored.

Despite the short deployment time, the clod card measurements are robust against tidal forces and other low-frequency waves. As a result, cards can be deployed at any point in the tidal cycle for six hours without generating error due to tidal processes. However, in locations where tidal height ranges more than one foot, dissolution of plaster might be more affected by the larger forces associated with more extensive tidal ranges. The study site we used to test the tidal effects on clod card dissolution rate has a characteristically low tidal range. More experimentation would be needed to test the effects in areas with more extensive tidal ranges.

Further improvements to the clod card predictability model are necessary for its use in field research. Incorporating the effect of turbulent forces on clod card dissolution would make

noticeable improvements to the model predictability in field applications. While the presented model was ineffective for predicting water flow in standard units during field applications, there is still a strong need for affordably monitoring water flow in aquaculture operations.

## Chapter 3: Biofouling treatment on long-line cages alters the growth strategies of cultured eastern oysters by affecting cage motion

### Abstract

Efficient aquaculture production of *Crassostrea virginica* requires the optimization of grow-out techniques to ensure cultured oysters' high growth and quality. Biofouling on oyster long-line cages, which can limit flow and reduce animal growth, is typically controlled by various methods to either desiccate (expose to air) or directly wash fouling organisms from cages. These biofouling treatments are thought to ensure high water flow and production rates and offset any labor and resource costs associated with added cage maintenance. However, the effectiveness of these treatments on internal cage conditions and resulting production are poorly understood. Tools to understand the physical forces acting upon cages were applied to understand the effects of fouling treatment on the production efficiency of cultured oysters in a two-month study (June–August 2019) conducted at the Horn Point Laboratory Demonstration Farm in the Choptank River of the Chesapeake Bay. We monitored cage motion and several production parameters (tissue growth, shell growth, and condition index) to determine the effect of biofouling species on production. This study used three fouling mitigation techniques (24-hour desiccation, weekly power washing, no treatment) and three commercial long-line cages (Seapa™, BST™, Hexcyl™) to determine how fouling treatment, cage style, and internal

physical cage conditions influence oyster production rates. Cage jostling was significantly affected by treatment. Additionally, cages treated for fouling had a significantly lower average shell length yet significantly higher condition index at the end of the field trial. This study introduced monitors that can monitor physical forcing inside oyster aquaculture gear to allow for the further optimization and profitability of oyster aquaculture operations. Interestingly, the significant differences in shell growth and condition index of oysters between treatments also indicated that aquaculturists should consider selecting a fouling mitigation technique tailored to their targeted half-shell or shucked market.

## **Introduction**

The culture of the eastern oyster, *Crassostrea virginica*, has developed significantly over the past several decades regarding annual harvest, economic growth, and educational investment (FAO 2020). Parallel to the commercial development in this industry, there has been an increased number of peer-reviewed publications in oyster-focused research, with a noticeable proportion being aquaculture-based (Guo et al. 2016). Despite the increased recent attention toward developing oyster aquaculture, little research addresses the biophysical interactions between cultured oysters and the immediate physical environment.

As suspension feeders, oysters require a specific range of water flow to capture and ingest food particles from the environment (Grizzle et al. 1992, Wilson-Ormond et al. 1997). A small change in flow or turbulence can create an unsuitable feeding environment for cultured species. While several studies have attempted to determine the suitable flow range that promotes suspension feeding activity in bivalves (Ehrich & Harris 2015, zu Ermgassen et al. 2013, Harsh

and Luckenbach 1999, Claereboudt et al. 1994), their results are inconsistent and do not consider potential influences of cages on physical forcing under dynamic field conditions (Campbell & Hall 2018, Powell et al. 1992, Lenihan et al. 1996). Inconsistencies in these studies are likely due to the location of the study and the ambient hydrodynamic conditions of the test site. Studies on other suspension feeders suggested that feeding behavior depends on hydrodynamic conditions (Lee et al. 2017, Newell et al. 2014, Vo et al. 2018).

Quantifying internal cage conditions represents a fundamental starting point for gear optimization that, when scaled to farm-level, could be reasonably expected to improve production and farm profitability. Indeed, understanding finfish pen hydrodynamics has helped improve culture sustainability by preventing anoxia in pens, but these studies also indicate that physical forces require greater consideration in future pen design (Dong et al. 2020, Klebert et al. 2013, Xu et al. 2019, Chen & Christensen 2017). Similarly, monitoring physical forces among shellfish cages should help discern the potential impacts of biological phenomena on flow, such as the settlement of fouling organisms on caged oysters.

Biofouling on culture cages prevents adequate water flow into cages and can limit food availability (Beristain & Malouf 1988, Ross et al. 2002). Excess biofouling can also impede growth in oysters and other bivalves (Mallet 2009, Ross et al. 2002, Wildish & Kristmanson 1997). Additionally, it is possible that waste material, such as ammonia, could accumulate in cages with high biofouling coverage if the flushing rate is low relative to the waste generation rate. Despite recent developments in biofouling research for aquaculture gear, information is

lacking about biofouling effects on caged bivalve growth and production or whether different fouling mitigation practices alter the physical forces experienced by these crops.

This study aimed to compare standard fouling mitigation practices (power wash, desiccation, no treatment) on the oyster morphology and condition within different commercial long-line cages (Seapa, BST, Hexcyl). By comparing three types of long-line cages and three mitigation techniques for biofouling, we sought to understand how changes in the biofouling mitigation approach influenced the physical forces acting upon aquaculture cages and, ultimately, oyster production.

## **Methods**

Natural diploid oysters raised under identical conditions were deployed at the Horn Point Laboratory Demonstration Oyster Farm (Horn Point Laboratory, Cambridge, MD) from June to August 2019 at average initial shell lengths of 35.8 mm +/- 0.5 mm. We treated triplicate cages for fouling in three ways: 24-hour desiccation once per week, power washing cages once per week, and a non-treated control. We compared three common commercial cage types (Seapa, BST, Hexcyl) in each fouling treatment. Cages were then monitored twice a month for the percent surface fouling in addition to cage movement among other environmental parameters (temperature, salinity, dissolved oxygen, pH, turbidity, chlorophyll A). Oyster performance, defined as oyster growth, dry weight, and condition index, was recorded at the end of the two-month study period.

## Study area

Field experiments were conducted at the Horn Point Demonstration Farm (Horn Point Laboratory, Cambridge, MD) between June and August 2019. The farm sits next to a (90 x 23 m) pier within the Choptank River, a major tributary of the Chesapeake Bay, which is considered a highly productive, eutrophic estuary (Kemp et al. 2005) (Figure 10). This area has a depth between one to two meters depending on tidal fluctuations and typically has a salinity ranging between 8 – 12 ppt. Given the pier and a nearby jetty, this area was mainly protected from the dominant currents during the study period and can be characterized as a low-energy environment with a homogenous flow rate typically not exceeding 10 cm/s.



Figure 10: Aerial map of the Horn Point Demonstration Farm, Choptank River, Chesapeake Bay, MD, US. Key features include the jetty and dock directly north of the lease space, reducing natural water flow to this area. The black square outlines the long-line systems on the farm. The blue line (closest to the pier) is where the control and power washed groups were placed during the experiment, while the purple (second from the pier) held the desiccated cages. The yellow lines were not used in this experiment but contained fully stocked oyster cages.

### Sample design

Three commercial cage types (i.e., Seapa, BST, Hexcyl) were sampled for each fouling treatment to show the potential effects that cage style had on biofouling accumulation and oyster performance. The Seapa and BST cages were 12 mm mesh and 15-liter volume cages, while the Hexcyl baskets were 15 mm mesh and 25-liter volume cages. The total open area of the Seapa, BST, and Hexcyl baskets are 127, 117, and 225 mm<sup>2</sup>, respectively. The Seapa and Hexcyl baskets have square pores, while the BST cage has hexagonal pores.

The oysters used in this experiment were from a diploid brood produced by the Horn Point Laboratory Oyster Hatchery and are considered wild oysters (Hornick & Plough 2022). They had been grown in identical conditions and graded to an average shell length of 35.8 mm (range 25-45 mm) before experimentation using a commercial sorting tumbler. We stocked each cage at 20 % of the total volume of the cage (3 L for BST and Seapa, 5 L for Hexcyl cages).

Cage fouling treatments followed standard methods used by growers. The desiccation treatment involves a 24-hour desiccation period once per week. To desiccate cages, we lifted the entire line above the maximum tidal range to be fully exposed to the air for 24 consecutive hours on days with low cloud cover and no rainfall. The power washing treatment consisted of bringing the cages to shore and spraying the cages (with oysters inside) with a 2000 PSI power washer to remove nearly all fouling from the external surface of the cages and some fouling from the oysters. Lastly, a group of cages were left continuously in the water and not treated for fouling.

We deployed oyster cages across two long-line systems, one line held the desiccated treatment, and the other held power washed and control treatments (Figure 10). Lines are secured on either end by 12” diameter pilings and supported along their 37-meter length by PVC riser posts outfitted with clips to distribute the weight of the line and ensure the baskets remain at a fixed position above the seafloor (~1 m). Both lines were arranged at the same height from the bottom and had the same potential exposure to tidal desiccation, which occurred on most low tides. These lines were parallel and spaced approximately five feet apart. Cages were arranged randomly across each line, and the arrangement of cages was redistributed randomly at least once weekly throughout the experiment.

#### *Biofouling coverage*

Biofouling was monitored bi-weekly by assessing the percent fouling coverage on the surface of the cages using methods adapted and modernized from Underwood & Anderson (1994). For a more quantitative result, we took pictures of a section of each cage. We used the image analytical program, ImageJ, to determine the percent of the white background shown in each image along with a scale for a reference to standardize the dimensions. Additionally, photographs were taken at the same time of day, three inches above the cage in the exact sample location on the top of the cage, to standardize the scale between photos. We compared images to clean baskets to act as a blank reference (Figure 11).

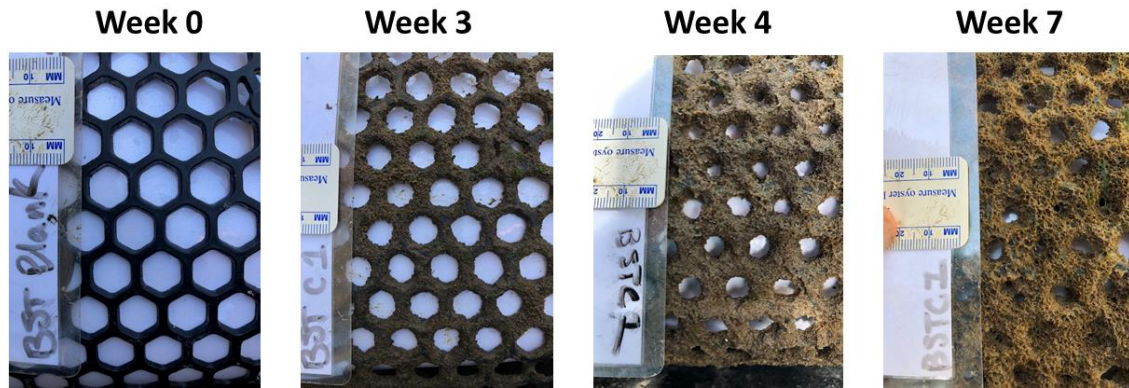


Figure 11: Sample of pictures taken to monitor biofouling accumulation rate. The percent of white space behind the cage will be used to derive biofouling coverage using Image J software.

### Physical forcing

Cage and oyster jostling was measured using accelerometers (Onset HOBO Pendant G Logger: UA-004-64), roughly the size and weight of adult oyster wet tissue (50 mm x 30 mm x 15 mm, 21 g). Accelerometers monitor the simulated three-dimensional displacement and velocity of the cage it is in, plus the motion experienced by one oyster. Devices were tethered to one replicate per cage type and mitigation treatment and left to move freely throughout the cages for the duration of the experiment. The measurement taken will describe the relative movement of one oyster inside of a cage plus the motion of the cage itself. We removed jostling data from all treatments during periods where at least one treatment was out of the water or being handled throughout the experiment.

### Environmental monitoring

Environmental conditions were monitored continuously throughout the experiment. Using a YSI EXO2 multiparameter sonde deployed at the end of the pier along the northwest

side of the study site, we monitored multiple environmental factors such as temperature, salinity, dissolved oxygen, turbidity, and chlorophyll-a. To track natural periods of desiccation among cages, we deployed a modified Stream Temperature, Intermittency, and Conductivity logger (STIC) (Chapin et al. 2014). After the experiment, an ADCP was used to determine the homogeneity of flow across the sample site to discern any unusual local flow patterns within the sample site that may alter the results.

### Oyster performance

Oyster performance was measured by assessing the final growth of individual oysters per treatment. We measured the shell length, width, depth, and dry mass of 30 random oysters per cage. Additionally, the condition index was estimated according to the specifications of Lawrence and Scott (1982) to show the ratio between dry tissue and shell mass per treatment (Eqn. 7). The condition index is a ratio that is commonly used to estimate the relative quality of tissue development in oysters and correlate positively with the value of an oyster's value.

$$\text{Eqn. 7: } CI = \frac{\text{dry tissue weight (g)} * 100}{\text{dry shell weight}}$$

### Statistical analysis

Since most of the data did not have normal distributions according to the Shapiro and Levene tests for normality and could not be corrected using standard data transformations, we primarily used non-parametric statistical approaches during analysis. We performed Kruskal-Wallis tests with Scheirer-Ray-Hare Adjustments to assess the statistical significance between

fouling treatments and cage style. Of the significant comparisons, a post-hoc Dunn test with a Bonferroni correction was used to test for statistical significance between respective treatments for the ammonia concentration and oyster shell sizes. We performed mixed linear effect models for measurements with unequal sample sizes, such as condition index and fouling coverage rate. General additive models were used to explain fluctuations in trends of jostling for each treatment and cage type. All statistical metrics were based on an alpha value of 0.05.

## **Results**

This research evaluated the effects of biofouling, biofouling mitigation, and cage conditions on the physical environment, and oysters grown in long-line cages. Prior to this work, there has been scant research to assess how the biofouling accumulation on long-line cages influences local physical forcing and oyster morphology. By growing oysters for two months in different cage styles and treating them for fouling using various techniques, we attempted to monitor how waste accumulation and cage jostling changed and assess how the altered physical environment changed the oyster growth and performance.

### *Environmental monitoring*

During the experiment, the experimental location experienced noticeable fluctuations in salinity (6-10 PSU) and water temperature (27-33 °C). Mean atmospheric temperature ranged between 20-32 °C throughout the season and experienced an average 9.6 °C daily fluctuation (NOAA/NCEI). Tidal desiccation caused all cages to be out of the water for a total of 113 hours

(10.8 %) throughout the experiment. The desiccated treated cages were out of the water for 248 hours (20.2 %) between tidal and manual desiccations (Figure 12).

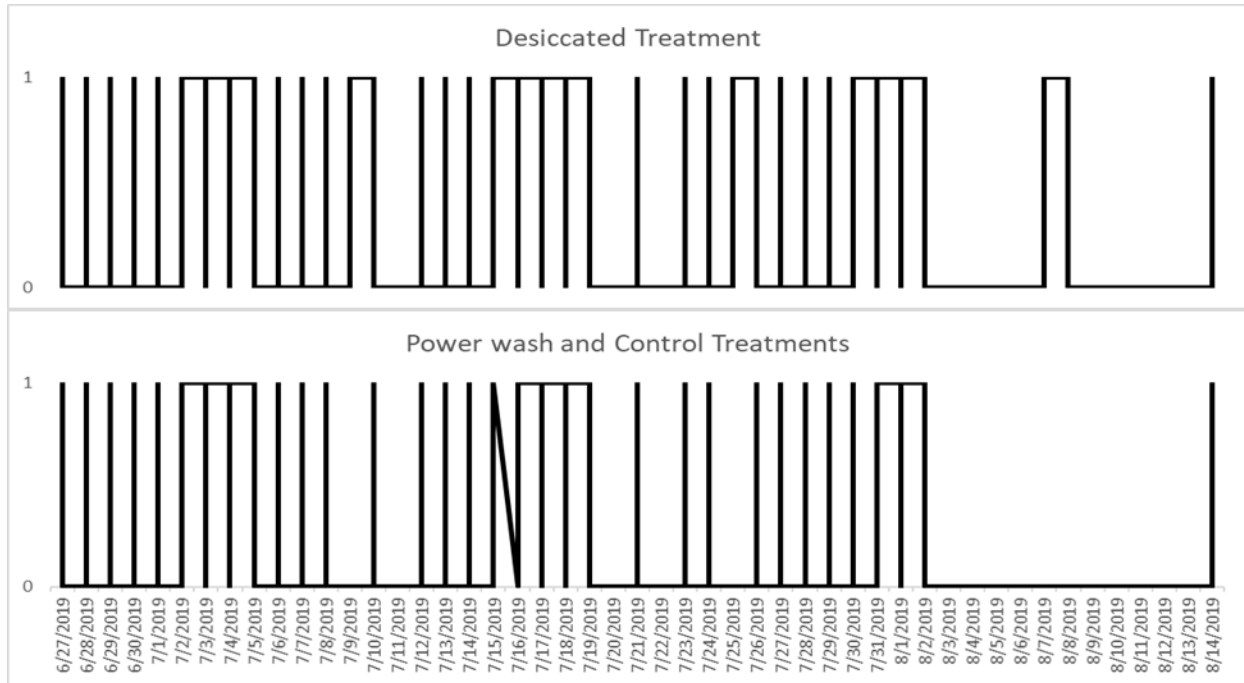


Figure 12: Time of desiccation for all treatments based on tidal fluctuations and lifted lines (Top: desiccated treatment; Bottom: Control and Power washed treatments). Lines at the ‘0’ position indicate periods in the water, while lines at position ‘1’ indicate periods of desiccation. Desiccated treatments spent 247.6 (20.2 %) hours out of the water, while Control and Power washed treatments spent 113.4 (10.8 %) hours out of the water.

### Biofouling coverage during field experiments

The percent coverage of fouling on cages by the end of the experimental period was significantly different between all cage styles used and fouling treatments ( $p = 0.004, 0.009$ , respectively). The BST style cages had the highest percentage of fouling coverage ( $87.20 \pm 4.40$  %), followed by Seapa ( $71.48 \pm 7.2$  %), then Hexcyl cages ( $58.48 \pm 8.29$  %). The desiccation and power washing treatments ( $63.43 \pm 10.82, 75.16 \pm 9.43$  %, respectively) had less fouling

coverage than the non-treated control group ( $78.58 \pm 11.2\%$ ) (Figure 13, 14) (Table 3). The dominant fouling organism observed in the study was *Victorella pavid*, a bryozoan that forms thick mats that block the mesh space in cages.

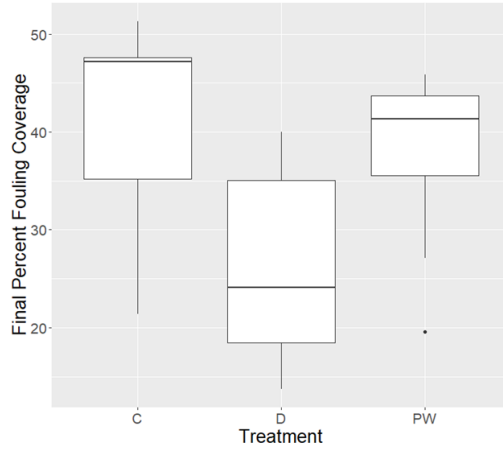


Figure 13: Boxplots showing the interquartile range of accumulated fouling coverage since the start of the experiment, separated by fouling treatment method (C = control, D = desiccated, PW = power washed). Values represent the total surface coverage of cages subtracted by the coverage of clean cages. Significant differences between fouling accumulation compared to both control and power washed treatments.

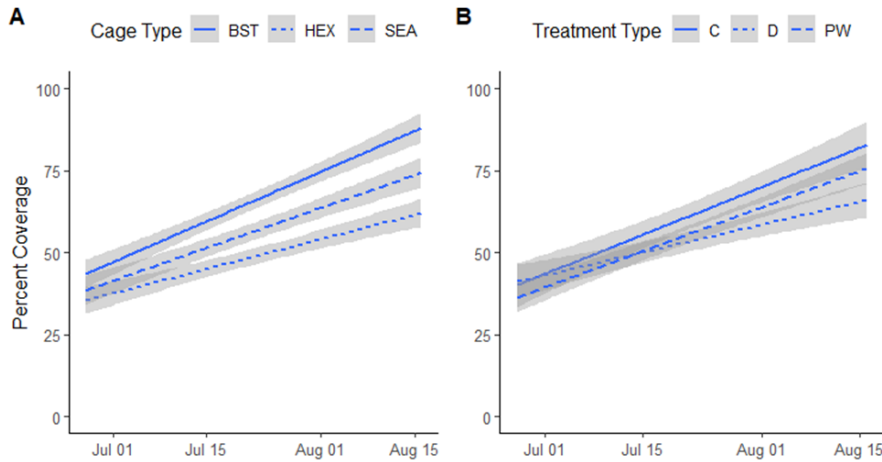


Figure 14: Percent fouling coverage on cages over time separated by cage type (A) and treatment type (B) (BST = BST cages, HEX = Hexcyl baskets, SEA = Seapa cages, C = control, D = desiccated, PW = power washed).

Table 3: Mean response for each variable with a 95 percent confidence interval separated by cage type and treatment method.

	Shell Length (mm)	Shell Width (mm)	Shell Depth (mm)	Whole Dry Mass (g)	Shape Index	Condition Index	Final Fouling Coverage (%)	Cage + Oyster Jostling (m/s <sup>2</sup> )
<b>Bag Type</b>								
Seapa	41.86 ± 0.63	38.99 ± 0.54	14.56 ± 0.17	14.53 ± 0.42	1.454 ± 0.015	3.460 ± 0.214	71.48 ± 7.2	10.72
BST	42.52 ± 0.59	39.03 ± 0.50	14.61 ± 0.19	14.47 ± 0.38	1.470 ± 0.015	3.413 ± 0.248	87.20 ± 4.4	10.57
Hexcyl	42.42 ± 0.63	39.21 ± 0.56	14.64 ± 0.17	14.70 ± 0.40	1.463 ± 0.016	3.688 ± 0.261	58.48 ± 8.29	10.39
<b>Treatment Type</b>								
Power Washed	40.63 ± 0.59	37.16 ± 0.48	14.55 ± 0.18	14.43 ± 0.41	1.486 ± 0.014	2.650 ± 0.223	75.16 ± 9.43	10.58
Desiccation	41.68 ± 0.54	39.16 ± 0.50	14.48 ± 0.18	14.01 ± 0.35	1.441 ± 0.015	4.222 ± 0.224	63.43 ± 10.82	10.61
Control	44.49 ± 0.62	40.91 ± 0.52	14.95 ± 0.17	15.25 ± 0.41	1.460 ± 0.016	3.291 ± 0.156	78.58 ± 11.2	10.49

Physical forcing

Seapa-style cages had the most significant internal movement, followed by BST and Hexcyl cages. The cage styles all showed similar trends of jostling rate over time, where halfway through the experiment, there was a notable decreasing trend in jostling. The continuous monitoring of cage jostling showed that desiccated treatments had more internal motion, followed by power washed and control treatments towards the end of the experiment (Figure 15). The desiccated cages appeared to have a constant rate of jostling throughout the experiment while the control and power washed oysters began trending negatively at the second half of the experiment.

Oyster performance

Fouling treatment and cage style showed to influence oyster growth during the duration of the experiment. Oysters in weekly desiccated cages had a significantly higher condition index ( $4.22 \pm 0.22$ ,  $p < 0.001$ ) than the other biofouling treatments (Control:  $3.29 \pm 0.156$ , power

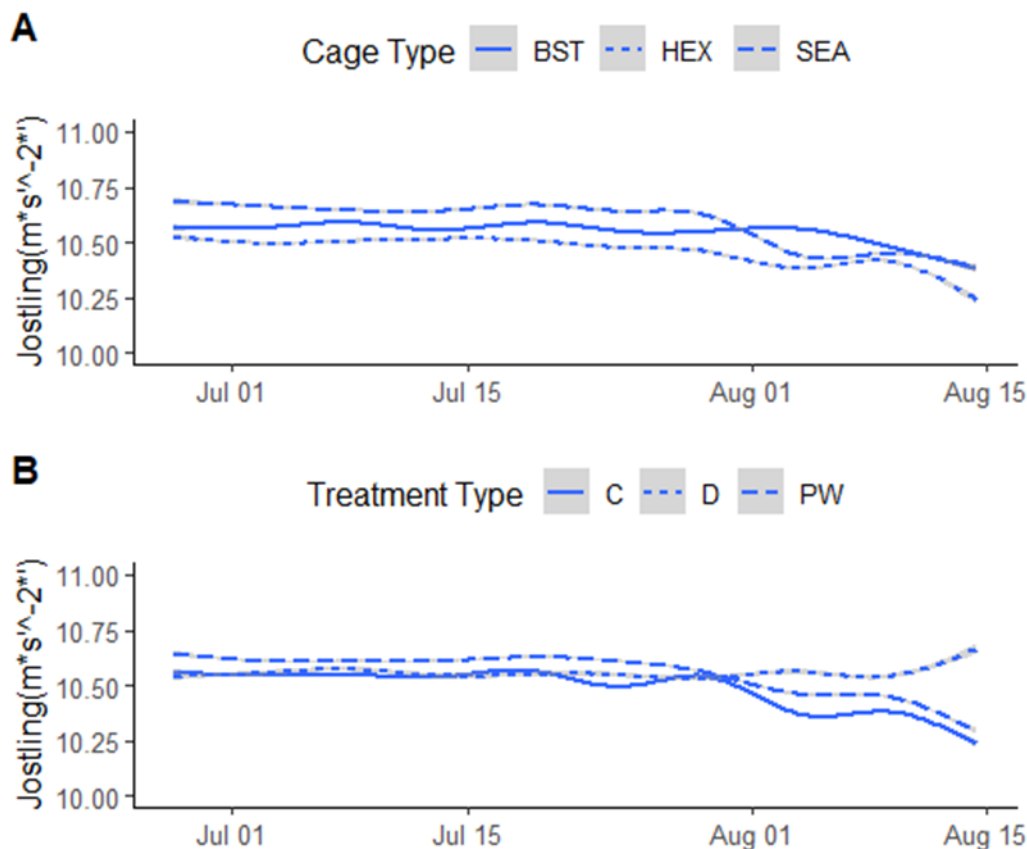


Figure 15: Cage and oyster jostling over time separated by cage type (top) and biofouling treatment method (bottom) (BST = BST cage, HEX = Hexcyl basket, SEA = Seapa cage, C = control treatment, D = desiccation treatment, PW = power washed treatment). A deviation in jostling rates between treatments starts to occur just before August 1.

washed:  $2.65 \pm 0.223$ ) (Figure 16b). Oyster condition index was not significantly influenced by cage style ( $p > 0.05$ ) (Table 4).

All treatment methods had significantly different shell lengths (control:  $44.49 \pm 0.62$  mm, desiccated:  $41.68 \pm 0.54$  mm, power washed:  $40.63 \pm 0.59$  mm,  $p < 0.001$ ) (Figure 16a). This trend persisted for shell width ( $p < 0.001$ ), shell depth ( $p < 0.001$ ), and total wet mass ( $p <$

0.001). Cage style was shown to not be a significant factor in oyster shell length ( $p = 0.15$ ), width ( $p = 0.78$ ), depth ( $p = 0.80$ ), or wet mass ( $p = 0.62$ ).

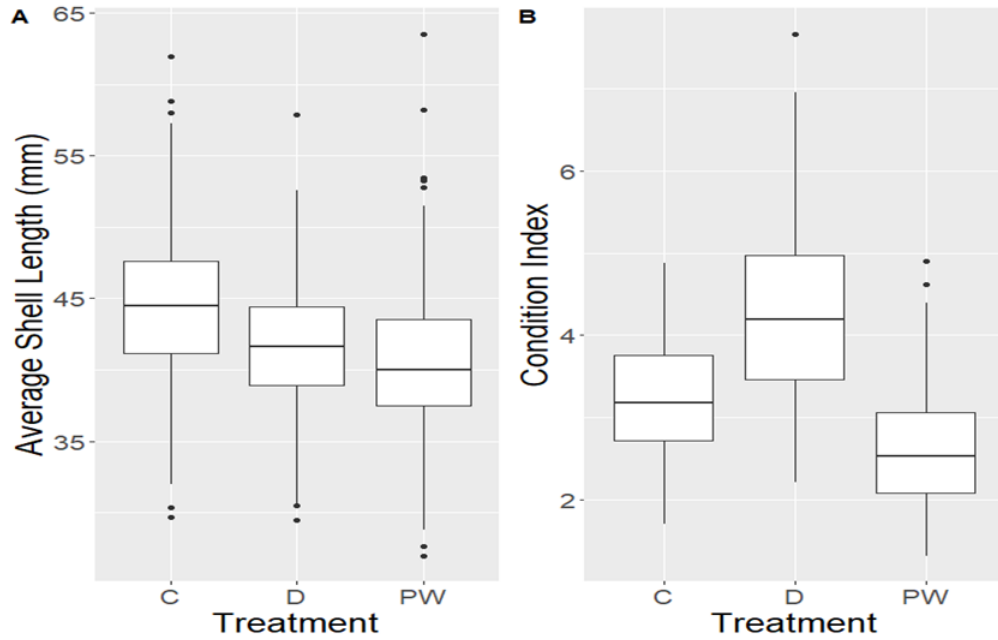


Figure 16: Boxplots showing the difference in average shell length (A) and condition index (B) between cages treated differently for biofouling (C = Control, D = Desiccation, PW = Power washed).

Table 4: Results of statistical Dunn tests following Kruskal Wallis test to represent significant differences within treatment groups ( $\alpha = 0.05$ ). Any changes in letters per variable indicate significant differences for individual variables

	Shell Length (mm)	Shell Width (mm)	Shell Depth (mm)	Shape Index	Dry Mass (g)
<b>Bag Type</b>					
Seapa	a	a	a	a	a
BST	a	a	a	a	a
Hexcyl	a	a	a	a	a
<b>Treatment Type</b>					
Power Washed	a	a	a	a	a
Desiccation	b	b	a	b	a
Control	c	c	b	ab	b

## Discussion

The use of physical tools to monitor the internal conditions of shellfish aquaculture cages in-situ exposed to varying biofouling mitigation treatments demonstrated this sampling method's practical application in better understanding shellfish aquaculture production. In our experimental region, cage jostling was a significant factor influencing oyster growth and condition index.

Despite no significant flow effect on oyster performance, we found differences in cage jostling associated with fouling coverage. The cages with less biofouling accumulation jostled more in the water, likely due to the fouling organisms' added weight, causing the cages to become more resistant to forcing and therefore jostling less. Adding weight to finfish cages is done intentionally in cases where hydrodynamic forces are strong enough to create deformities in nets. The added weight to the bottom of the finfish cages prevents movement and helps to preserve the shape of nets in the water (Klebert et al. 2013).

The desiccation regime was the most effective means for biofouling reduction. Despite the power washing method fully clearing the surfaces of the cages each week, there was rapid biofouling development soon after redeployment. In the power washing treatment, new fouling organisms have a new surface to attach to and the surface of the cage can be filled quickly. In the desiccation treatment, the thin layer of dead fouling material may shield the cages, preventing additional fouling organisms from attaching to the cage surface and resulting in an overall slower fouling rate. Additionally, since the power washing technique only removes the surface material from the cages, there is still an existing populace of biofouling that can continue to grow and

quickly reinhabit the surface of the cages. The desiccation treatment kills most of the fouling which slows the rate of fouling accumulation over time.

After taking length measurements and testing the condition index of oysters, we noticed a trade-off between those found in cages with high fouling and those grown in cages with low fouling coverage. There were significantly larger shell lengths in the cages with more fouling coverage compared to the other treatments. Interestingly, we found that the condition index of the oysters had an inverse relationship with shell length. The oysters in cages with lower fouling coverage had a nearly two-fold increase in condition index, meaning that the oysters treated with desiccation regimens had much more tissue weight per shell weight than the non-treated, highly fouled cages and would likely be more valuable. This trade-off between more tissue growth for shorter shell lengths driven by fouling treatment is an essential distinction for growers looking to alter the development of oysters to improve market-specific demands for oysters (Figure 17). Based on the results of this work, a grower can change the method for treating fouling to maintain a precise level of fouling on their cages to optimize either faster growth of the shells at the expense of tissue mass or for fuller shells at the expense of shell growth. This control also helps growers to better target their ideal market. If a grower wishes to sell to a higher-end half-shell market, they may need to perform desiccation regimes to produce fuller shells with deeper cups to increase the value of their crop to reach that market (Brake et al. 2003). Interestingly, the trade-off between shell growth and the condition index is not a consistent trend. Similar research comparing ploidy and gear type on oyster growth determined that shell growth and condition index amongst gear types were positively correlated (Walton et al. 2013b).

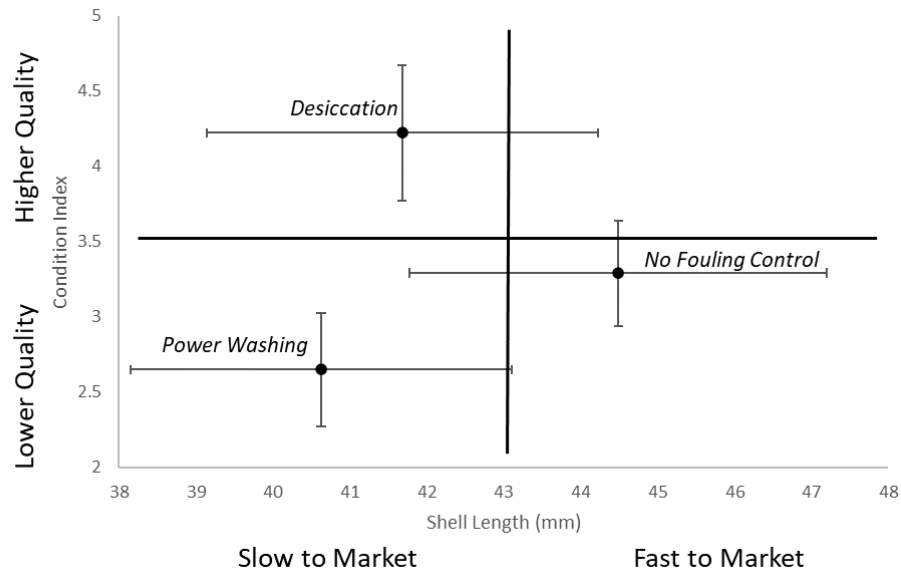


Figure 17: Scatter plot showing the relationship between oyster quality and time to market metrics when applying each biofouling mitigation technique. Error bars indicate the standard error in the measured data. The plot is separated into quadrants by adding lines through the center of the axes to emphasize the different production outcomes when each technique was applied.

The difference in oyster growth compared to untreated and desiccated cages agrees with the findings of previous work. Kreeger et al. (1990) determined that intertidal populations of *Geukensia demissa* with limited exposure to resources and long periods exposed to air had higher carbon absorption rates than subtidal populations by allocating energy to digestive enzyme production and maximizing absorption efficiency. We hypothesize that larger-bodied oysters associated with desiccated or 'intertidal' treatments may also alter their digestive strategy similarly. Power washed treatments were also exposed to air; however, exposure was momentary and apparently not enough for these oysters to diverge their feeding or digestive strategy from gear held permanently in the subtidal region. Another study by Gillmor (1982) further shows compensatory growth between intertidal and subtidal populations of *Crassostrea virginica*,

where the intertidal populations showed larger growth rates than the subtidal populations. In our study, the desiccated treatments were out of the water twice as much as the other treatments. Since the desiccated oysters were out of the water more and for extended periods, it is possible that the difference in oyster tissue mass can be due to intertidal effects rather than fouling coverage effects.

While previous research explains the mechanism behind the differential shell sizes between treatments, it does not show why the non-treated cages had larger shell lengths than the desiccated cages. The reduced shell sizes are likely due to the increased jostling in the cages that break off the ends of the oyster shell and inhibit new shell growth. However, no previous work has quantitatively described the rate of shell chipping to jostling intensity.

Future trials of this experiment should include more extended grow-out periods, additional common gear types, and a region of higher mean flow rate to better represent relationships between oyster growth and physical forcing. Additionally, a rate of fouling treatment intensity should be used instead of different methods of fouling treatment to better describe a gradient of fouling accumulation on bags to make for a less complicated comparison. For example, power washing as a biofouling treatment method created a system with low growth and low biofouling, likely caused by stress associated with the treatment regimen rather than physical forcing. A follow up study comparing power washing techniques where oysters are removed from cages prior to power washing or are placed in clean cages weekly may be insightful for better characterizing these conditions.

## Chapter 4: Effect of off-bottom oyster grow-out method on physical forces and oyster production

### **Abstract**

While the influx of new oyster culture systems provided growers with the ability to grow oysters throughout the water column, there is still uncertainty as to how these new technologies influence physical conditions inside cages and the production and quality of oysters. Since oysters are suspension feeders, potential changes in water flow will likely influence the overall survival, growth rate, and quality of oysters since oysters rely on local currents to deliver suspended food within their siphoning range. Additionally, the motion, or jostling, of cages are thought to cause chipping on the outer portion of oyster shells, influencing the overall shape and growth of oysters. However, the rate at which this chipping occurs has been seldomly researched. A gear comparison was conducted between three commonly used oyster cultivation methods (Virginia-style bottom cages, long-line cages, and floating cages) to better understand how the use of culture gear throughout the water column influences internal cage conditions and oyster performance. The average and variance in jostling between each cultivation method was noticeably different, which resulted in significant differences in the growth rate and quality of oysters. The changes in physical conditions inside each cultivation method demonstrated a trade-off between growth rate (a metric of time to market) and shell and meat quality (representative of

crop value). These results can help inform growers wishing to strategically adopt cultivation methods that are most aligned with their production goals.

## **Introduction**

Within the aquaculture industry, oyster aquaculture has been one of the fastest growing aquaculture industries globally (Botta et al. 2020). The use of cages and artificial structure to grow individual oysters has been widely used to produce oysters with more uniformity and more desirable shell shape, which typically command a premium from consumers in the raw, half-shell market. While oysters grown using off-bottom culture methods enhance the value of oysters and the overall profitability of a commercial operation, there is a much higher initial cost and considerable risk involved with this method (Huang et al. 2013, Engle et al. 2021). Much of this risk associated with caged aquaculture lies within identifying a productive lease space and choosing the appropriate gear type, husbandry method, and oyster species and genetic family needed for that lease space (Walton et al. 2013a, Walton et al. 2013b). While some water quality characteristics that are important for growing oysters can be easily understood and quantified (e.g. temperature and salinity), other site characteristics and how they interact with specific gear types are more cryptic. Specifically, there is a limited understanding of how physical factors that influence oyster growth rate and quality; there is less understanding of how these factors interact with shellfish culture gear. Therefore, it can be difficult for growers to account for the role of physical forces when evaluating a site or estimating its effects on yield.

To help mitigate risk and crop variability on cages oyster aquaculture farms, research efforts are needed establish the relationship between the physical environment, aquaculture gear,

and its relation to oyster performance and farm profitability. Since oysters are filter feeders, they rely on the ambient physical environment to deliver food for growth and development (Grizzle et al. 1992, Lenihan et al. 1995, Wilson-Ormond et al. 1997, Lee et al. 2017, Cranford et al. 2011). While the relationship between oyster filtration ability and ambient conditions has been well researched its role can be ambiguous (Campbell & Hall 2018) and is rarely accounted for during field studies. In laboratory experiments, the presence of cage material has also been shown to alter the local hydrodynamics, indicating it may be an important factor under some conditions (Lin et al. 2016, Grant & Bacher 2001, Stevens et al. 2011, Dong et al. 2020, Gaurier et al. 2011, Liu et al. 2020, Duarte et al. 2014). The growth and quality of oysters has also been found to change across different culture gear (Haché et al. 2021, Walton et al. 2013b, Mallet et al. 2013, Comeau 2013, Thomas 2016, Mizuta & Wikfors 2019). While the change in hydrodynamics and oyster production has been documented independently, there has been a limited amount of field research conducted to compare the physical effects among different gear types in a single location and its effect on oyster growth and performance. One study has determined that cultured oyster quality and growth rate has also been shown to change in response to changes in physical forcing, such as biofouling mitigation techniques (see Chapter 3), suggesting that cage and oyster motion are underlying factors that influence oyster shape.

The study presented here was designed to compare differences in the physical forcing and oyster performance across a series of commonly used oyster aquaculture cultivation methods (bottom, long-line, floating) in a low-energy environment. Through this assessment, we sought to understand how the use of different cultivation methods alter the physical environment within

cages, and how the changes in that environment influence the growth and quality of cultured oysters. We assessed physical forcing by monitoring the movement of both oyster cages and individual oysters deployed along one line. Oyster performance was monitored by tracking mortality, shell growth, tissue condition, and the shape ratio of oysters to assess oyster growth and quality using commercial standards (Galtsoff 1964, Ward et al. 2005). We anticipate that the results of this work will help to provide a better understanding of how physical processes affect risk and yield variability across various grow-out methods used in off-bottom oyster aquaculture. The results of this work will likely help to point out key factors that explain the variability in growth and quality between different culture methods and help growers in better understanding how culture method can influence the production of cultured oysters.

## **Methods**

Triploid LOLA family oysters produced by Hooper's Island Oyster Company and wintered at the Horn Point Demonstration Farm (HPLDF) were deployed from June 2020 to November 2020 using three commonly used grow-out methods (bottom Virginia-Style Cages, SEAPA long-line cages, OysterGro floating cages). Throughout the duration of the experiment, oyster and cage jostling was monitored continuously. Oyster growth was measured at the middle and conclusion of the deployment period and condition was assessed immediately after the end of the experiment.

### Study area

The field study was conducted at HPLDF on a specialized line designed to hold all three grow-out methods in parallel (Figure 18). HPLDF is located within a cove along the Choptank River, which is a major tributary branching from the northern end of the Chesapeake Bay, in roughly 1 to 2 meters of water depending on the tidal cycle. This farm site is located downstream from a jetty and a large setting pier which results in typically low water flow through this area during a large portion of the day, where the water velocity likely does not exceed 10 cm/s. During outgoing tides and wind-driven currents, water flow can be stronger. Oysters were graded prior to deployment and had an initial average shell length of 16.2 +/- 0.83 mm.

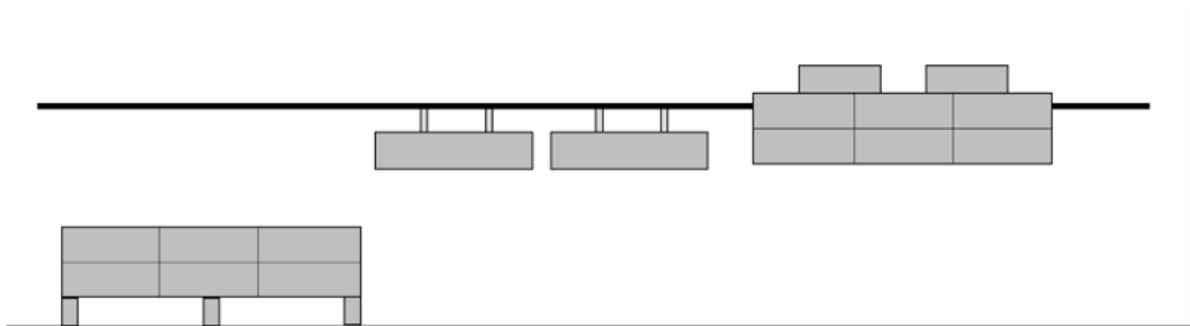


Figure 18: Depiction of the order of cages during the experiment. One bottom cage (left) was deployed directly below the line followed by two SEAPA long-line cages (center) then one OysterGro floating cage (right). This pattern was repeated three times along the same line at HPL.

### Experimental design

Oysters were deployed on a specialized line fit for holding bottom, long-line, and floating cages in parallel. Three grow-out methods were used that span the vertical distribution of the water column (bottom Virginia-Style Cages, SEAPA long-line cages, OysterGro floating cages). Three cages from each grow-out method were used. The bottom cages hold a maximum six

cages and are raised eight inches from the bottom. The bottom row of the bottom cage was used to hold three bags per cage in this study and each set of bags were averaged to represent the entire cage. SEAPA long-line cages were deployed just below the surface of the water in pairs. Each pair were averaged to act as one replicate long-line cage. Lastly, the floating cages were left on the surface of the water and contain up to six bags. Like the bottom cages, three bags were placed at the bottom row of the floating cage and were averaged to act as one replicate for this cage type. Each bag was stocked with approximately 900 oysters per bag at the start of the experiment which were graded so that each bag started with an average shell length of 16.2 +/- 0.83 mm.

#### Oyster growth and performance

Oyster performance was assessed by taking measurements of the shell length (distance between the hinge and the furthest point on the mantle), shell width (the widest distance perpendicular to the shell length), and shell depth (the widest point from the top shell to the bottom shell) of thirty random individuals per bag at the conclusion of the field deployment. Additionally, a condition index was performed with ten individuals per cage using methods by Lawrence and Scott (1982, eqn. 7). Condition index roughly estimates the quality of oysters by taking the ratio of dry tissue weight to dry shell weight which is a common metric used for describing the relative quality or value of an oyster. Using these measurements, a series of indexes were also taken to assess the quality of the oysters grown in each method. Specifically, shape index, (eqn. 8), width index (eqn. 9), and elongation index (eqn. 10) were calculated (Galtsoff 1964, Ward et al. 2005). Again, these shell indices are general metrics used for

characterizing the relative quality and value of oysters grown. While the ideal shape and quality of an oyster's condition index and shell indices vary from one individual to another, we will scale our study based on meat quality correlating positively with the condition index value and shell quality will be the highest when the shape index reaches 2 and the width and elongation indexes approach 1.

$$\text{Eqn. 8: } SI = \frac{\text{shell length } h \text{ (mm)} + \text{shell depth } h \text{ (mm)}}{3 * \text{shell width } h \text{ (mm)}}$$

$$\text{Eqn. 9: } WI = \frac{\text{shell length } h \text{ (mm)}}{\text{shell width } h \text{ (mm)}}$$

$$\text{Eqn. 10: } EI = \frac{2 * \text{shell length } h \text{ (mm)}}{3 * \text{shell width } h \text{ (mm)}}$$

### Physical forcing

Accelerometers (Onset HOBO Pendant G Logger: UA-004-64) were deployed continuously to monitor the movement of oysters and oyster cages throughout the experiment. One accelerometer was tethered to the inside of each bag to simulate the gross movement of one oyster under culture conditions (i.e. cage + oyster). A second accelerometer was securely fastened to the outside of each cage to monitor the total movement of the cage. The difference between the two accelerometers is indicative of the net movement of one oyster inside a bag for each method (Figure 19).

### Environmental monitoring

Environmental conditions at HPLDF were monitored continuously at five-minute intervals using a calibrated YSI EXO2 multiparameter sonde to record temperature, salinity,

dissolved oxygen, turbidity, and chlorophyll-a to identify any periods of abnormal environmental condition. The YSI was mounted at the far end of the pier northwest and upstream of the experimental site.

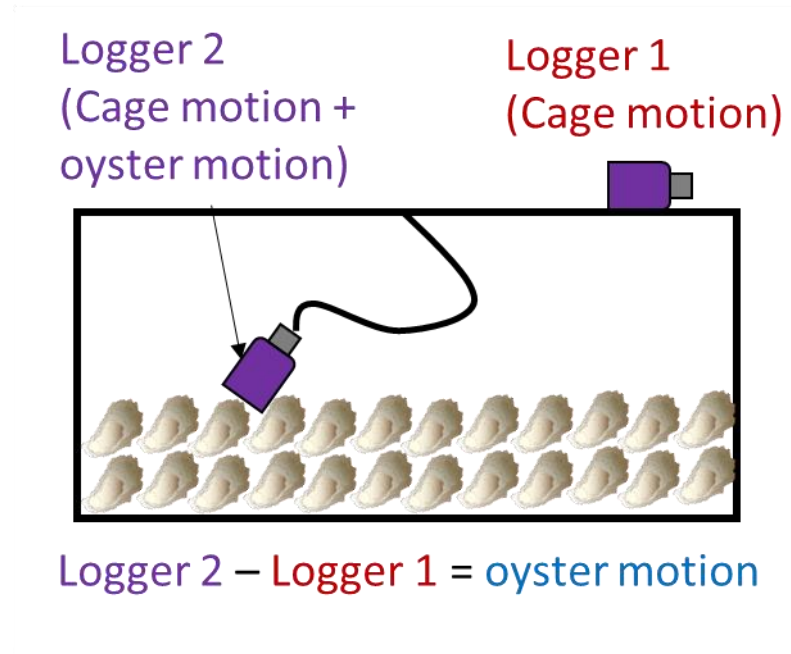


Figure 19: Diagram of how the two accelerometers were deployed per cage. The first accelerometer was attached directly to the exterior of the cage while the second was attached to a tether in the center of the inside of the cage alongside the oysters.

### Statistical analysis

The assumptions of normal distribution were tested using a Levene test and a Shapiro test. Most of the oyster growth data produced were not found to be normally distributed despite attempts to transform data using logarithmic, square-root, and box-cox methods. Due to the lack of normality found, mainly non-parametric statistical approaches were applied to the data. Kruskal-Wallis tests with Scheirer-Ray-Hare Adjustments were used to determine statistical

significance between the oyster performance and physical conditions of different husbandry practices. Of the comparisons that were significant, a post-hoc Dunn test using a Bonferroni correction was used to test for statistical significance between respective treatments. Mixed linear effect models were used when comparing differences in condition index and fouling coverage rate between fouling treatments and cage types due to an unequal sampling size. To process the jostling time series data and provide a forecast of the future trend in jostling, an autoregressive integrated moving average model (ARIMA) was produced using the ‘auto.arima’ function within the forecast package in R. In this package, ARIMA conditions are performed by detrending the original time series then finding the optimal  $p$ ,  $d$ , and  $q$  parameters. With these parameters, a trend can be produced of the original timeseries which will be used to produce a projection beyond the observed values given the modeled trend considering linear trends and any possible oscillation in trend that may occur. Using the provided parameters, the data was projected over a two-month forecast to predict any potential changes in jostling that would occur during the remainder of the growing season. Lastly, a principal component analysis (PCA) was produced to determine any separation in physical conditions and changes in growth associated with different culture techniques. Since the number of measures were not equal for each parameter analyzed in this experiment, the PCA integrated the average shell growth, condition index, mortality, and physical parameters from each treatment to plot one point per treatment that is representative of all the data that was collected. The separation between points in scatter plot of the two major principal component axes will describe how the growth performance and physical environment are collectively different between these culture methods. All statistical metrics were based on an alpha value of 0.05.

## Results

The following study evaluated the internal conditions of three oyster culture methods and the potential implications on oyster growth and productivity. Previously, minimal work has been conducted in the field to address the internal condition of cages. Additionally, research conducted in minimally energetic environments have not been well documented. By growing oysters in a range of culture methods that span the depth of the water column, we aimed to find differences in the physical characteristics within each cage system and determine if there is any relationship between those physical changes and differences between oyster productivity.

### Environmental monitoring

HPLDF experienced noticeable yet expected fluctuations in environmental conditions over the experimental season. Water temperature decreased over time without any large, acute changes. Water temperature at the beginning of the experiment averaged at about 30 °C and decreased to 10 °C by November. The average temperature of the whole experimental period was 24.10 °C with a standard deviation of 6.13 °C. Salinity fluctuated across the time series but overall trended positively with time starting at 6 ppt and rising to roughly 14 ppt. There were some acute drops in salinity that went as low as 4 ppt during the treatment period. Average salinity for the season was 9.84 ppt with a standard deviation of 2.95 ppt. The observed range in salinity was low compared to historical trends in this area. A small increasing trend in optical dissolved oxygen (ODO) was shown with high fluctuations ranging from 0 – 17 mg/L. The seasonal average of ODO was 7.25 mg/L with a standard deviation of 2.12 mg/L. Chlorophyll concentration was highly variable throughout the season with several large peaks, suggesting

algal bloom activity, which reached up to 312.79  $\mu\text{g/L}$  but averaged at 13.55  $\mu\text{g/L}$  with a standard deviation of 14.82  $\mu\text{g/L}$ .

### Physical forcing

There were noticeable differences in the average and variance in the cage jostling experienced by the oysters in each cultivation method (Table 5). The long-line system had the highest relative average cage jostling followed by the bottom cage, then the floating cage (jostling = 10.743  $\text{m/s}^2$ , 10.569  $\text{m/s}^2$ , 10.382  $\text{m/s}^2$ , respectively, Figure 20a). However, the bottom cages had the most relative oyster jostling, followed by the longline cage, then the floating cage (jostling = 0.5394  $\text{m/s}^2$ , 0.4270  $\text{m/s}^2$ , 0.2789  $\text{m/s}^2$ , respectively). The variance in oyster jostling per culture method was not proportionate to the average. While the long-line cages had both the highest average and variance in cage motion, the bottom cage had the least variance in cage motion and the floating cage had a high variance comparable to the long-line cages (variance = 0.037  $\text{m/s}^2$ , 0.017  $\text{m/s}^2$ , 0.033  $\text{m/s}^2$ , respectively, Figure 20b).

The time series of jostling for each gear type shows little trend in jostling over time for any of the culture methods (Figure 21). At multiple points throughout each of the time series, there appears to be points of larger motion that are seemingly consistent across all treatments which are likely derived from more turbulent conditions such as storms or high winds. Our prediction of future oyster jostling shows that the oysters grown in bottom and floating cages should have higher average motion compared to the long-line system which remained more constant.

Table 5: Average and confidence interval of all relevant parameters measured in this study separated by cultivation method. The alpha used to determine confidence intervals was 0.05.

Culture Method	Shell Length (mm)	Shell Width (mm)	Shell Depth (mm)	Shape Index	Width Index	Elongation Index	Condition Index	Cage Jostling (m/s <sup>2</sup> )	Oyster Jostling (m/s <sup>2</sup> )
Bottom Cage	60.63 ± 2.41	48.60 ± 0.92	19.03 ± 0.34	1.649 ± 0.02	3.201 ± 0.047	0.8358 ± 0.0111	7.185 ± 0.541	10.041	0.5394
Longline Cage	60.96 ± 1.56	50.61 ± 1.20	20.36 ± 0.64	1.614 ± 0.025	3.042 ± 0.067	0.8067 ± 0.0141	7.921 ± 0.528	10.099	0.4270
Floating Cage	54.46 ± 1.01	48.85 ± 0.84	20.03 ± 0.38	1.530 ± 0.015	2.743 ± 0.044	0.7449 ± 0.0079	8.376 ± 0.674	9.819	0.2789

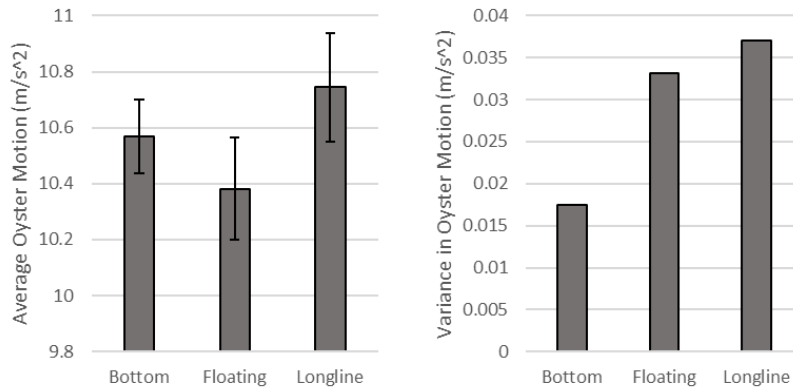


Figure 20: Average (left) and variance (right) in oyster movement per cultivation method measured continuously throughout the experiment. Error bars on the left represent one standard deviation from the average.

### Oyster performance

Oyster growth and performance were highly variable amongst each tested culture method. Given the growth trends in figure 22, the growth of the oysters appeared to initially separate between the second and third sampling date. The growth rate of the long-line and bottom caged oysters was greater than that of the floating cage. The shell length of bottom and long-line oysters was significantly higher than those grown in floating cages ( $p < 0.001$ ) (Figure 23). While the mean shell length of the bottom and long-line cage was statistically similar ( $p = 0.096$ ) there was still a noticeable difference between the standard deviation of the shell lengths

of the oyster in each of these treatments (bottom = 10.03 mm, long-line = 10.64 mm, floating = 8.47 mm). Shell width was found to be statistically significant between all treatments ( $p = 0.041$ ); however, Dunn tests showed no statistically significant differences within treatments directly. Shell depth was found to be statistically significant across all treatments ( $p < 0.001$ ) and the long-line and floating cages were found to grow oysters with significantly deeper shells than in bottom cages ( $p < 0.001$ ).

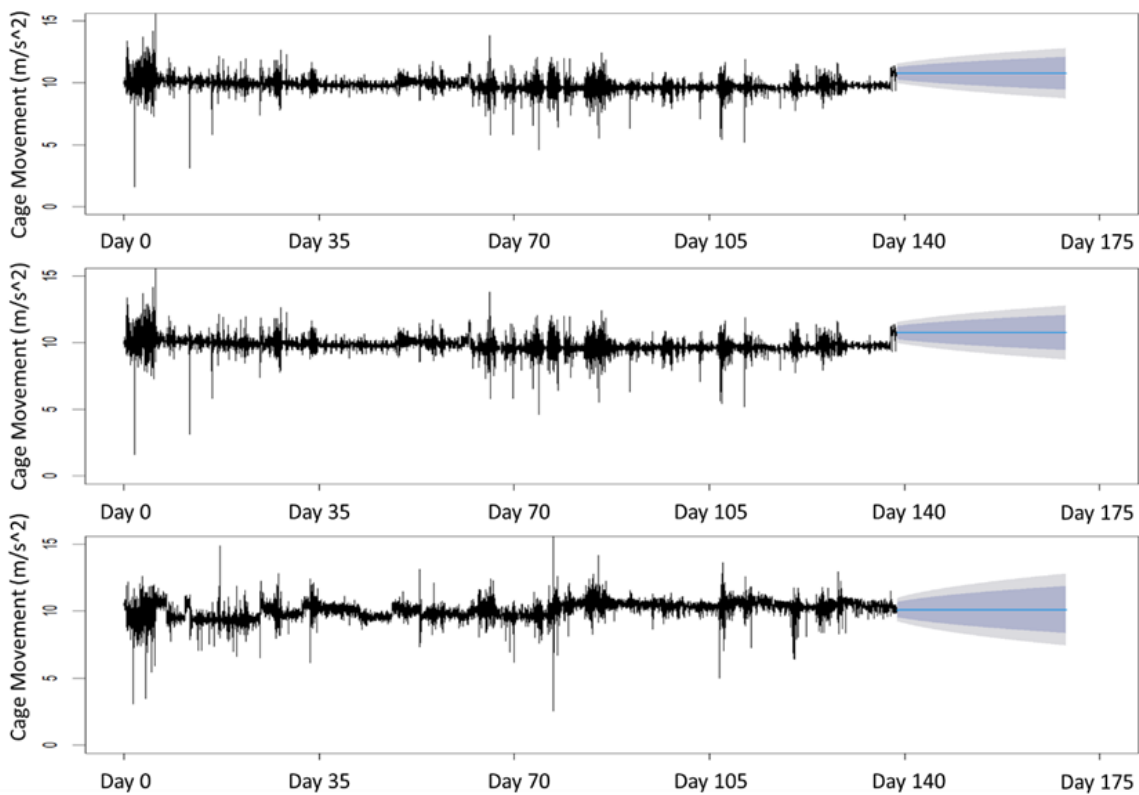


Figure 21: Trend in cage jostling for bottom cages (top), floating cages (middle), and longline cages (bottom) throughout the sampling period with a two-month prediction. An optimized ARIMA was used to model the forecast per treatment (ARIMA coefficients: bottom, 3,1,2; floating, 0,1,1; longline, 4,1,3).

All shell shape indices were shown to have highly statistical differences between each treatment ( $p < 0.001$ ). Condition index of oysters grown in floating and long-line cages were significantly higher than the condition index of bottom cage oysters ( $p = 0.013$ ,  $p = 0.021$ , respectively). The total mortality of oysters grown in floating cages were significantly higher than that of long-line cages ( $p = 0.034$ ), however neither were significantly different from the mortality from bottom cages ( $p = 0.11$ ,  $p = 0.50$ , respectively). Table 5 lists the average of each measured attribute of oyster performance per treatment with a 95 % confidence interval. Figure 24 shows the results of a PCA that was produced to determine the separation of growth parameters of the oysters and the ambient physical environment measured. Across the first principal component, there were some similarities between the bottom and longline cages which explained most of the difference in environment between these treatments (71.4 %) but notable separation between all three cage types in the second component.

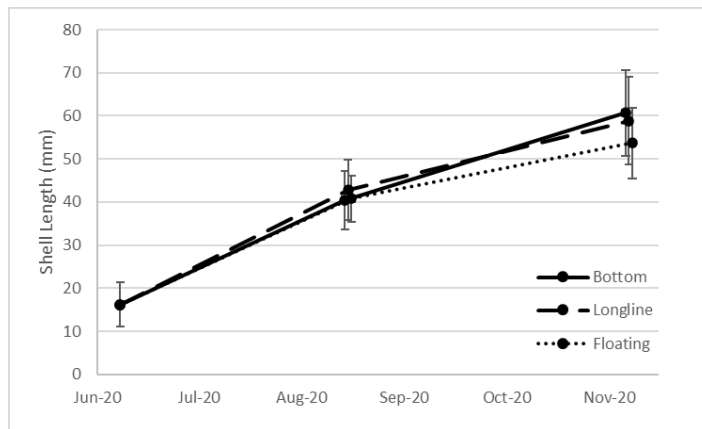


Figure 22: Recorded shell length growth of oysters per cultivation method for the entire experiment. Initial shell length was determined before splitting oysters into respective treatments and therefore, all treatments have identical initial shell lengths. Error bars represent one standard deviation among the data. August and November sampling points were jittered to better show the error bars.

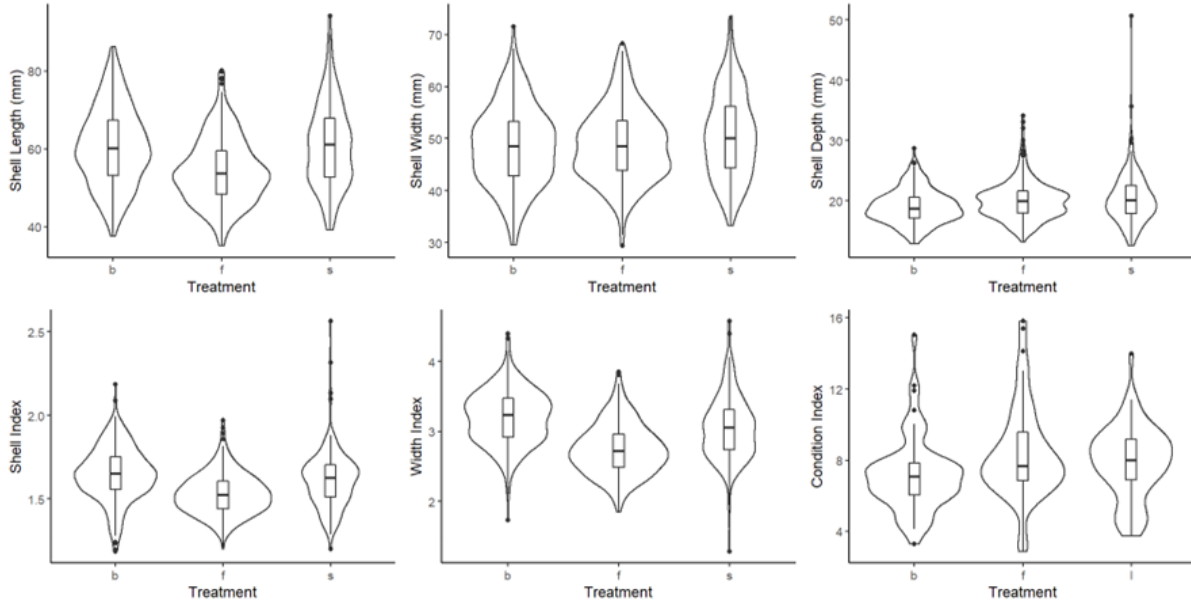


Figure 23: Violin plots of each measured shell performance metric for bottom cages (b), floating cages (f), and longline cages (s). A boxplot is centered within each violin and the spread over the data is indicated by the width of each violin.

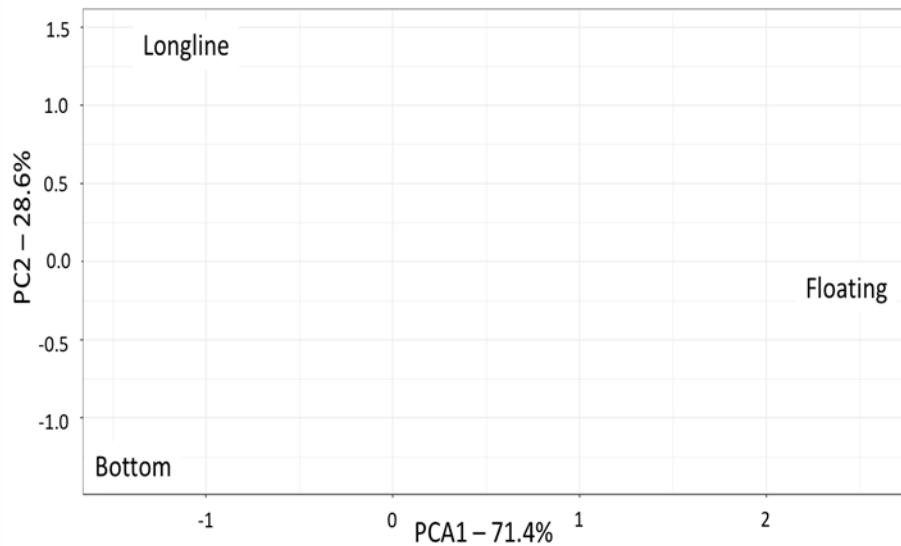


Figure 24: PCA of the two primary components dictating oyster performance and hydrodynamic forces for each cultivation method.

## Discussion

At the start of this experiment, the ambient salinity was at the lower range of what is expected at our study site. This initial low salinity was at a range that has been shown to negatively impact oyster reproductive processes, growth, and survival (Butt et al. 2006, La Peyre et al. 2013, Du et al. 2021). It is likely that the overall shell growth might have been slowed by this low salinity. However, since all growth methods were exposed to similar environmental conditions, there effects on culture conditions and growth should also be similar among gear types.

Oyster performance varied significantly across each culture method in our demonstration site. This observation has been well observed in previous studies but appear to be site and species specific (Bishop & Petersen 2005, Hamilton et al. 2004, Davis 2013). These differences highlight some practical trade-offs that can be used strategically to optimize production on farms that utilize more than one culture method. Bottom cages provided the fastest average shell length growth at the expense of meat quality and shape. They happen to also create more consistent growth than the other methods with moderate survival. This growth response makes the bottom culture method a useful method for sustaining early growth and ensuring all crops start growing thicker shells at an even pace. Interestingly, a similar study comparing the production of oysters using these methods showed higher mortality and slower shell growth at their farm site in the Gulf of Mexico, suggesting that these results are likely site specific (Walton et al. 2013a). The long-line system produced oysters with higher condition index and high survival, at the cost of slower, less consistent shell growth. This method could work well as an intermediate stage for

growing oysters. Since the bottom cages already produced a longer shell length at a consistent rate, the long-line systems can be used to begin shaping the oyster and providing a system that supports meat development while preventing mortality risk. Lastly, the floating cages offer the most optimal shell shape and can be used as a finishing tool to optimize the shape of the oyster, a component that heavily dictates the cost of oysters sold to the half-shell market. The concept of using floating cage systems as a finishing step to optimize oyster shape has been discussed by Thomas (2016). It is important to note that the interpretation of these results as they pertain to actual farm management decisions may change based on what the specific grower and buyer perceives as ‘ideal.’

Within HPLDF, a relatively low energy culture site, each oyster cultivation method produced different physical environments. There were notable differences between the movement of the cages. The way in which each method was supported and their position in the water column allowed different reactions to physical processes and affected either the average movement of the cages throughout the season and the intensity of the movement that occurred. The bottom cage, which rests along the waterbed, provided the most resistance to water movement. While the average movement of the cages was medial, the variance in movement was half that of the other cultivation methods, suggesting that the cages are being affected by consistent, lower frequency movement. Since the cages are positioned lower in the water column, they are likely not being exposed to wave-generated movement. The long-line cages, which are suspended freely below a line with floats are much less resistant to water movement. As such, this cultivation method is exposed to all forms of water movement hence, why the bags

had the highest movement at a variance very similar to the floating cages. It is important to note that there are several ways to deploy long-line cages that can offer more resistance if needed. For example, a cage that was attached more directly to a taught line would be very resistant to water movement. Lastly, the floating cages, which have floats directly attached to the structure had some resistance to lower frequency motion but likely offered little resistance to wave energy, since the floats force the cage to move along with oncoming waves. As a result, floating cages receive the least bag movement, but have a high variance in motion, due to exposure to only high energy wave events.

While the effect of these physical disturbances on oysters have not been well studied, there is evidence to suggest that disturbances that chip new shell growth too frequently may have a negative impact on growth (Mallet et al. 2009). Cages that affected by higher energy movements in moderately stocked cages are most likely to result in shell chipping than those in lower energy environments. This concept agrees with our findings where the cages with larger variations in cage movement (floating and long-line systems) resulted in slower shell growth than the more protected cages (bottom cages). The response in shell shape and meat quality is also likely derived from this relationship. The loss in shell length and shell mass inadvertently increases the shell shape ratios to produce more optimal shells. Additionally, since tissue mass is conserved in this process, the meat index is increased as more shell mass is lost. Hence, the cage systems that are influencing the environment that the oysters are being exposed to are also responsible for shaping the oysters. A theoretical diagram identifying the cages associated with average and variance in cage motion, along with the growth characteristics observed was

produced using this data (Figure 25). While this relationship has been generally understood, it has not been effectively measured in the field. By quantifying the variance and average motion of gear in active aquaculture sites, growers can further optimize the outcome of their crop by manipulating the type of gear used and furthermore, the progression of culture methods used across the grow-out period for their crops. Similar studies should be conducted in more energetic environments comparing different gear types, species, and ploidy. A culmination of studies monitoring the physical conditions of cages across gear types in varying environments could lend itself invaluable to growers wishing to optimize their production. Furthermore, a study attempting to utilize a series of growing techniques across the grow out stage of a single cohort would further validate the hypotheses made from these results.

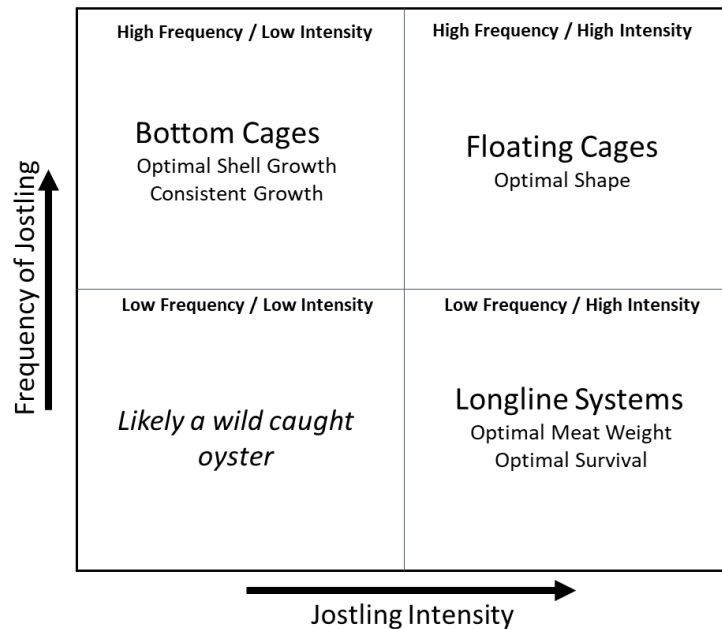


Figure 25: Theoretical chart to depict the environment created by each cultivation method and the resulting oyster performance that was observed in our study.

## Chapter 5: Assessing the variability of the physical environment surrounding an off-bottom oyster lease and its influence on eastern oyster growth performance

### **Abstract**

As the shellfish aquaculture industry continues to expand, the size of individual shellfish farms is also like to become larger. Physical processes in natural water bodies are dynamic and can vary across small spatial scales. Additionally, the presence of aquaculture equipment may contribute to physical changes across a system. Alterations in water flow, which control the delivery of food to oysters and other suspension-feeding species, may influence production. It is important to understand how the physical environment can change across a shellfish lease space so that growers can account for changes in water movement and optimize their production. This project seeks to understand the amount of variability in production that can be attributed to water flow across an active commercial lease site. A series of bags were deployed on a commercial, off-bottom aquaculture farm in the Patuxent River, Maryland to understand the possible variation in oyster growth and quality along the horizontal extent of a shellfish aquaculture lease. Tools were deployed inside each cage to understand the relative mass transfer and movement of cages and oysters. In our study site, we were able to determine noticeable changes in oyster growth and quality across the farm site. Additionally, the changes in oyster performance seem to be correlative with the rate of movement of oysters within the bottom cages. Lastly, water quality

transects throughout the farm showed increased chlorophyll and low flow downstream of the farm, which may have been caused by the farm itself, although follow-up work is necessary to draw further conclusions. The results demonstrate farm-scale variability of culture conditions that could be optimized for greater yield and more consistent production.

## **Introduction**

To fulfill the growing need for alternative forms of sustainable protein, expansion of shellfish aquaculture is essential (Shumway et al. 2003, Garlock et al. 2019). Currently, the oyster aquaculture industry has been growing at an average rate of 2.09 percent since 1950 (Botta et al. 2020). Despite the historic growth in the industry, there are still efforts to rapidly expand the industry further. Even in high-production areas such as the Chesapeake Bay, there is a clear underutilization of lease space occurring, signaling the potential for high expansion well into the future (Beckensteiner et al. 2021).

In attempt to optimize shellfish production further, models have been developed to identify optimal environmental and biological conditions for shellfish aquaculture leasing (Ferreira et al. 2007, Newell et al. 2013, Hawkins et al. 2013, Jiang et al. 2022). These models use a combination of remote sensing, water sampling, and hydrographic monitoring to identify zones with optimal food inputs, temperature, salinity, and flushing rates and then provide an estimate on the carrying capacity and relative production of the area. While these models are all necessary for the growth of the industry, they do not fully account for the physical environment including culture equipment, nor can they predict the relative quality of the shellfish produced.

Oysters are suspension feeders that rely on the external physical environment to deliver food items towards their siphons at a particular flux (Wilson-Ormond et al. 1997, Lee et al. 2017). Local hydrodynamics are important to consider in oyster aquaculture practices, but past research on the effects of water flow on suspension feeding behavior has been inconsistent and primarily conducted in controlled laboratory settings (Campbell and Hall 2018). While faster water flow is generally considered to be better suited for oyster production, there is an upper limit where caged oysters can become stressed, which can result in increased mortality and stunted growth (Mallet et al. 2009). This effect is likely attributed to increased motion of the caged oysters that produces shell chipping and the inability for oysters to feed (Mizuta and Wikfors 2019).

The relationship between oyster suspension feeding and physical forcing becomes further complicated when additional structures are considered. For example, in finfish aquaculture, the presence of nets and pens have been shown to have significant effects on ambient hydrodynamic conditions (Klebert et al. 2013, Chen and Christiansen 2017, Xu et al. 2019, Dong et al. 2020). Studies on shellfish have shown how hydrodynamic conditions are altered significantly with the introduction of mussel ropes (Newell and Richardson 2014) and between damaged and restored oyster reefs (Kitsikoudis et al. 2020, Yurek et al. 2021). The effects of oyster aquaculture gear on ambient physical forcing have been rarely tested in the field and offer little quantitative explanation as to how these conditions affect oyster growth and quality in cages. Additionally, the variation of hydrodynamic conditions across one oyster aquaculture lease space has only

been measured in one other study (Turner et al. 2019), although the movement of oysters and cages have not been assessed in this study, nor was the effect on the oysters themselves.

This research seeks to understand how water flow and cage motion are affected across the extent of an existing bottom cage farm and what influence those changes have on oyster performance. For this analysis we sampled a series vexar bags containing adult oysters placed inside bottom cages at specific grid points along an oyster farm on the Patuxent River, MD. For each of these sample points, the mass transfer within cages, cage motion, and oyster motion were measured along with several growth measurements of subsampled oysters. This work aims to assess the spatial effects of bottom cage oyster aquaculture on the physical environment, water quality, and oyster performance. The goal of this research is to create a methodology for growers to consider when designing farm orientation that may improve production.

## **Methods**

Triploid LOLA family oysters, produced by Hooper's Island Oyster Company and wintered at the Horn Point Demonstration Farm (HPLDF), were deployed from May 2021 to November 2021 across the horizontal extent of an existing bottom cage oyster farm (roughly 420 bottom cages) on the Patuxent River, Maryland to observe potential changes in growth performance associated with location on a farm and the local hydrodynamics. In May of 2021, oysters had an average shell length of 53 mm upon deployment. Throughout the duration of the experiment, physical forces, water flow, and water quality relevant to oyster culture were monitored.

### Study area

This experiment was conducted at a shellfish lease owned and operated by 38 North Oyster Farm located on the Patuxent River in Solomons, Maryland. The Patuxent River is a major tributary of the Chesapeake Bay stemming from the southwestern portion of the bay. This lease is split into four major sections each operated by different growers. Along the center of the lease is a pier that splits the two sections. This experiment was conducted on the southmost, inshore section of the lease. The region surrounding the lease is highly exposed to wind-driven waves and frequent disturbance from commercial (mainly from the northeast to southwest) and recreational (mainly from the northwest) boat traffic. The inner-most section of the lease where the study was conducted was believed to reduce some of the major disturbances that occur from the boat traffic according to conversations with the grower (Figure 26).

### Experimental design

A 6 x 3 grid was derived along the horizontal extent of an existing oyster farm on the Patuxent River in Solomons, Maryland (Figure 27). At each grid point, an oyster test bag stocked with 185 oysters at an initial average shell length of 53 mm on the top of a fully stocked, Virginia-style bottom cage from May 2021 to November 2021. Oysters were hand-graded to include oysters that have shell lengths between roughly 50 mm and 60 mm. Each test bag was fastened to the top of a bottom cage using four bag pins to secure the corners of the bag and a bungee cord to keep the center of the bag flush with the cage (Figure 28). The growth and survival of each test bag was monitored throughout the duration of the experiment. Tools were used to periodically measure mass transfer and motion through cages and continuously log cage

and animal movement. Environmental conditions were monitored continuously throughout the length of the experiment and a series of vertical and horizontal transects were conducted between deployed bags at one timepoint in September 2021.

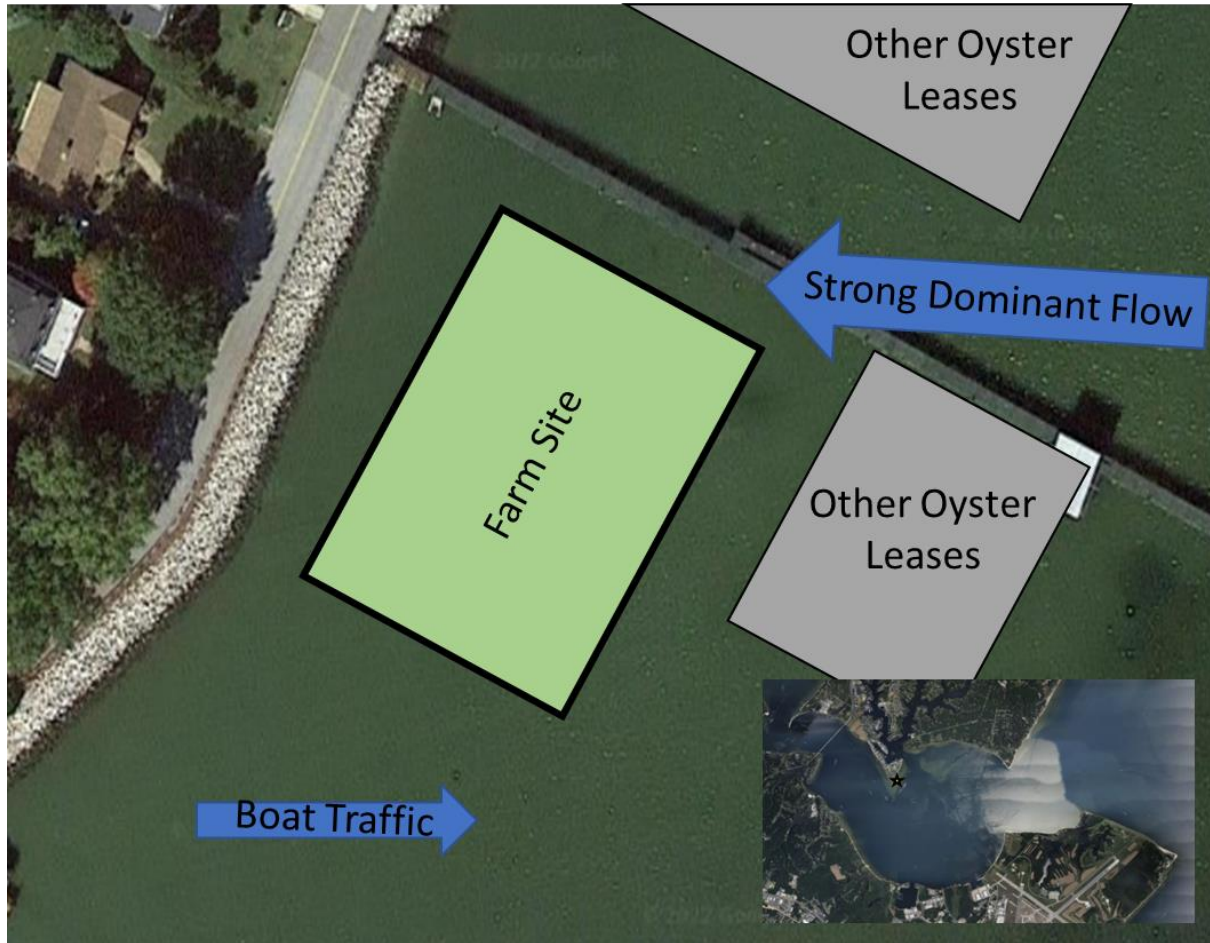


Figure 26: Map of the experimental site. This farm is located off Solomons Island within the mouth of the Patuxent River, Maryland. This site is surrounded by other oyster farms and has dominant current from the east and frequent surface disturbances in wave motion from the south of the farm due to boat activity.

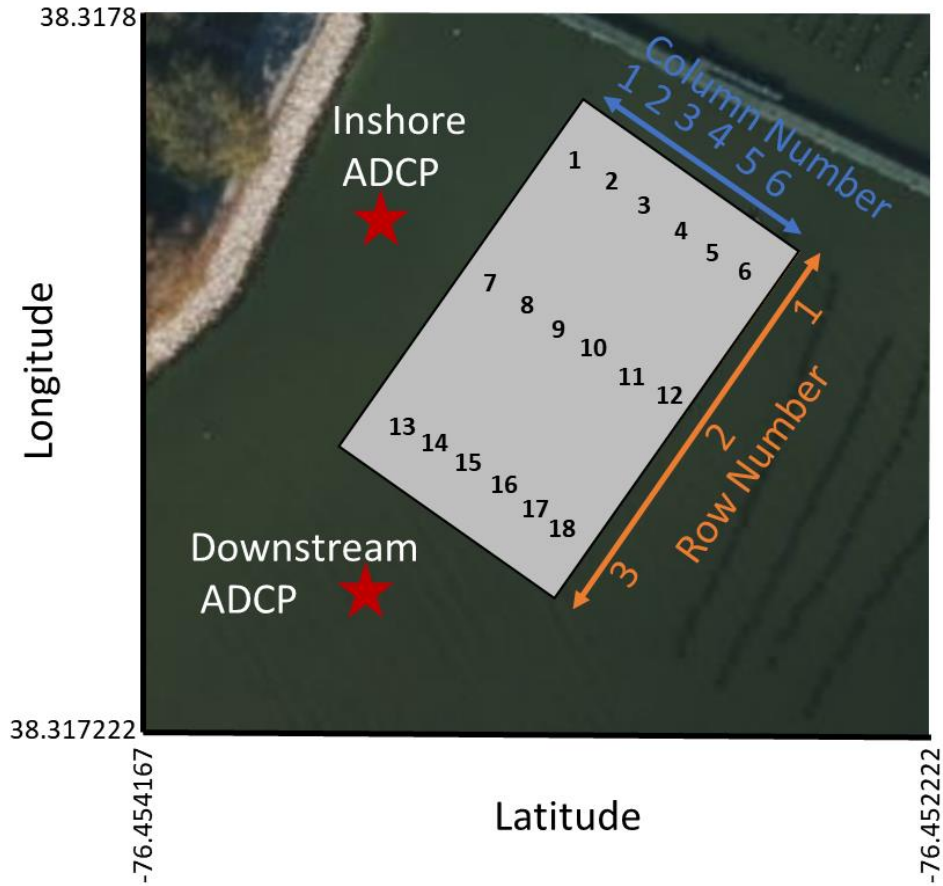


Figure 27: Locations of all deployed test bags across the farm site. Each bag is numbers to correspond with Table X and Y. ADCP deployments were conducted in the red stars.

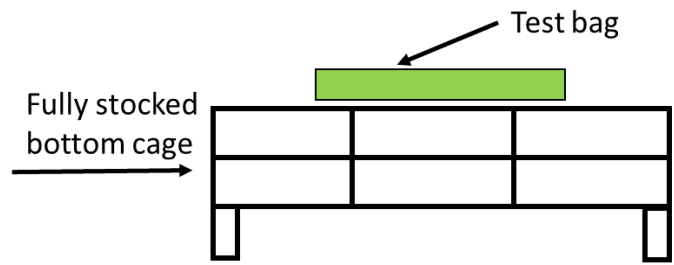


Figure 28: Diagram showing how test bags were deployed on bottom cages. A test bag was fastened to the top of a fully stocked bottom cage using crab pins at each corner and a bungee cord was used as a security to further hold the bag down to the cage.

### Oyster growth and performance

Oyster performance was assessed by measuring shell length (base of the hinge to the farthest point on the mantle), shell width (widest point perpendicular to the shell length), and shell depth (the widest point between the top and bottom shells) of 30 random individuals per bag at the start of deployment, twice during deployment, and once at the end of deployment. Additionally, the dried meat to shell ratio was measured for 10 random animals per bag using the methods to derive the condition index from Lawrence and Scott (1982, eqn. 7). Condition index is commonly used as an index for understanding the relative quality and value of an oyster which scales positively with quality. Using the shell measurements, a series of shell quality indices were taken to assess the shell quality of the oysters grown in each method. Specifically, the shape index (eqn. 8) (Galtsoff 1964), width index (eqn. 9), and elongation index (eqn. 10) were calculated. The shell indices give a metric of shell shape which overall indicates the value of an oyster for the half-shell market. While different growers and buyers have varied definition of an ‘ideal’ oyster, we will define ‘ideal’ when each of these shell indices approach 1. Lastly, total mortality was taken at each day of measurement to track the mortality that occurs throughout the duration of the experiment. The measurements and respective quality ratios were then extrapolated across the farm site using contouring methods derived from the plotly package of R.

### Physical forcing

Clod cards were used to estimate mass transfer rate occurring inside oyster cages. Cards were made based on the f-type card described by Jokiel and Morrissey (1993) with modifications that shrink the card to a 2.5 cm diameter and add a protective cage along the perimeter. Neither

of these modifications significantly influenced the dissolution rate of the clod card (see Chapter 2). Since these modifications were performed, the dissolution of the clod cards will not definitively express relative water flow. Instead, these devices will detect mass transfer rate which expresses the relative exchange that the clod card has with its environment which can be used as a proxy to understand the environment inside the cage. Following construction, a triplicate of cards was then deployed per bag in six-hour intervals to align with tidal cycles. Five total clod card deployments were made during the experiment, roughly once a month during the trial period. To provide context to the clod card measurements and describe the relative flow of water surrounding the field site, two 2 Mhz Nortek™ Aquadopp ADCP units were deployed inshore and downstream of the oyster farm from June 23 to July 7 to monitor water velocity at various depth bins at these locations at 15-minute intervals (Figure 27).

Two accelerometers (Onset HOBO Pendant G Logger: UA-004-64) were deployed continuously in each bag to monitor the movement of oysters and oyster cages throughout the experiment (Figure 19). One accelerometer was placed on the inside of each bag and left to move freely on the inside of the bag to simulate the additive movement between the oysters inside the bag and the bag itself. The other accelerometer was tightly fastened to the exterior of the bag to measure the movement of the bag. The difference between the two accelerometers simulates the movement of one oyster in a bag relative to the other bags. The average clod card dissolution rate and jostling were then extrapolated across the farm site using a contouring method derived from the plotly package in R.

### *Environmental monitoring*

Using a YSI EXO2 sonde, a series of vertical and horizontal profiles were taken at each bag location to monitor the change in environmental conditions at each site. The vertical transects began at the northeast corner of the farm and continued up and down every third row of cages. The YSI was deployed for a total of 21 minutes. The vertical transects were then extrapolated across the farm site using ordinary kriging through ArcMap to extrapolate water quality across the full extent of the experiment location. Vertical profiles were taken immediately next to each bag site and integrated with depth to determine the average environmental conditions at each bag site.

## **Results**

This research evaluated the spatiotemporal physical characteristics of active oyster bottom culture farms and its potential implications on oyster performance. Historically, few have sought to understand these characteristics and even fewer have attempted to sample the movement of oysters due to physical forcing. The seasonal deployment of oyster bags along an active oyster bottom culture and the monitoring of water quality, oyster performance, and physical forcing will likely be capable of characterizing the variability that occurs within oyster aquaculture operations.

### *Environmental monitoring*

Overall, the EXO YSI sonde transects across the farm site showed little spatial variation in water quality (Figure 29). The surface temperature remained constant, not exceeding 1 °C in range. There was a noticeable, yet insignificant, spatial change in the chlorophyll content across

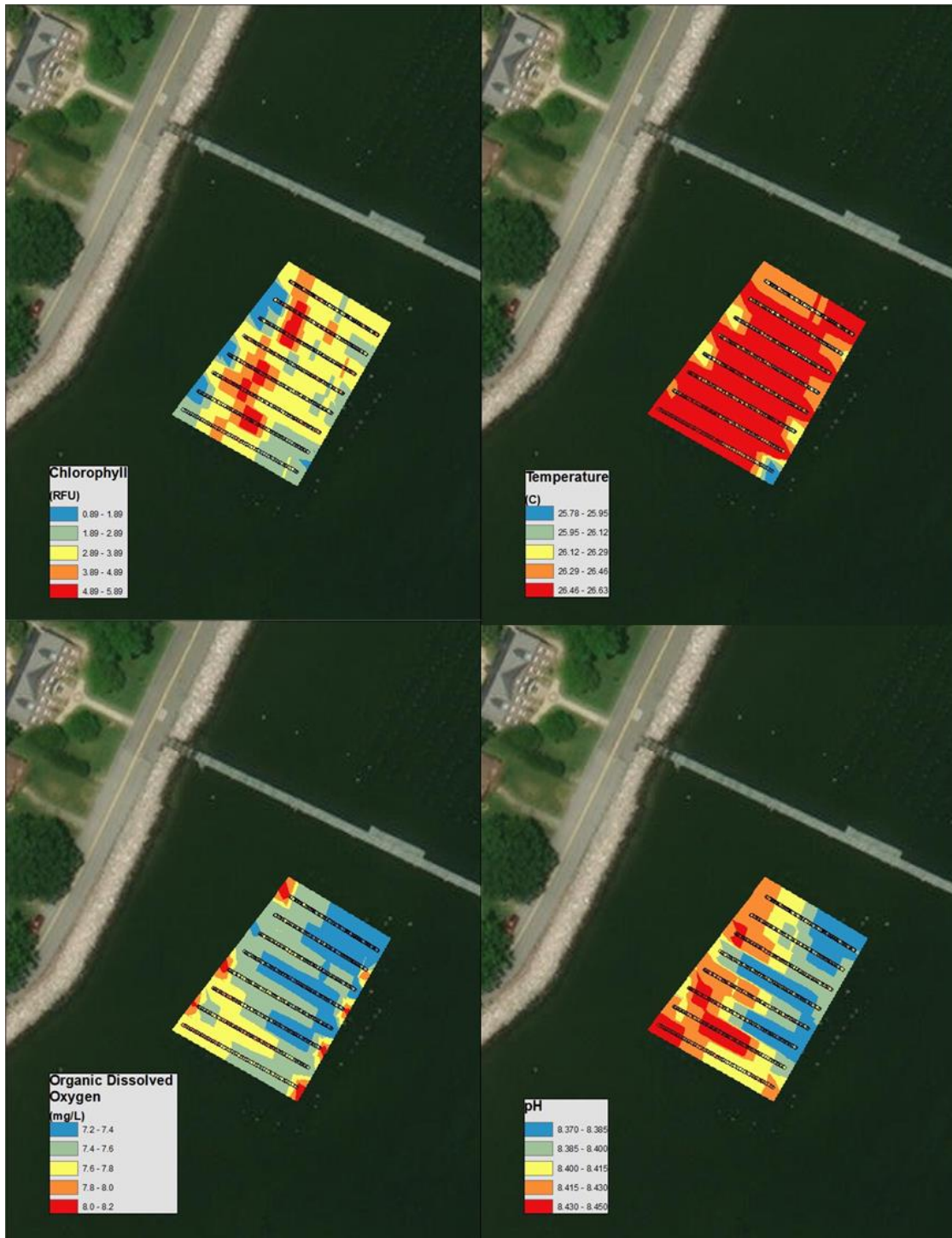


Figure 29: Water quality monitoring of the oyster farm site using a YSI EXO2 sonde. Dots represent the sampling path taken. The remaining area was extrapolated using kriging techniques.

the farm site ( $p = 0.608$ , Moran's spatial autocorrelation). Along the western plane of the grid space; however, there was a band of high chlorophyll present ( $> 5$  RFU) that exceeded the average chlorophyll present (2.50 RFU). In this region of high chlorophyll, there was also a subsequent increase in optical dissolved oxygen (ODO) and pH that was spatially significant ( $p < 0.001$ ;  $p < 0.001$ , respectively, Moran's spatial autocorrelation). From this region moving eastward, there was a decreasing trend in ODO spanning from roughly 7.7 mg/L in the western corner and dropping to roughly 7.3 mg/L in the eastern corner. A similar trend occurs with pH but over a much smaller range (pH range = 8.44 - 8.38) (Figure 29).

### Physical forcing

According to the ADCP deployments, water velocity downstream of the farm averaged at 8.98 cm/s with an RMS velocity of 8.70 cm/s and a maximum velocity of 41.3 cm/s. Average maximum ebb tide velocity downstream was 6.40 cm/s with an RMS of 7.40 cm/s while the maximum flood tide velocity was 7.43 cm/s with an RMS of 8.77 cm/s. Water velocity inshore of the farm was similar to the downstream region of the with an average velocity of 9.05 cm/s, an RMS velocity of 9.21 cm/s, and a maximum velocity of 35.9 cm/s. Average of the maximum ebb tide inshore of the farm was 5.84 cm/s with an RMS velocity of 7.00 cm/s while the average maximum flood tide velocity was 7.60 cm/s with an RMS velocity of 9.05 cm/s (Figure 30). This experimental site is also subject to semi-diurnal tidal cycles (Figure 31). The water velocities observed over this sample period falls in line with the range of water velocities tested by Thompson and Glenn (1994) and Jokiel and Morrissey (1993), making the clod card measurements as reasonable measures for relative mass transfer in this scenario. However, our

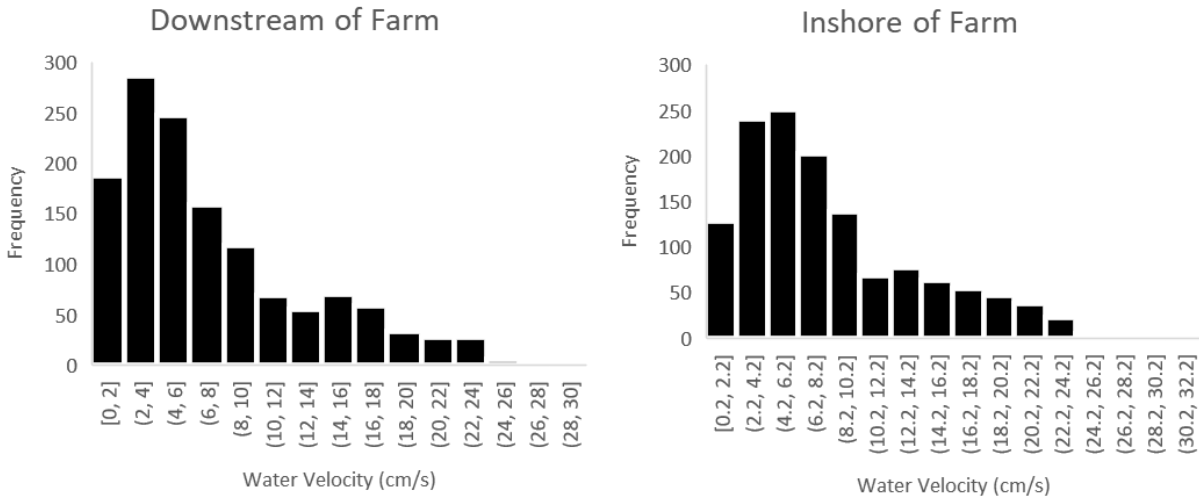


Figure 30: Histogram of all water velocity measurements collected by the ADCP between June 23 to July 7 downstream (left) and inshore (right) of the farm.

study in Chapter two indicates a high level of noise when deploying these cards at low flow velocity (0 – 5 cm/s), indicating that these measures may be noisy at lower average flow velocities. Clod card deployments on sample bags show three distinct zones throughout the farm with varying mass transfer rates (Figure 32). The north and east corners of the farm experienced the highest relative mass transfer rate with respect to the rest of the farm (4.0 – 4.8% clod card dissolution per hour). Toward the center of the farm, there was a steep reduction in mass transfer rate (3.6 – 4.1% clod card dissolution per hour) which persisted into the southern portion of the farm (3.4 – 3.7% clod card dissolution per hour). Overall, clod card dissolution was spatially correlated over the farm site ( $p = 0.002$ , Moran’s spatial autocorrelation). Interestingly, the spatial effects on the dissolution of clod cards were significantly correlated with rows of cages and insignificantly correlated across columns ( $\rho = -0.673$ ,  $p = 0.002$ ;  $\rho = 0.101$ ,  $p = 0.69$ , respectively, Spearman’s rank correlation) (Figure 33).

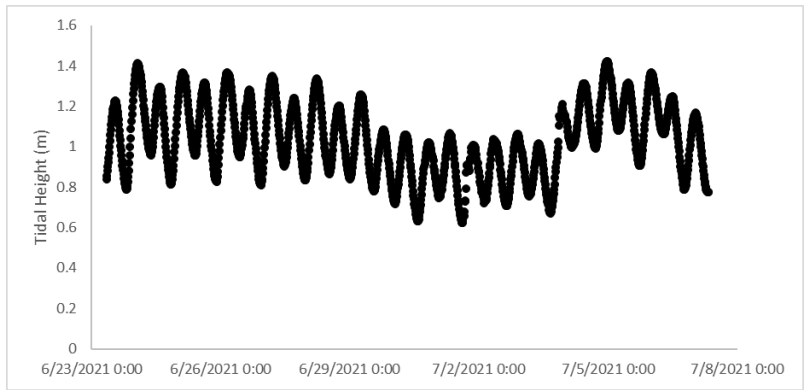


Figure 31: Time series of the tidal height of the water column just downstream of the farm site. Patterns in tidal change indicate a semi-diurnal cycle.

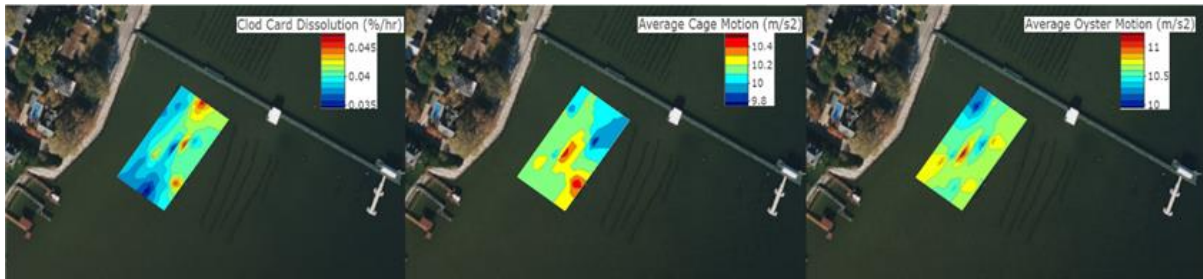


Figure 32: Contour plots of the average mass transfer rate, cage motion, and oyster + cage motion throughout the season.

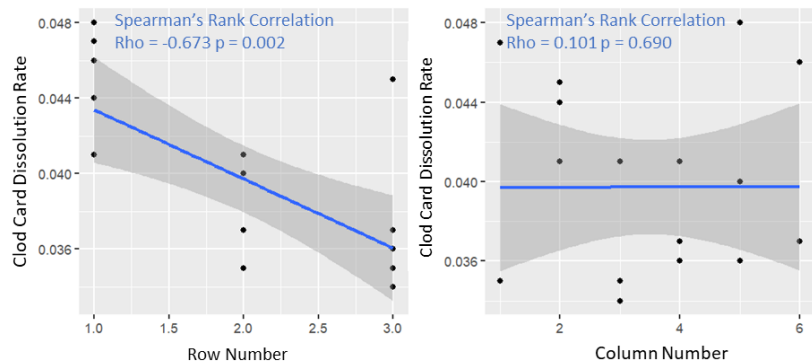


Figure 33: Scatter plot of clod card dissolution rate against the row number (left) and column number (right) of the farm site as depicted in figure 27. A linear trendline was fit with a 95% confidence interval and Spearman's ranked correlation was performed.

The average movement was the highest in the center and the southeast portion of the farm (10.2 – 10.5 m/s<sup>2</sup>). Interestingly, in the area with high cage movement, there was subsequently low water flow. The north and northeastern portion of the farms had the lowest average cage movement (10.0 – 10.2 m/s<sup>2</sup>). Oyster movement had a similar spatial distribution as the cage movement was a high rate of movement in the center of the farm (10.5 – 11.3 m/s<sup>2</sup>) and lower movement along the perimeter of the farm (10.0 – 10.5 m/s<sup>2</sup>) where the lowest average movement was found in the northern corner of the farm (Table 6). While there were noticeable changes in cage and oyster movement across the farm, the average movement at each sample point across the season was not spatially significant ( $p = 0.831$ ,  $p = 0.524$ , respectively, Moran's spatial autocorrelation). Using the mass transfer rate data and the motion data, three noticeable zones were identified across this farm (Figure 34). The northern most section, we will refer to as the 'protected' area due to its relatively low mass transfer and low cage motion. The 'intermediate' zone occurs southwest of the farm and has low relative mass transfer, yet higher cage motion. Lastly, the 'exposed' region located in the northeast section of the farm where the dominant current enters the farm saw the fastest relative rate of mass transfer with a medial amount of cage motion.

### Oyster performance

The growth and performance patterns of oysters across the farm site were complex (Figure 35) (Table 7). The final shell length and width of oysters grown across all cages were statistically significant ( $p = 0.00863$ ,  $p = 0.0124$ , respectively, ANOVA); however, shell depth was not found to be statistically significant ( $p = 0.588$ , ANOVA). Shell length and shell depth

Table 6: Average and 95% confidence interval of physical and water quality measurements taken at each sample bag site on the farm. Bag numbers coincide with figure 1. Clod card dissolution was monitored at 5 different time intervals throughout the experiment. Cage and oyster movement was monitored continuously, and the water quality data was a summary of transects that occurred in one day during the experiment.

Bag Number	Clod Card Dissolution Rate	Average Cage Motion (m/s <sup>2</sup> )	Average Oyster Motion (m/s <sup>2</sup> )	Chlorophyll (RFU)	Optical Dissolved Oxygen (mg/L)	pH	Temperature (C)
1	0.047 ± 0.0064	10.01	0.511	2.605 ± 0.51	7.914 ± 0.077	8.47 ± 0.005	25.97 ± 0.164
2	0.044 ± 0.0095	10.08	0.601	2.324 ± 0.42	7.736 ± 0.075	8.46 ± 0.003	26.25 ± 0.070
3	0.041 ± 0.0079	10.24	0.090	3.407 ± 0.31	7.665 ± 0.050	8.43 ± 0.001	26.37 ± 0.062
4	0.041 ± 0.0068	10.02	-0.030	2.429 ± 0.26	7.600 ± 0.064	8.44 ± 0.009	26.26 ± 0.075
5	0.048 ± 0.0055	9.91	0.437	3.222 ± 0.63	7.626 ± 0.079	8.42 ± 0.004	26.24 ± 0.077
6	0.046 ± 0.0055	10.28	0.139	2.471 ± 0.44	7.643 ± 0.071	8.42 ± 0.005	26.07 ± 0.118
7	0.035 ± 0.0055	9.74	1.150	2.800 ± 0.31	7.790 ± 0.045	8.46 ± 0.004	26.50 ± 0.035
8	0.041 ± 0.0069	10.21	0.016	2.547 ± 0.32	7.779 ± 0.069	8.42 ± 0.002	26.49 ± 0.018
9	0.035 ± 0.0040	10.33	0.235	3.392 ± 0.49	7.877 ± 0.045	8.46 ± 0.008	26.24 ± 0.106
10	0.037 ± 0.0046	10.52	0.708	2.792 ± 0.38	7.786 ± 0.055	8.47 ± 0.002	26.52 ± 0.021
11	0.040 ± 0.0049	9.97	0.377	2.710 ± 0.38	7.734 ± 0.049	8.44 ± 0.007	26.39 ± 0.052
12	0.037 ± 0.0046	10.26	0.643	2.145 ± 0.21	7.700 ± 0.025	8.43 ± 0.000	26.40 ± 0.047
13	0.035 ± 0.0060	10.36	0.194	2.801 ± 0.48	8.025 ± 0.064	8.48 ± 0.002	26.15 ± 0.164
14	0.045 ± 0.011	10.50	0.252	3.114 ± 0.43	7.953 ± 0.053	8.48 ± 0.001	26.33 ± 0.094
15	0.034 ± 0.0055	10.20	0.567	2.911 ± 0.26	7.886 ± 0.063	8.49 ± 0.002	26.45 ± 0.049
16	0.036 ± 0.0076	10.10	0.342	3.084 ± 0.63	8.016 ± 0.055	8.49 ± 0.003	26.16 ± 0.124
17	0.036 ± 0.0094	10.12	0.468	3.678 ± 0.10	7.831 ± 0.097	8.48 ± 0.002	26.50 ± 0.056
18	0.037 ± 0.0061	10.11	0.428	2.773 ± 0.52	8.009 ± 0.044	8.47 ± 0.002	26.07 ± 0.134

appeared to have similar growth patterns. The exposed region of the farm had the largest shell growth followed by the intermediate, then the protected area. The center and southeastern portion of the farm also showed high relative shell length following the experiment. Shell width had a similar pattern of shell growth however, the areas with the largest shell with were exclusively in the center of the farm.

The shape index and elongation index of the oysters grown on the farm were representative of higher quality oysters. The shape index was statistically significant across the study site ( $p = 0.0236$ , ANOVA), but the width index and elongation index were not ( $p = 0.0684$ ,



Figure 34: Based on characteristics driven from the mass transfer rate and cage motion, three distinct locations were identified based on their physical properties. The 'protected' zone with low mass transfer and cage movement is shown in the green section. The 'intermediate' zone in yellow has a low relative mass transfer rate and high cage movement. The 'exposed' zone in red has the highest relative mass transfer rate and moderate cage movement.

$p = 0.0684$ , respectively, ANOVA). Ideal ranges for shape index fall between 1 – 3 depending on personal preference. For this study, we will characterize an 'ideal' oyster as one that has a shape index that approaches 1.5. The oysters in this experiment had overall high-quality shell indexes, ranging from 1.25 to 2.5. Shape index was shown to fluctuate throughout the farm space. There was a horizontal band in the center of the farm where shell index was comparably high (shell index =  $\sim 1.5$ ) while the corners of the farm were notably lower (shell index = 1.75 – 2.5). A similar pattern was shown for the elongation index. An ideal elongation index value range between 0.5 and 1, depending on consumer preference. Some oysters in the farm exceeded an

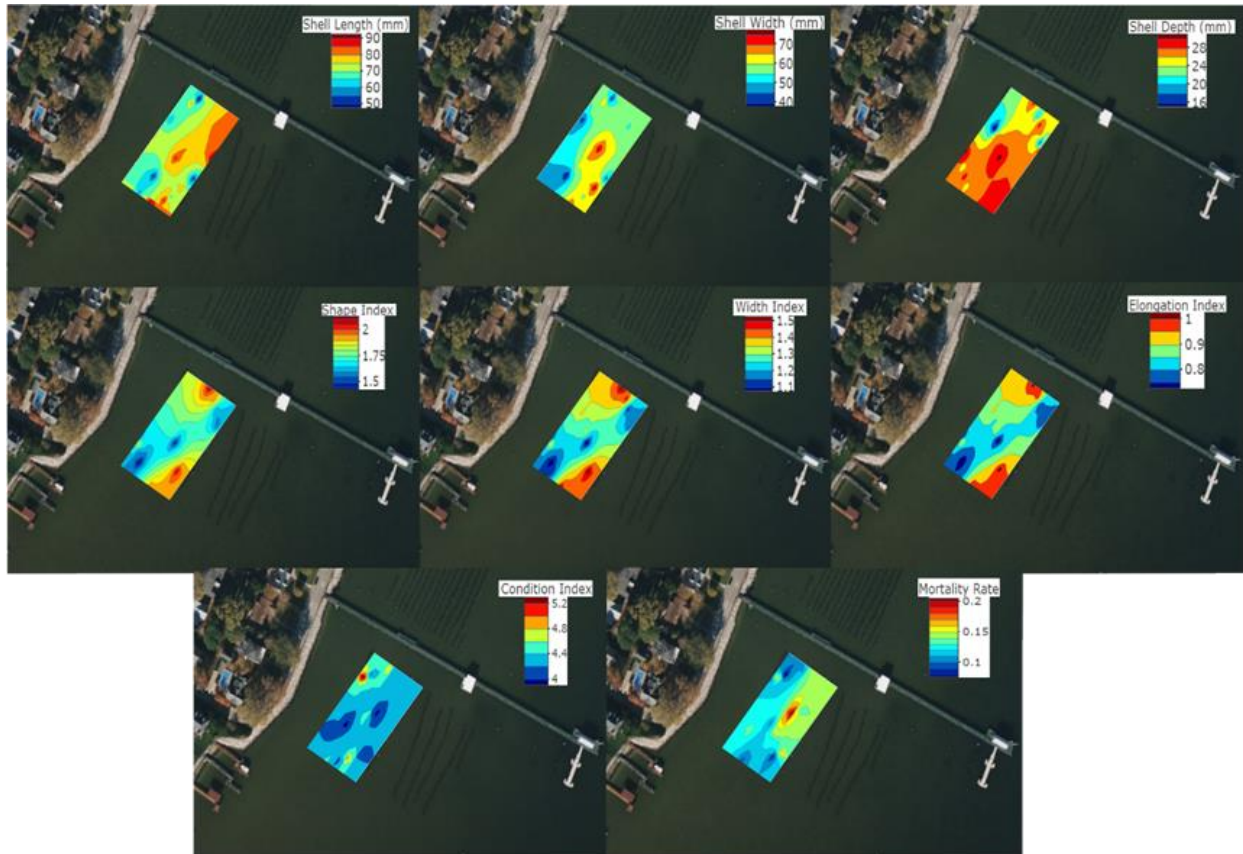


Figure 35: Contour plots of each measured parameter for oyster performance. Contours were extrapolated from 18 sample points which reflect an average of measurements from each test bag at the end of the experiment.

elongation index of 1 and only a small number of oysters were below 0.5. In the northern corner and southern portion of the farm, where the shape index was considerably high, there was a shape index that exceeded one, suggesting that the oysters are too long compared to an ideal shape. The oysters with an optimal elongation index (elongation index =  $\sim 0.75$ ) were found in the center of the farm, where shape index was lower. Across the three distinct physical areas across the farm, the protected area had a lower overall shell shape compared to the intermediate and exposed regions of the farm based on our definitions of ‘ideal’ oyster shape.

Table 7: Average and 95% confidence interval of all final oyster growth parameters measured for each sample bag site. Bag number corresponds to the map in figure 1. Welch t-tests were performed to compare individual bags with the mean across the farm and significant treatments were marked with an asterisk (\*  $p < 0.1$ ; \*\*  $p < 0.05$ ; \*\*\*  $p < 0.01$ ).

Bag Number	Shell Length (mm)	Shell Width (mm)	Shell Depth (mm)	Shape Index	Width Index	Elongation Index	Condition Index	Mortality (%)
1	75.93 ± 4.06	59.73 ± 3.33	28.30 ± 1.83	1.757 ± 0.069	1.297 ± 0.070	0.8528 ± 0.0346	4.217 ± 1.095	15.14
2	74.37 ± 3.50	61.47 ± 3.73	27.83 ± 1.50	1.682 ± 0.062*	1.225 ± 0.054	0.8166 ± 0.0363	4.783 ± 1.100	10.81
3	73.40 ± 3.64	60.10 ± 2.92	28.03 ± 1.71	1.694 ± 0.049	1.227 ± 0.044	0.8181 ± 0.0293	4.393 ± 0.690	10.81
4	73.50 ± 3.64	59.73 ± 3.36	27.90 ± 1.39	1.712 ± 0.066	1.239 ± 0.047	0.8263 ± 0.0315	4.118 ± 1.045	7.03
5	72.17 ± 3.16	56.17 ± 2.53**	27.30 ± 1.43	1.777 ± 0.057	1.290 ± 0.044	0.8599 ± 0.0290	5.375 ± 0.762**	15.14
6	68.6 ± 3.03***	56.27 ± 2.94*	26.7 ± 1.48	1.705 ± 0.049	1.226 ± 0.034*	0.8176 ± 0.0227*	4.430 ± 0.713	10.27
7	75.93 ± 4.13	61.27 ± 3.95	27.23 ± 1.69	1.699 ± 0.062	1.252 ± 0.052	0.8348 ± 0.0349	4.217 ± 0.646	12.97
8	75.90 ± 4.14	58.60 ± 3.36	27.60 ± 1.90	1.770 ± 0.040	1.300 ± 0.034*	0.8665 ± 0.0223*	3.885 ± 0.544*	20.54
9	74.20 ± 3.15	60.57 ± 3.04	27.93 ± 1.62	1.697 ± 0.049	1.236 ± 0.050	0.8241 ± 0.0335	4.578 ± 0.946	15.68
10	74.80 ± 3.54	59.03 ± 2.93	28.57 ± 1.97	1.762 ± 0.071	1.276 ± 0.056	0.8509 ± 0.0377	4.333 ± 1.015	10.27
11	69.57 ± 3.19**	57.27 ± 3.34	26.00 ± 1.51*	1.684 ± 0.065	1.228 ± 0.054	0.8190 ± 0.0362	3.820 ± 0.728	12.43
12	76.70 ± 5.14	57.67 ± 3.61	28.13 ± 1.68	1.837 ± 0.082**	1.335 ± 0.053	0.8900 ± 0.0356**	4.286 ± 0.600	14.05
13	71.20 ± 3.63	57.50 ± 3.28	26.67 ± 1.59	1.712 ± 0.047	1.245 ± 0.037**	0.8303 ± 0.0248	4.280 ± 1.004	13.51
14	74.90 ± 4.04	58.73 ± 3.32	26.40 ± 2.45	1.736 ± 1.668	1.283 ± 0.045	0.8555 ± 0.0299	4.035 ± 0.605	15.68
15	70.97 ± 5.46	54.70 ± 4.08**	26.60 ± 1.92	1.808 ± 0.128	1.316 ± 0.102	0.8773 ± 0.0678	4.190 ± 1.170	8.11
16	80.37 ± 3.79***	64.43 ± 3.48***	28.77 ± 1.73	1.713 ± 0.083	1.264 ± 0.071	0.8429 ± 0.0474	4.907 ± 1.329	11.35
17	74.77 ± 3.87	58.10 ± 3.53	27.87 ± 1.50	1.805 ± 0.133	1.312 ± 0.094	0.8745 ± 0.0628	4.071 ± 0.616	11.35
18	73.83 ± 5.42	60.07 ± 3.02	27.23 ± 1.39	1.683 ± 0.07	1.228 ± 0.069	0.8187 ± 0.0457	4.565 ± 1.067	8.65

The condition index of oysters also showed a dynamic pattern across the farm site but was not found to be statistically significant ( $p = 0.566$ , ANOVA). Overall, the condition index of all sample locations was of higher quality (greater than 1) and did not vary much across the farm site. Condition index ranges from 4 - 5.2 where the highest condition index was in the protected area and the remainder of the farm was lower.

The farm experienced an average of 12.4 percent mortality across the growing season. There was no significant effect on mortality from the farm ( $p = 0.287$ , ANOVA). The center of the farm experienced the highest mortality at twenty percent in one of the bags. The exposed area of the farm had the second highest mortality rate that was consistently over twelve percent. The remaining portion of the farm had lower mortality which generally did not exceed twelve percent.

## Discussion

Noticeable changes in water quality throughout the extent of the farm seem to be attributed to enhanced primary productivity in the downstream portion of the farm. The increase in productivity led to an increase in dissolved oxygen and pH. With the current data, it is uncertain what produced the surge in productivity. One hypothesis is that the ammonia-rich waste produced by the oysters in the surrounding farms might be pooling into that area, as water movement was reduced downstream, allowing for the proliferation of a small, localized phytoplankton bloom. Ray et al. (2015) observed that oyster aquaculture could enhance inorganic nitrogen immediately downstream of their test site. However, Turner et al. (2019) found in their study site, with high water flushing and low stocking density, that oyster aquaculture had minimal influence on local water quality. The area where we observed the increase in productivity lies between two convergent currents that reduce the residence of the area, likely creating a nutrient sink where phytoplankton could be abnormally abundant. Future sampling efforts using water quality sonde transects in parallel with water sampling and surface current profiling over a longer time span would be necessary to confirm the source of this observation and derive the role that oyster aquaculture played in this change in local water quality.

The two distinct regions of high mass transfer rate across the farm are likely derived from a combination of the local currents and marine traffic producing water movement and the attenuation of water motion produced by the surrounding aquaculture farms. In the protected region of the farm, the cages are not downstream of any of the surrounding bottom cage leases

due to the large pier located between them, hence why there is likely high mass transfer present in one thin band parallel to the dominant current. Similarly, the small, southern pool of higher mass transfer is likely being caused by heavy recreational boat traffic that exists within roughly fifty meters of the farm site due to a nearby marina. The remaining area is well protected by the surrounding off-bottom aquaculture farms, resulting in a much lower mass transfer rate.

Interestingly, there was a weak negative linear correlation between the relative mass transfer and cage and oyster jostling. Given that this environment has a particularly fast current running through it, it is likely that the exceedingly strong water flow is forcing all the oysters to one side of the bag and restricting movement. The region that is more protected likely has just enough water flow to allow more back-and-forth movement of oysters across the bag. This suggests that there is likely an optimal range of ambient water flows that will enhance the motion of oysters, providing chipping to the outer shell and producing higher quality oysters for the half-shell market. Additionally, the variability in the direction of water flow might also be factored into the rate of jostling amongst cages however, this has not been tested directly.

The observed changes in physical forcing across the farm appear to be associated with changes in oyster performance. While only mass transfer rate was spatially correlated using statistical approaches, there are regions across the farm that appear noticeably correlated when the datum was extrapolated across the entire site. Oysters that were grown in bags with more jostling were shown to have wider, deeper shells, producing more optimal shell ratios. In the northern region with high mass transfer rates and low jostling, the oysters had higher mortality,

reduced growth and overall lower shell and meat ratios, likely indicating a physical stress that is negatively impacting their growth.

By deploying novel and tools and using innovative approaches, it was possible to observe differences in oyster performance across one off-bottom aquaculture lease and speculate on the role of physical forcing in affected oyster production. It is likely that this observation extends into other farm locations. By knowing regions of a farm site that result in poor or optimal growth, farmers can better leverage specific regions of their farm to achieve specific production goals. For example, oysters that are near ready for market would likely be enhanced by finishing in a region that produces oysters with higher shell and meat ratios to sell to higher quality half-shell markets. Additionally, having foresight on the physical environment within a potential aquaculture site can provide guidance on whether the site is optimal for growing oysters. A grower could also strategically plan a grow out rotation that favors more consistent growth that matches with grower preferences. Figure 36 shows an example of a rotation that can be applied to this farm that would likely produce more consistent well-shaped oysters with a predictable mortality. Future studies should expand upon this work to study the physical conditions that are optimal for growth using other gear types. Prior knowledge of the physical characteristics of a farm could also allow for a study using multiple cultivation methods to determine if growers that utilize multiple grow out methods can strategically place gear with regards to the local environment to enhance production. Furthermore, the cumulation of studies with similar frameworks can be used to inform a random forest model capable of deciding optimal grow out strategies.

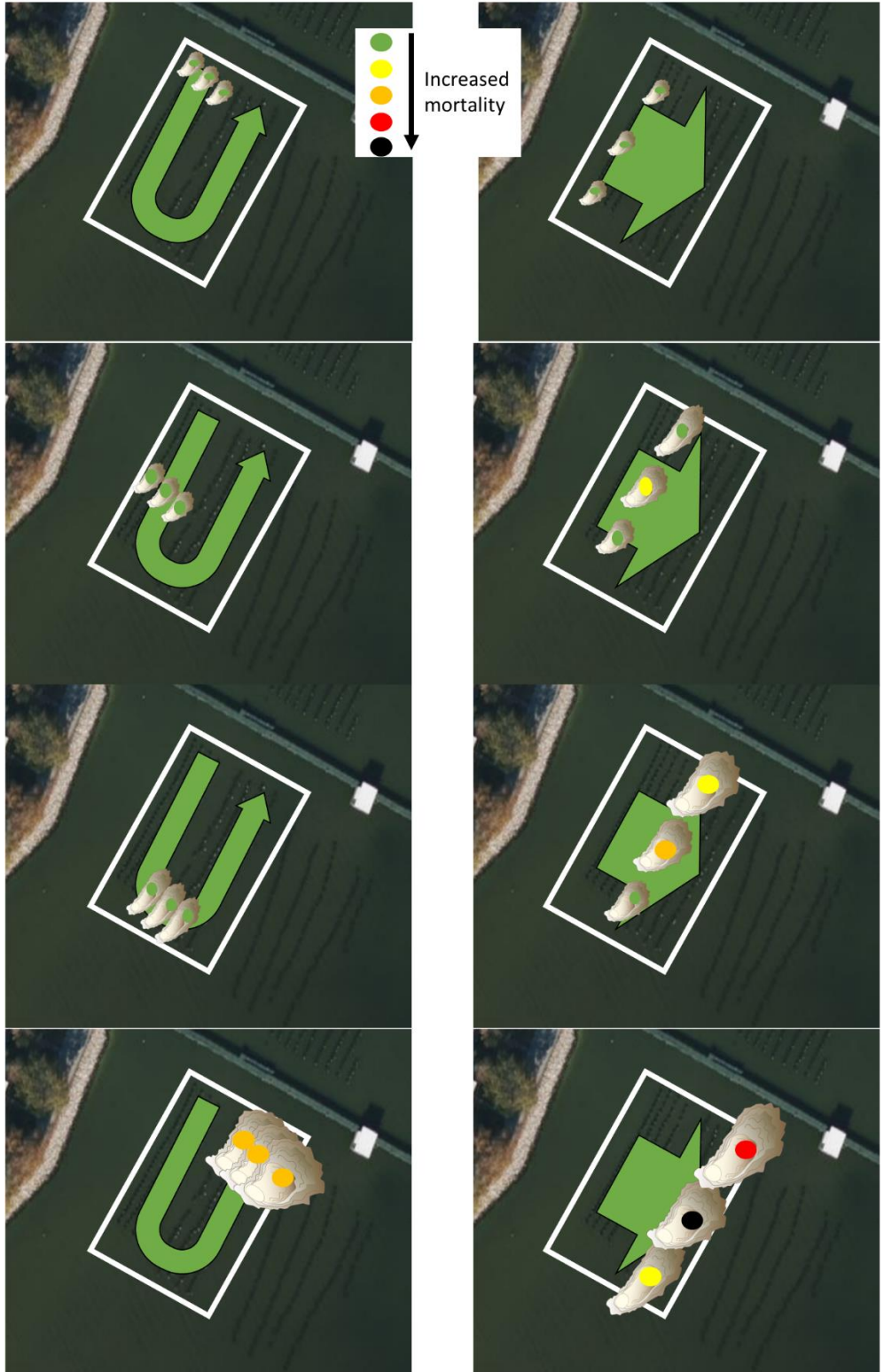


Figure 36: Hypothetical speculations of projected oyster growth throughout two grow-out scenarios. The series on the right demonstrates a circular progression through the farm that is suggested based on the spatial oyster performance and physical forcing data. The second projection follows a more common grow-out rotation observed on farms. The scale of the oysters in each figure represents the speculated size and shape of oysters at discrete timepoints in this scenario. The colored dots on the shells indicate the projected mortality of oysters over time.

## Bibliography

- Adams, C.M., Shumway, S.E., Whitlach, R.B., & Getchis, T. (2011). Biofouling in marine molluscan shellfish aquaculture: a survey assessing the business and economic implications of mitigation. *Journal of the World Aquaculture Society*, 42(2), 242-252. doi: 10.1111/j.1749-7345.2011.00460.x
- Baker, S.M. & Mann, R. (1994). Feeding ability during settlement and metamorphosis in the oyster *Crassostrea virginica* (Gmelin, 1791) and the effects of hypoxia on post-settlement ingestion rates. *Journal of Experimental Marine Biology and Ecology*, 181, 239-253. doi: 10.1016/0022-0981(94)90131-7
- Bartol, I.K., Mann, R., & Luckenbach, M. (1999). Growth and mortality of oysters (*Crassostrea virginica*) on constructed intertidal reefs: effects of tidal height and substrate level. *Journal of Experimental Marine Biology and Ecology*, 237, 157-184. doi: 10.1016/S0022-0981(98)00175-0
- Barton, A., Hales, B., Waldbusser, G.G., Langdon, C., & Feely, R.A. (2012). The Pacific oyster, *Crassostrea gigas*, shows negative correlation to naturally elevated carbon dioxide levels: implications for near-term ocean acidification effects. *Limnology and Oceanography*, 57(3), 698-710. doi: 10.4319/lo.2012.57.3.0698698
- Beckensteiner, J., Scheld, A.M., St-Laurent, P., Friedrichs, M.A.M., & Kaplan, D.M. (2021). Environmentally-determined production frontiers and lease utilization in Virginia's eastern oyster aquaculture industry. *Aquaculture*, 542, 736883. doi: 10.1016/j.aquaculture.2021.736883
- Beristain, M.A. & Malouf, R.E. (1988). The effect of epibionts on the growth of *Mytilus edulis* cultured in Long Island Sound. *Journal of Shellfish Research*, 7(1), 149.
- Bi, C.W., Zhao, Y.P., Dong, G.H., Wu, Z.M., Zhang, Y., & Xu, T.J. (2018). Drag on and flow through the hydroid-fouled nets in currents. *Ocean Engineering*, 161, 195-204. doi: 10.1016/j.oceaneng.2018.05.005
- Bi, S., Chen, L., Sun, Z., Wen, Y., Xue, Q., Xue, C., Li, Z., & Liu, H. (2021). Physiological responses of the triploid Pacific oyster (*Crassostrea gigas*) to varying salinities of aquaculture seawater. *Aquaculture Research*, 52, 2907-2914. doi: 10.1111/are.15117
- Bihan, V.L., Pardo, S., & Guillotreau, P. (2013). Risk perception and risk management strategies of oyster farmers. *Marine Resource Economies*, 28(3), 285-304. doi: 10.5950/0738-1360-28.3.285
- Bishop, M.J. & Hooper, P.J. (2005). Flow, stocking density and treatment against *Polydora spp.*: influences on nursery growth and mortality of the oysters *Crassostrea virginica* and *C. ariakensis*. *Aquaculture*, 246, 251-261. doi: 10.1016/j.aquaculture.2005.01.021

- Bishop, M.J. & Peterson, C.H. (2005). Constraints to *Crassostrea ariakensis* aquaculture: season and method of culture strongly influence success of grow-out. *Journal of Shellfish Research*, 24(4), 995-1006. doi: 10.2983/0730-8000(2005)24[995:CTCAAS]2.0.CO;2
- Botta, R., Asche, F., Borsum, J. S., & Camp, E. V. (2020). A review of global oyster aquaculture production and consumption. *Marine Policy*, 117, 103952. doi: 10.1016/j.marpol.2020.103952
- Brake, J., Evans, F., & Langdon, C. (2003). Is beauty in the eye of the beholder? Development of a simple method to describe desirable shell shape for the Pacific oyster industry. *Journal of Shellfish Research*, 22, 767-771.
- Bricker, S.B., Getchis, T.L., Chadwick, C.B., Rose, C.M., & Rose, J.M. (2016). Integration of ecosystem-based models into an existing interactive web-based tool for improved aquaculture decision-making. *Aquaculture*, 453, 135-146. doi: 10.1016/j.aquaculture.2015.11.036
- Buitrago, J., Rada, M., Hernández, H., & Buitrago, E. (2005). A single-use site selection technique, using GIS, for aquaculture planning: choosing locations for mangrove oyster raft culture in Margarita Island, Venezuela. *Environmental Management*, 35(5), 544-556. doi: 10.1007/s00267-004-0087-9
- Byron, C.J., Jin, D., & Dalton, T.M. (2015). An integrated ecological-economic modeling framework for the sustainable management of oyster farming. *Aquaculture*, 447, 15-22. doi: 10.1016/j.aquaculture.2014.08.030
- Butt, D., Shaddick, K., & Raftos, D. (2005). The effect of low salinity on phenoloxidase activity in the Sydney rock oyster, *Saccostrea glomerata*. *Aquaculture*, 251, 159-166. doi: 10.1016/j.aquaculture.2005.05.045
- Campbell, M.D. & Hall, S.G. (2018). Hydrodynamic effects on oyster aquaculture systems: a review. *Reviews in Aquaculture*, 1-11. doi: 10.1111/raq.12271
- Chapin, T.P., Todd, A.S., & Zeigler, M.P. (2014). Robust, low-cost data loggers for stream temperature, flow intermittency, and relative conductivity monitoring. *Water Resources Research*, 60, 6542-6548. doi: 10.1002/2013WR015158
- Chávez-Villalba, J., Pommier, J., Andriamiseza, J., Pouvreau, S., Barret, J., Cochard, J.C., & Le Pennec, M. (2002). *Aquaculture*, 214, 115-130. doi: 10.1016/S0044-8486(01)00898-5
- Chen, H. & Christensen, E.D. (2017). Development of a numerical model for fluid-structure interaction analysis of flow through and around an aquaculture net cage. *Ocean Engineering*, 142, 597-615. doi: 10.1016/j.oceaneng.2017.07.033
- Claereboudt, M.R., Himmelman, J.H., & Côté, J. (1994). Field evaluation of the effect of current velocity and direction on the growth of the giant scallop, *Placopecten magellanicus*, in suspended culture. *Journal of Experimental Marine Biology and Ecology*, 183, 27-39. doi: 10.1016/0022-0981(94)90154-6

- Coen, L.D., Dumbauld, B.R., & Judge, M.L. (2011). Expanding shellfish aquaculture: a review of the ecological services provided by and impacts of native and cultured bivalves in shellfish-dominated ecosystems, in: Shumway, S.E. Shellfish aquaculture and the environment. John Wiley & Sons, United Kingdom, pp. 185-225.
- Comeau, L. (2013). Suspended versus bottom oyster culture in eastern Canada: comparing stocking densities and clearance rates. *Aquaculture*, 410-411, 57-65. doi: 10.1016/j.aquaculture.2013.06.017
- Cranford, P.J., Li, W., Strand, Ø., & Strohmeier, T. (2008). Phytoplankton depletion by mussel aquaculture: high resolution mapping, ecosystem modeling and potential indicators of ecological carrying capacity. *International Council for the Exploration of the Seas*.
- Cranford, P.J., Ward, J.E., & Shumway, S.E. (2011). Bivalve filter feeding: variability and limits of the aquaculture biofilter, in: Shumway, S.E. Shellfish aquaculture and the environment. John Wiley & Sons, United Kingdom, pp. 185-225.
- Cranford, P.J. (2019). Magnitude and extent of water clarification services provided by bivalve suspension feeding, in: Smaal, A.C., Ferreira, J.G., Grant, J., Petersen, J.K., & Strand, Ø. Goods and Services of Marine Bivalves. Springer, Switzerland, pp. 119-142.
- Delaux, S., Stevens, C.L., & Popinet, S. (2011). High-resolution computational fluid dynamics modelling of suspended shellfish structures. *Environmental Fluid Mechanics*, 11, 405-425. doi: 10.1007/s10652-010-9183-y
- Davis, J.E. (2016). Effects of basket arrangement and stocking density when using the adjustable long-line system for oyster grow-out. Auburn University.
- Dong, F.M. (2009). The nutritional value of shellfish. Washington Sea Grant
- Dong, S., You, X., & Hu, F. (2020). Effects of wave forces on knotless polyethylene and chain-link wire netting panels for marine aquaculture cages. *Ocean Engineering*, 207, 107368. doi: 10.1016/j.oceaneng.2020.107368
- Doty, M.S. (1971). Measurement of water movement in reference to benthic algal growth. *Botanica Marina*, 14, 32-35. doi: 10.1515/botm.1971.14.1.32
- Du, J., Park, K., Jensen, C., Dellapenna, T.M., Zhang, W.G., & Shi, Y. (2021). Massive oyster kill in Galveston Bay caused by prolonged low-salinity exposure after Hurricane Harvey. *Science of the Total Environment*, 774, 145132. doi: 10.1016/j.scitotenv.2021.145132
- Duarte, P., Alvarez-Salgado, X.A., Fernández-Reiriz, M.J., Piedracoba, S., & Labarta, U. (2014). A modeling study on the hydrodynamics of a coastal embayment occupied by mussel farms (Ria de Ares-Betanzos, NW Iberian Peninsula). *Estuarine, Coastal and Shelf Science*, 147, 42-55. doi: 10.1016/j.ecss.2014.05.021

- Dumbauld, B.R. & McCoy, L.M. (2015). Effect of oyster aquaculture on seagrass *Zostera marina* at the estuarine landscape in Willapa Bay, Washington (USA). *Aquaculture Environment Interactions*, 7, 29-47. doi: 10.3354/aei00131
- Ehrich, M.K. & Harris, L.A. (2015). A review of existing eastern oyster filtration rate models. *Ecological Modeling*, 297, 201-212. doi: 10.1016/j.ecolmodel.2014.11.023
- Engle, C., van Senten, J., Parker, M., Webster, D., & Clark, C. (2021). Economic tradeoffs and risk between traditional bottom and container culture of oysters on Maryland farms. *Aquaculture Economies & Management*, 1-32. doi: 10.1080/13657305.2021.1938295
- FAO. (2020). The state of world fisheries and aquaculture 2020. Sustainability in action. Rome.
- Ferreira, J.G., Hawkins, A.J.S., & Bricker, S.B. (2007). Management of productivity, environmental effects and profitability of shellfish aquaculture – the Farm Aquaculture Resource Management (FARM) model. *Aquaculture*, 264, 160-174. doi: 10.1016/j.aquaculture.2006.12.017
- Ferretto, G., Verges, A., Poore, A.G.B., Gribben, P.E., & Glasby, T.M. (2022). Floating bags have the potential to minimize oyster farming impacts on *Posidonia australis* seagrass meadows. *Aquaculture*, 560, 738594. doi: 10.1016/j.aquaculture.2022.738594
- Filgueira, R., Comeau, L.A., Landry, T., Grant, J., Guyondet, T., & Mallet, A. (2013). Bivalve condition index as an indicator of aquaculture intensity, a meta-analysis. *Ecological Indicators*, 25, 215-229. doi: 10.1016/j.ecolind.2012.10.001
- Filgueira, R., Guyondet, T., Comeau, L.A., & Grant, J. (2014). A fully-spatial ecosystem-DEB model of oyster (*Crassostrea virginica*) carrying capacity in the Richibucto Estuary, Eastern Canada. *Journal of Marine Systems*, 136, 42-54. doi: 10.1016/j.jmarsys.2014.03.015
- Folkard, A.M. & Gascoigne, J.C. (2009). Hydrodynamics of discontinuous mussel beds: laboratory flume simulations. *Journal of Sea Research*, 62, 250-257. doi: 10.1016/j.seares.2009.06.001
- Galtsoff, P.S. (1964). The American oyster, *Crassostrea virginica* Gmelin. *Fishery Bulletin of the USA, Fish and Wildlife Service*, 64, pp. 16-45.
- Gangnery, A., Bacher, C., & Buestel, D. (2004). Modelling oyster population dynamics in a Mediterranean coastal lagoon (Thau, France): sensitivity of marketable production to environmental conditions. *Aquaculture*, 230, 323-347. doi: 10.1016/S0044-8486(03)00413-7
- Garlock, T., Asche, F., Anderson, J., Bjørndal, T., Kumar, G., Lorenzen, K., Ropicki, A., Smith, M.D., & Tveterås, R. (2020). A global blue revolution: aquaculture growth across regions, species, and countries. *Reviews in Fisheries Sciences & Aquaculture*, 1, 107-116. doi: 10.1080/23308249.2019.1678111

- Gaurier, B., Germain, G., Kervella, Y., Davourie, J., Cayocca, F., & Lesueur, P. (2011). Experimental and numerical characterization of an oyster farm impact on the flow. *European Journal of Mechanics B/Fluids*, 30, 513-525. doi: 10.1016/j.euromechflu.2011.05.001
- Gerard, V.A. & Mann, K.H. (1979). Growth and production of *Laminaria longicruris* (phaeophyta) populations exposed to different intensities of water movement. *Journal of Phycology*, 15, 33-41. doi: 10.1111/j.1529-8817.1979.tb02958.x
- Gillmor, R.B. (1982). Assessment of intertidal growth and capacity adaptations in suspension-feeding bivalves. *Marine Biology*, 68, 277-286. doi: 10.1007/BF00409594
- Girard, S. & Pérez Agúndez, J.A. (2014). The effects of the oyster mortality crisis on the economics of the shellfish farming sector: preliminary review and prospects from a case study in Marennes-Oleron Bay (France). *Marine Policy*, 48, 142-151. doi: 10.1016/j.marpol.2014.03.024
- Grant, J. & Bacher, C. (2001). A numerical model of flow modification induced by suspended aquaculture in a Chinese bay. *Canadian Journal of Fisheries and Aquatic Sciences*, 58, 1003-1011. doi: 10.1139/cjfas-58-5-1003
- Gray, M.W., Alexander, S.T., Beal, B.F., Bliss, T., Burge, C.A., Cram, J.A., De Luca, M., Dumhart, J., Glibert, P.M., Gonsior, M., Heyes, A., Huebert, K.B., Lyubchich, V., McFarland, K., Parker, M., Plough, L.V., Schott, E.J., Wainger, L.A., Wikfors, G.H., & Wilbur, A.E. (2021). Hatchery crashes among shellfish research hatcheries along the Atlantic coast of the United States: a case study of production analysis at Horn Point Laboratory. *Aquaculture*, 546, 737259. doi: 10.1016/j.aquaculture.2021.737259
- Grizzle, R.E., Langan, R., & Howell, W.H. (1992). Growth responses of suspension-feeding bivalve molluscs to changes in water flow: differences between siphonate and non siphonate taxa. *Journal of Experimental Marine Biology and Ecology*, 162, 213-228. doi: 10.1016/0022-0981(92)90202-L
- Grizzle, R., Ward, K., Burdick, D., Payne, A., & Berlinsky, D. (2020). Eastern oyster *Crassostrea virginica* growth and mortality in New Hampshire (USA) using off-bottom farm gear. *North American Journal of Aquaculture*, 82(2), 132-142. doi: 10.1002/naaq.10135
- Grovhoug, J.G. (1978). Piti power plant intake survey. November 1977. *Naval Ocean Systems Center Technical Report*, 288, San Diego, CA.
- Guo, L., Xu, F., Feng, Z., & Zhang, G. (2016). A bibliometric analysis of oyster research from 1991 to 2014. *Aquaculture International*, 24, 327-344. doi: 10.1007/s10499-015-9928-1
- Guzmán-Agüero, J.E., Nieves-Soto, M., Hurtado, M.A., Piña-Valdez, P., & Garza-Aguirre, M.d.C. (2013). Feeding physiology and scope for growth of the oyster *Crassostrea corteziensis* (Hertlein, 1951) acclimated to different conditions of temperature and salinity. *Aquaculture International*, 21, 283-297. doi: 10.1007/s10499-012-9550-4

- Haché, R., Plante, S., & Doiron, S. (2021). Growth of Eastern oyster (*Crassostrea virginica*) using two oyster – bag float configurations. *Journal of Applied Aquaculture*, 1-12. doi: 10.1080/10454438.2021.1955803
- Hamilton, K.A., Swann, D.L., & Rikard, F.S. (2004). Evaluation of two off-bottom oyster, *Crassostrea virginica*, culture methods for use in oyster gardening in Alabama. *Journal of Applied Aquaculture*, 16(3/4), 1-16. doi: 10.1300/J028v16n03\_01
- Handley, S.J. & Bergquist, P.R. (1997). Spionid polychaete infestations of intertidal Pacific oysters *Crassostrea gigas* (Thunberg), Mahurangi Harbour, northern New Zealand. *Aquaculture*, 3-4, 191-205. doi: 10.1016/S0044-8486(97)00032-X
- Harsh, D. & Luckenbach, M.W. (1999). Materials processing by oysters in patches: interactive roles of current speed and seston composition, in: Luckenbach, M.W., Mann, R., & Wesson, J.A. Oyster reef habitat restoration: a synopsis and synthesis of approaches. Virginia Institute of Marine Science, College of William and Mary, pp. 251-266.
- Hawkins, A.J.S., Pascoe, P.L., Parry, H., Brinsley, M., Black, K.D., McGonigle, C., Moore, H., Newell, C.R., O'Boyle, N., O'Carroll, T., O'Loan, B., Service, M., Smaal, A.C., Zhang, X.L., & Zhu, M.Y. (2013). ShellSIM: a generic model of growth and environmental effects validated across contrasting habitats in bivalve shellfish. *Journal of Shellfish Research*, 32(2), 237-253. doi: 10.2983/035.032.0201
- Hensey, S.M. (2020). Improving the (off)-bottom line: assessing the costs and benefits of different culture techniques on an Alabama commercial oyster farm. Auburn University.
- Ho, L.M., Huang, J.F., & Lee, J.M. (2016). The effects of price changes on oyster farmers in Changhua County, Taiwan, who cultivate oysters at low and high densities. *Aquaculture International*, 24, 623-635. doi: 10.1007/s10499-015-9952-1
- Honkoop, P.J.C. & Bayne, B.L. (2002). Stocking density and growth of the Pacific oyster (*Crassostrea gigas*) and the Sydney rock oyster (*Saccostrea glomerata*) in Port Stephens, Australia. *Aquaculture*, 213, 171-186. doi: 10.1016/S0044-8486(02)00030-3
- Hood, S., Webster, D., Meritt, D., Plough, L., & Parker, M. (2020). Oyster production equipment comparisons 2016-2018. Maryland Sea Grant.
- Hornick, K.M. & Plough, L.V. (2021). Genome-wide analysis of natural and restored eastern oyster populations reveals local adaptation and positive impacts of planting frequency and broodstock number. *Evolutionary Applications*, 15, 40-59. doi: 10.1111/eva.13322
- Huang, J.F. & Lee, J.M. (2013). Production economies and profitability analysis of horizontal rack culture and horizontal rack culture coupled with raft-string culture methods: a case study of Pacific oyster (*Crassostrea gigas*) farming in Chiayi and Yunlin Counties, Taiwan. *Aquaculture International*, 22, 1131-1147. doi: 10.1007/s10499-013-9733-7

- Jiang, B., Boss, E., Kiffney, T., Hesketh, G., Bourdin, G., Fan, D., & Brady, D.C. (2022). Oyster aquaculture site selection using high-resolution remote sensing: a case study in the Gulf of Maine, United States. *Frontiers in Marine Science*, *9*, 802438. doi: 10.3389/fmars.2022.802438
- Jokiel, P.L. & Morrissey, J.I. (1993). Water motion on coral reefs: evaluation of the 'clod card' technique. *Marine Ecology Progress Series*, *93*, 175-181. doi: 10.3354/meps093175
- Kawai, H., Marui, M., & Kurogi, M. (1982). Measurement of water movement with a hemispherical block of plaster. *Japanese Journal of Phycology*, *30*, 161-162.
- Kemp, W.M., Boynton, W.R., Adolf, J.E., Boesch, D.F., Boicourt, W.C., Brush, G., Cornwell, J.C., Fisher, T.R., Glibert, P.M., Hagy, J.D., Harding, L.W., Houde, E.D., Kimmel, D.G., Miller, W.D., Newell, R.I.E., Roman, M.R., Smith, E.M., & Stevenson, J.C. (2005). Eutrophication of Chesapeake Bay: historical trends and ecological interactions. *Marine Ecology Progress Series*, *303*, 1-29. doi: 10.3354/meps303001
- Kitsikoudis, V., Kibler, K.M., & Walters, L.J. (2020). In-situ measurements of turbulent flow over intertidal natural and degraded oyster reefs in an estuarine lagoon. *Ecological Engineering*, *143*, 105688. doi: 10.1016/j.ecoleng.2019.105688
- Klebert, P., Lader, P., Gansel, L., & Oppedal, F. (2013). Hydrodynamic interactions on net panel and aquaculture fish cages: a review. *Ocean Engineering*, *58*, 260-274. doi: 10.1016/j.oceaneng.2012.11.006
- Kobayashi, M., Msangi, S., Batka, M., Vannuccini, S., Dey, M.M., & Anderson, J.L. (2015). Fish to 2030: the role and opportunity for aquaculture. *Aquaculture, Economies & Management*, *19*(3), 282-300. doi: 10.1080/13657305.2015.994240
- Kreeger, D.A., Newell, R.I.E., & Langdon, C.J. (1990). Effect of tidal exposure on utilization of dietary lignocellulose by the ribbed mussel *Geukensia demissa* (Dillwyn) (Mollusca : Bivalvia). *Journal of Experimental Marine Biology and Ecology*, *144*, 85-100. doi: 10.1016/0022-0981(90)90021-4
- La Peyre, M.K., Eberline, B.S., Soniat, T.M., & La Peyre, J.F. (2013). Differences in extreme low salinity timing and duration differentially affect eastern oyster (*Crassostrea virginica*) size class growth and mortality in Breton Sound, LA. *Estuarine, Coastal and Shelf Science*, *135*, 146-157. doi: 10.1016/j.ecss.2013.10.001
- Lacoste, E., Le Moullac, G., Levy, P., Gueguen, Y., & Gaertner-Mazouni, N. (2014). Biofouling development and its effect on growth and reproduction of the farmed pearl oyster *Pinctada margaritifera*. *Aquaculture*, *434*, 18-26. doi: 10.1016/j.aquaculture.2014.07.012

- Lacoste, E. & Gaertner-Mazouni, N. (2015). Biofouling impact on production and ecosystem functioning: a review for bivalve aquaculture. *Reviews in Aquaculture*, 7, 187-196. doi: 10.1111/raq.12063
- Lawrence, D.R. & Scott, G.I. (1982). The determination and use of condition index of oysters. *Estuaries*, 5, 23–27. doi: 10.2307/1352213
- Lee, Y.J., Kang, H.Y., Lee, W.C., & Kang, C.K. (2017). Hydrodynamic effects on growth performance of the Pacific oyster *Crassostrea gigas* cultured in suspension in a temperate bay on the coast of Korea. *Estuaries and Coasts*, 40, 1551-1565. doi: 10.1007/s12237-017-0252-z
- Lenihan, H.S., Peterson, C.H., & Allen, J.M. (1996). Does flow speed also have a direct effect on growth of active suspension-feeders: an experimental test on oysters. *Limnology and Oceanography*, 41(6), 1359-1366. doi: 10.4319/lo.1996.41.6.1359
- Li, A., Li, L., Song, K., Wang, W., & Zhang, G. (2017). Temperature, energy metabolism, and adaptive divergence in two oyster subspecies. *Ecology and Evolution*, 7, 6151-6162. doi: 10.1002/ece3.3085
- Lin, J., Li, C., & Zhang, S. (2016). Hydrodynamic effect of a large offshore mussel suspended aquaculture farm. *Aquaculture*, 451, 147-155. doi: 10.1016/j.aquaculture.2015.08.039
- Liu, Z. & Huguenard, K. (2020). Hydrodynamic response of a floating aquaculture farm in a low inflow estuary. *Journal of Geophysical Research*, 125, e2019JC015625. doi: 10.1029/2019JC015625
- Llorente, I. & Luna, L. (2016). Bioeconomic modelling in aquaculture: an overview of the literature. *Aquaculture International*, 24, 931-948. doi: 10.1007/s10499-015-9962-z
- Lodeiros, C., Galindo, L., Buitrago, E., & Himmelman, J.H. (2007). Effects of mass and position of artificial fouling added to the upper valve of the mangrove oyster *Crassostrea rhizophorae* on its growth and survival. *Aquaculture*, 262, 168-171. doi: 10.1016/j.aquaculture.2006.10.002
- Madin, J., Chong, V.C., & Hartstein, N.D. (2010). Effects of water flow velocity and fish culture on net biofouling in fish cages. *Aquaculture Research*, 41, e602-e617. doi: 10.1111/j.1365-2109.2010.02567.x
- Mallet, A.L., Carver, C.E., & Hardy, M. (2009). The effect of floating bag management strategies on biofouling, oyster growth and biodeposition levels. *Aquaculture*, 287, 325-323. doi: 10.1016/j.aquaculture.2008.10.023
- Mallet, A.L., Carver, C.E., & Thériault, M.H. (2013). Growth performance of Eastern oysters *Crassostrea virginica* in Atlantic Canada: effect of the culture gear. *Aquaculture*, 396-399, 1-7. doi: 10.1016/j.aquaculture.2013.02.019

- Marshall, R.D. & Dunham, A. (2013). Effects of culture media and stocking density on biofouling, shell shape, growth, and survival of the Pacific oyster (*Crassostrea gigas*) and the Manila clam (*Venerupis philippinarum*) in suspended culture. *Aquaculture*, 406-407, 68-78. doi: 10.1016/j.aquaculture.2013.05.003
- Martinell, D.P., Vergara-Solana, F.J., Almendarez-Hernández, L.C., & Araneda-Padilla, M.E. (2019). Econometric models applied to aquaculture as tools for sustainable production. *Reviews in Aquaculture*, 1-16. doi: 10.1111/raq.12385
- McCarty, A.J., McFarland, K., Small, J., Allen, S.K.J., & Plough, L.V. (2020). Heritability of acute low salinity survival in the Eastern oyster (*Crassostrea virginica*). *Aquaculture*, 529, 735649. doi: 10.1016/j.aquaculture.2020.735649
- Mizuta, D.D., Silveira, N.J., Fischer, C.E., & Lemos, D. (2012). Interannual variation in commercial oyster (*Crassostrea gigas*) farming in the sea (Florianópolis, Brazil, 27°44' S; 48°33' W) in relation to temperature, chlorophyll *a* and associated oceanographic conditions. *Aquaculture*, 366-367, 105-114. doi: 10.1016/j.aquaculture.2012.09.011
- Mizuta, D.D. & Wikfors, G.H. (2019). Seeking the perfect oyster shell: a brief review of current knowledge. *Reviews in Aquaculture*, 11, 586-602. doi: 10.1111/raq.12247
- Munroe, D.M., Grothues, T.M., Cleary, N.E., Daw, J., & Estrada, S. (2020). Oyster aquaculture does not impede spawning beach access for Atlantic horseshoe crabs *Limulus polyphemus*. *Aquaculture Environment Interactions*, 12, 81-90. doi: 10.3354/aei00351
- Muus, B.J. (1968). A field method for measuring “exposure” by means of plaster balls: a preliminary account. *Sarsia*, 34(1), 61-68. doi: 10.1080/00364827.1968.10413371
- Naylor, R.L., Williams, S.L., & Strong, D.R. (2001). Aquaculture – a gateway for exotic species. *Science*, 294, 1655-1656. doi: 10.1126/science.1064875
- Needler, A.W.H. (1935). Rearing separate oyster spat on trays. *Biological Board of Canada*, 48, 1-12.
- Newell, C.R., Hawkins, A.J.S., Marros, K., Richardson, J., Davis, C., & Getchis, T. (2013). ShellGIS: a dynamic tool for shellfish farm site selection. *World Aquaculture*, 52-55.
- Newell, C.R. & Richardson, J. (2014). The effects of ambient and aquaculture structure hydrodynamics on the food supply and demand of mussel rafts. *Journal of Shellfish Research*, 33(1), 257-272. doi: 10.2983/035.033.0125
- Newell, C.R., Hawkins, A.J.S., Morris, K., Boss, E., Thomas, A.C., Kiffney, T.J., & Brady, D.C. (2021). Using high-resolution remote sensing to characterize suspended particulate organic matter as bivalve food for aquaculture site selection. *Journal of Shellfish Research*, 40(1), 113-118. doi: 10.2983/035.040.0110

- Palmer, S.C.J., Barillé, L., Kay, S., Ciavatta, S., Buck, B., & Gernez, P. (2021). Pacific oyster (*Crassostrea gigas*) growth modelling and indicators for offshore aquaculture in Europe under climate change uncertainty. *Aquaculture*, 532, 736116. doi: 10.1016/j.aquaculture.2020.736116
- Parker, M. & Bricker, S. (2020). Sustainable oyster aquaculture, water quality improvement, and ecosystem service value potential in Maryland Chesapeake Bay. *Journal of Shellfish Research*, 39(2), 269-281. doi: 10.2983/035.039.0208
- Pilditch, C.A., Grant, J., & Bryan, K.R. (2001). Seston supply to sea scallops (*Placopecten magellanicus*) in suspended culture. *Canadian Journal of Fisheries and Aquatic Sciences*, 58, 241-253. doi: 10.1139/cjfas-58-2-241
- Pit, J.H. & Southgate, P.C. (2003). Fouling and predation; how do they affect growth and survival of the blacklip pearl oyster, *Pinctada margaritifera*, during nursery culture?. *Aquaculture International*, 11, 545-555. doi: 10.1023/B:AQUI.0000013310.17400.97
- Poizot, E., Verjus, R., N'Guyen, H.Y., Angilella, J.R., & Méar, Y. (2016). Self-contamination of aquaculture cages in shallow water. *Environmental Fluid Mechanics*, 16, 793-805. doi: 10.1007/s10652-016-9450-7
- Porter, E.T., Sanford, L.P., & Suttles, S.E. (2000). Gypsum dissolution is not a universal integrator of 'water motion'. *Limnology and Oceanography*, 45(1), 145-158. doi: 10.4319/lo.2000.45.1.0145
- Powell, E.N., Hofmann, J.M., Klinck, J.M., & Ray, S.M., 1992. Modeling oyster populations: I. a commentary on filtration rate. is faster always better?. *Journal of Shellfish Research*, 11(2), 387-398.
- Proestou, D.A., Vinyard, B.T., Corbett, R.J., Piesz, J., Allen, S.K.J., Small, J.M., Li, C., Liu, M., DeBrosse, G., Guo, X., Rawson, P., & Gómez-Chiarri, M. (2016). Performance of selectively-bred lines of eastern oyster, *Crassostrea virginica*, across eastern US estuaries. *Aquaculture*, 464, 17-27. doi: 10.1016/j.aquaculture.2016.06.012
- Rauch, H.E., Botsford, L.W., & Shleser, R.A. (1975). Economic optimization of an aquaculture facility. *Transactions on Automatic Control*, 20(3), 310-319. doi: 10.1109/TAC.1975.1100952
- Ray, N.E., Li, J., Kangas, P.C., & Terlizzi, D.E. (2015). Water quality upstream and downstream of a commercial oyster aquaculture facility in Chesapeake Bay, USA. *Aquacultural Engineering*, 68, 35-42. doi: 10.1016/j.aquaeng.2015.08.001
- Ray, N.E., Maguire, T.J., Al-Haj, A.N., Henning, M.C., & Fulweiler, R.W. (2019). Low greenhouse gas emissions from oyster aquaculture. *Environmental Science & Technology*, 53, 9118-9127. doi: 10.1021/acs.est.9b02965
- Richardson, N.F., Ruesink, J.L., Naeem, S., Hacker, S.D., Tallis, H.M., Dumbauld, B.R., & Wisheart, L.M. (2008). Bacterial abundance and aerobic microbial activity across natural and

- oyster aquaculture habitats during summer conditions in a northeastern Pacific estuary. *Hydrobiologia*, 596, 269-278. doi: 10.1007/s10750-007-9102-5
- Ross, L.G., Telfer, T.C., Falconer, L., Soto, D., & Aguilar-Manjarrez, J. (2013). Site selection and carrying capacities for inland and coastal aquaculture. *FAO/Institute of Aquaculture, University of Stirling, Expert Workshop 6-8 December 2010*, Rome.
- Sala, A. & Lucchetti, A. (2008). Low-cost tool to reduce biofouling in oyster longline culture. *Aquacultural Engineering*, 39, 53-58. doi: 10.1016/j.aquaeng.2008.06.001
- Scanes, E., Parker, L.M., O'Connor, W.A., Dove, M.C., & Ross, P.M. (2020). Heatwaves alter survival of the Sydney rock oyster, *Saccostrea glomerata*. *Marine Pollution Bulletin*, 158, 111389. doi: 10.1016/j.marpolbul.2020.111389
- Shaw, W.N. (1969). The past and present status of off-bottom oyster culture in North America. *Transactions of the American Fisheries Society*, 98(4), 755-761. doi: 10.1577/1548-8659(1969)98[755:TPAPSO]2.0.CO;2
- Shumway, S.E., Davis, C., Downey, R., Karney, R., Kraeuter, J., Parsons, J., Rheault, R., & Wikfors, G. (2003). Shellfish aquaculture – in praise of sustainable economies and environments. *World Aquaculture*, 34(4), 15-18.
- Silva, C., Ferreira, J.G., Bricker, S.B., DelValls, T.A., Martín-Díaz, M.L., & Yáñez, E. (2011). Site selection for shellfish aquaculture by means of GIS and farm-scale models, with an emphasis on data-poor environments. *Aquaculture*, 318(3-4), 444-457. doi: 10.1016/j.aquaculture.2011.05.033
- Snyder, J., Boss, E., Weatherbee, R., Thomas, A.C., Brady, D.C., & Newell, C.R. (2017). Oyster aquaculture site selection using landsat 8-derived sea surface temperature, turbidity, and chlorophyll *a*. *Frontiers in Marine Science*, 4, 190. doi: 10.3389/fmars.2017.00190
- Stevens, C.L. & Petersen, J.K. (2011). Turbulent, stratified flow through a suspended shellfish canopy: implications for mussel farm design. *Aquaculture Environmental Interactions*, 2(1), 87-104. doi: 10.3354/aei00033
- Tan, K., Deng, L., & Zheng, H. (2021). Effects of stocking density on the aquaculture performance of diploid and triploid, Pacific oyster *Crassostrea gigas* and Portuguese oyster *C. angulata* in warm water aquaculture. *Aquaculture Research*, 1-12. doi: 10.1111/are.15489
- Thiyagarajan, V. & Ko, G.W.K. (2012). Larval growth response of the Portuguese oyster (*Crassostrea angulata*) to multiple climate change stressors. *Aquaculture*, 370-371, 90-95. doi: 10.1016/j.aquaculture.2012.09.025
- Thomas, L.L. (2016). The effect of aquaculture gear and tidal zone on the growth and shape of the oyster *Crassostrea virginica* during a “finishing period” in Chesapeake Bay. University of Maryland.

- Thompson, T.L. & Glenn, E.P. (1994). Plaster standards to measure water motion. *Limnology and Oceanography*, 39(7), 1768-1779. doi: 10.4319/lo.1994.39.7.1768
- Tsarau, A., Lugni, C., Lucarelli, A., Kristiansen, D., & Lader, P. (2021). Sloshing in a rotating liquid inside a closed sea cage for fish farming. *Physics of Fluids*, 33, 037114. doi: 10.1063/5.0037408
- Turner, J.S., Kellogg, M.L., Massey, G.M., & Friedrichs, C.T. (2019). Minimal effects of oyster aquaculture on local water quality: examples from southern Chesapeake Bay. *Plos One*, 14(11), e0224768. doi: 10.1371/journal.pone.0224768
- Underwood, A.J. & Anderson, M.J. (1994). Seasonal and temporal aspects of recruitment and succession in an intertidal estuarine fouling assemblage. *Journal of the Marine Biological Association of the United Kingdom*, 74, 563-584. doi: 10.1017/S0025315400047676
- Vo, M., Mehrabian, S., Villalpando, F., Etienne, S., Pelletier, D., & Cameron, C.B. (2018). The fluid dynamics on *Balanus glandula* barnacles: adaptations to sheltered and exposed habitats. *Journal of Biomechanics*, 71, 225-235. doi: 10.1016/j.jbiomech.2018.02.011
- Walton, W.C., Davis, J.E., & Supan, J.E. (2013a). Off-bottom culture of oysters in the Gulf of Mexico. *Southern Regional Aquaculture Center*, 4308, 1-6.
- Walton, W.C., Rikard, F.S., Chaplin, G.I., Davis, J.E., Arias, C.R., & Supan, J.E. (2013b). Effects of ploidy and gear on the performance of cultured oysters, *Crassostrea virginica*: survival, growth, shape, condition index and *Vibrio* abundances. *Aquaculture*, 414-415, 260-266. doi: 10.1016/j.aquaculture.2013.07.032
- Wang, T., Li, Q., Zhang, J., & Yu, R. (2018). Effects of salinity, stocking density, and algal density on growth and survival of Iwagaki oyster *Crassostrea nippona* larvae. *Aquaculture International*, 26, 947-958. doi: 10.1007/s10499-018-0261-3
- Wang, X.X., Swift, M.R., Dewhurst, T., Tsukrov, I., Celikkol, B., & Newell, C. (2014). Dynamics of submersible mussel rafts in waves and current. *Chinese Ocean Engineering Society*, 29(3), 431-444. doi: 10.1007/s13344-015-0030-2
- Ward, R.D., Thompson, P.A., Appleyard, S.A., Swan, A.A., & Kube, P.D. (2005). Sustainable genetic improvement of Pacific oysters in Tasmania and South Australia. *Fisheries Research and Development Corporation final report*, Canberra, Australia, pp. 66-81.
- Whalen, M.A. & Stachowicz, J.J. (2017). Suspension feeder diversity enhances community filtration rates in different flow environments. *Marine Ecology Progress Series*, 570, 1-13. doi: 10.3354/meps12133
- Wildish, D. & Kristmanson, D. (1997). Benthic suspension feeders and flow. *Cambridge University Press*, Cambridge, UK.

- Willer, D.F., Nicholls, R.J., & Aldridge, D.C. (2021). Opportunities and challenges for upscaled global bivalve seafood production. *Nature Food*, 2, 935-943. <https://doi.org/10.1038/s43016-021-00423-5>
- Wilson-Ormond, E.A., Powell, E.N., & Ray, S.M. (1997). Short-term and small-scale variation in food availability to natural oyster populations: food, flow and flux. *Marine Ecology*, 18(1), 1-34. doi: 10.1111/j.1439-0485.1997.tb00424.x
- Xu, P., Zhang, S., Cai, H., Chen, W., Huang, H., & Liu, C. (2019). Characteristics of vertical mixing in a sea-cage farm and its environmental influences in a strong tide system: a case study in the Nanji Archipelago, East China Sea. *Aquaculture*, 512, 734344. doi: 10.1016/j.aquaculture.2019.734344
- Yokoyama, H., Inoue, M., & Abo, K. (2004). Estimation of the assimilative capacity of fish-farm environments based on the current velocity measured by plaster balls. *Aquaculture*, 240, 233-247. doi: 10.1016/j.aquaculture.2004.06.018
- Yu, L. & Gan, J. (2021). Mitigation of eutrophication and hypoxia through oyster aquaculture: an ecosystem model evaluation off the Pearl River Estuary. *Environmental Science & Technology*, 55, 5506-5514. doi: 10.1021/acs.est.0c06616
- Yurek, S., Eaton, M.J., Lavaud, R., Laney, R.W., DeAngelis, D.L., Pine III, W.E., La Peyre, M., Martin, J., Frederick, P., Wang, H., Lowe, M.R., Johnson, F., Camp, E.V., & Mordecai, R. (2021). Modeling structural mechanics of oyster reef self-organization including environmental constraints and community interactions. *Ecological Modelling*, 440, 109389. doi: 10.1016/j.ecolmodel.2020.109389
- zu Ermgassen, P.S.E., Spalding, M.D., Grizzle, R.E., & Brumbaugh, R.D. (2013). Quantifying the loss of a marine ecosystem service: filtration by the eastern oyster in US estuaries. *Estuaries and Coasts*, 36, 36–43. doi: 10.1007/s12237-012-9559-y